Table of contents

List of figures

ABBREVIATIONS

ABC Transporter	ATP Binding Cassette Transporter
Ag	Antigen
ATP	Adenosine triphosphate
BFA	Bafilomycin A_1
Bfa	Brefeldin A
^oC	Degrees Celsius
cDNA	Complementary DNA
Cnx	Calnexin
FACS	Fluorescence Activated Cell Sorter
DMEM	Dulbecco's Modified Eagle Medium
DMSO	Dimethylsulfoxide
DNA	Deoxyribonucleic acid
DRiPs	Defective Ribosomal Products
ER	Endoplasmic Reticulum
ERAD	ER-associated degradation
FCS	Fetal calf serum
HC	MHC class I heavy chain
IFN	Interferon
kDa	Kilo Dalton
Leup	Leupeptin
NBD	Nucleotide-binding domain

MHC	Major Histocompatibility Complex
mRNA	Messenger RNA
M6PR	Mannose-6-phosphate receptor
mM	millimolar
PAGE	polyacrylamide gel electrophoresis
PBS	Phosphate buffered saline
PCR	Polymerase chain reaction
PDI	Protein disulfide isomerase
PLC	Peptide loading complex
PVDF	Polyvinylidene fluoride
SDS	sodium dodecyl (lauryl) sulfate
S8L	SIINFEKL
SP	signal peptidase
siRNA	Small interfering RNA
TAP	Transporter associated with antigen presentation
TCR	T cell receptor
TGN	*trans*-Golgi network
Tpn	tapasin
TPPII	Tripeptidyl peptidase II
TfR	Transferrin receptor

Summary

MHC class I molecules usually present peptides derived from antigens digested in the cytosol by proteasomes and transported into the ER by TAP. However, also antigens that are internalized into the endocytic tract can be processed for class I-mediated presentation in either a proteasome/TAP-dependent or a TAP-independent fashion. While this cross-presentation pathway is established for exogenous soluble and particulate antigens in professional antigen presenting cells (pAPC), little is known about the endolysosomal processing of endogenous transmembrane antigens into class I-binding peptides by non-pAPCs.

In my thesis I investigated the K^b-restricted presentation of class I-peptide fusion proteins as a model antigen system. I studied the alternative, TAP-independent MHC class I antigen processing pathway in $TAP1^{-/-}$ and $tapasin^{-/-}$ immortalized fibroblasts as well as TAP-deficient RMA-S T lymphoma cells.

I showed that the ovalbumin (OVA)-derived epitope SIINFEKL (S8L) is cleaved out of various sequence contexts when tethered to the N terminus of K^d and K^b and presented to SIINFEKL/K^b specific B3Z T hybridoma cells.

Antigen presentation was inhibited by acidophilic amines and inhibitors of the vacuolar proton pump indicating processing in endosomes. Inhibitors of endolysosomal cysteine and aspartic proteases also interfered with presentation, whereas the ER aminopeptidase ERAP1 and the trans-Golgi endoprotease furin did not detectably contribute to processing.

Fusion proteins containing short N-terminal extensions of S8L and different C-terminal flanking residues were efficiently presented while longer N-terminal extensions showed reduced presentation. Also, proline introduced as N- or C-terminal flanking residue of the S8L epitope resulted in reduced presentation. Not only TAP-deficient cells but also TAP-competent P815 and Ltk^- cells utilized the vacuolar pathway for processing of peptide-tagged class I molecules.

I have characterized the mode of fusion protein internalization from the cell surface and the intracellular location of SIINFEKL-loaded K^b molecules. Both filipin and chlorpromazine partially blocked antigen presentation in reappearance assays after acid

stripping of the cell surface, suggesting both clathrin-independent and -dependent pathways of internalization. Unexpectedly, the cytoplasmic tail of class I harboring several putative sorting signals could be truncated without any loss of the capacity of class I-peptide conjugates to be targeted to vacuolar processing compartments and of peptide-loaded class I molecules to recycle to the surface.

SIINFEKL-loaded K^b molecules recognized by the antibody 25.D1-16 were found in small peripheral vesicles that showed a substantial colocalization with the early endosomal marker EEA1. A subset of 25.D1-16-positive vesicles were also labeled for the late endosomal marker mannose-6-phosphate receptor.

I thus present evidence in this thesis for a TAP-independent, class I-restricted pathway operative in non-professional antigen presenting cells that result in the efficient presentation of endogenous, membrane-associated antigens after processing in endosomes.

Zusammenfassung

MHC-Klasse-I-Moleküle präsentieren gewöhnlich Peptide, die aus zytosolischen Antigenproteinen durch proteasomalen Verdau generiert und anschließend vom TAP-Peptidtransporter ins endoplasmatische Retikulum transportiert werden. Es können jedoch auch endozytierte Antigene für die MHC-Klasse-I-vermittelten Antigenpräsentation prozessiert werden, wobei dieser alternative Weg entweder in einer Proteasom/TAP-abhängigen oder unabhängigen Weise abläuft. Während diese so genannte „Kreuzpräsentation“ für einige exogene lösliche bzw. partikuläre Antigen beschrieben war, war zu Beginn dieser Arbeit die endolysosomale Prozessierung von MHC-Klasse-I-bindenden Peptiden aus zelleigenen, membranständigen Proteinen noch weitgehend unverstanden**.**

In meiner Dissertation habe ich die H-2K^b-vermittelte Antigenpräsentation von Klasse-I-Peptid-Fusionsproteinen als Modellantigensystem verwendet. Ich untersuchte den alternativen, TAP-unabhängigen Prozessierungsweg in immortalisierten Fibroblasten aus TAP-defizienten bzw. Tapasin-defizienten Mäusen sowie mit Hilfe von TAP-defizienten Maus-T-Lymphomzellen. Ich verwendete das aus dem Ovalbumin stammende K^b-bindende Peptid SIINFEKL in kovalenter Verknüpfung mit dem Aminoterminus von K^b- und K^d-Klasse-I-Molekülen, wobei die SIINFEKL-Sequenz am N-terminalen Ende durch verschiedene natürlich vorkommende und artifizielle Sequenzen verlängert wurde. Ich konnte zeigen, dass das SIINFEKL-Epitop aus zahlreichen Sequenzkontexten herausprozessiert und effizient gegenüber SIINFEKL/K^b-spezifischen B3Z T-Hybridomzellen präsentiert wurde. Die Präsentation dieser Peptid-Klasse-I-Konjugate war inhibierbar durch azidophile Amine und Inhibitoren der vakuolären Protonenpumpe, welche den pH von endosomalen Vesikeln anheben. Diese Inhibition weist auf eine Antigenprozessierung im endolysosomalen Weg hin, da sowohl die Funktion von endosomalen Hydrolasen als auch der vesikuläre Transport im endozytischen Weg pH-abhängig sind. Pepstatin A als Inhibitor der endolysosomalen Endoproteasen Cathepsin E und D war ebenfalls in der Lage, die Prozessierung von SIINFEKL-Peptiden aus SIINFEKL-K^d-Konjugaten zu blockieren. Ich konnte jedoch keine Hinweise auf eine Beteiligung der ER-Aminopeptidase ERAP1 bzw. der im trans-Golgi-Netzwerk exprimierten Endoprotease Furin bei der Prozessierung unserer membranassoziierten Modellproteine finden. N-terminale

Verlängerungen des SIINFEKL-Epitops und verschiedene C-terminal flankierende Aminosäuren wurden in der Regel effizient entfernt, wobei Prolin als flankierende Aminosäure einschränkend auf die Prozessierung wirkte. Bemerkenswerterweise verwenden nicht nur TAP-defiziente, sondern auch Zellen mit voll funktionsfähigem TAP-abhängigen Peptidbeladungskomplex den alternativen endosomalen Weg der Antigenprozessierung. Dieser neuartige Befund ergab sich durch die gleichfalls in Wildtypzellen vorhandene Blockade der Präsention unserer Fusionsproteine durch Inhibitoren der endosomalen Ansäuerung.

Darüberhinaus untersuchte ich den Mechanismus der Internalisierung der Peptid-Klasse-I-Konjugate von der Zelloberfläche. Inhibitorstudien zeigten, dass sowohl die Clathrin-abhängige wie die Clathrin-unabhängige Endozytose bei der Internalisierung der Konjugate beteiligt war. Interessanterweise spielten Sortierungssignale in der zytoplasmatischen Domäne von Klasse-I-Molekülen keine Rolle für das Erreichen von prozessierungsaktiven Kompartimenten, da diese Domäne ohne Verlust der Antigenpräsentation deletiert werden konnten. Die Rezyklierung von peptidbeladenen K^b-Molekülen aus Endosomen zur Zelloberfläche zeigte sich ebenfalls unbeeinflusst durch Signale in der zytoplasmatischen Domäne. SIINFEKL-beladene K^b-Moleküle konnten durch konfokale Immunfluoreszenzmikroskopie in frühen und späten Endosomen nachgewiesen werden.

Diese Arbeit belegt die funktionelle Relevanz eines bislang noch wenig untersuchten, alternativen Antigenpräsentationswegs, der nach Internalisierung und endosomaler Prozessierung von internalisierten, endogen synthetisierten Transmembranproteinen zur Präsentation von Antigenpeptiden auf rezyklierenden MHC-Klasse-I-Molekülen führt.

1. Introduction

1.1 The immune system

1.1.1 Function

Our body is under a continuous exposure to various microorganisms such as bacteria, virus, fungi, and plants as well as other animals. The immune system of our body has the ability to distinguish between self and non-self and generates highly specific and often very protective responses against potentially pathogenic microorganisms that inhabit our environment.

1.1.2 Overview

The immune system can be classified into two subdivisions, the innate immune system and the adaptive immune system. The **innate immune system** establishes a first line of defense, which consists of anatomical barriers such as skin and mucosa, physiological barriers such as lysozyme, interferons and complement, macrophages and natural killer cells.

The **adaptive immune response** is characterized by four main features: specificity, diversity, memory and the recognition of self, altered self and non-self. The cells of the adaptive immune system, which contain all these essential features of defense, are called lymphocytes. The B-lymphocytes constitute the main effectors of the humoral immune response, whereas T-lymphocytes represent the main effectors of the cellular defense system.

1.1.3 Function of MHC molecules

It is important for our immune system to stringently recognize healthy versus abnormal conditions. Cells of the adaptive immune system, mainly T cells, survey the body cells for such abnormalities. First, is it a host (self) cell or foreign (non-self) cell? Second, the T cells control whether a host cell is healthy or infected by a pathogen. Even malignant transformation of cells lead to characteristic changes in the host cells (altered self).

All the features of self, non-self, foreign and altered self can be distinguished with the help of molecules encoded by the major histocompatibility complex (MHC). These molecules are specialized peptide receptors and serve to display antigenic peptides at

the cell surface for recognition by T lymphocytes. So to say, they serve as a passport for host cells. On the basis of their structure and their modes of antigen presentation, they can be further divided into two main subclasses, MHC I and MHC II.

Most nucleated cells carry MHC I molecules, while MHC II molecules are mainly found on the surface of professional antigen presenting cells (pAPC) such as dendritic cells (DC), B cells, macrophages and thymic epithelial cells.

1.1.4 The Major Histocompatibility Complex (MHC) Genes

The major histocompatibility complex (MHC) is a large genomic region or gene family which is found in most vertebrates and contains many genes with important immune functions. Sequencing of the MHC was preceded by a large series of mapping studies, which established the basic organization of both the human and mouse MHC. In the mouse it is located on chromosome 17 and in humans it is located on the short arm of chromosome 6. The role of the MHC was first identified for its effect on tumor rejection in mice by Snell and Gorer (Gorer *et al*., 1948) and later by skin transplantation studies by Medawar (Billingham *et al*., 1953).

The genomic regions where the MHC class I and II molecules are encoded are called class I and class II regions. The class III region is defined simply as the segment between the class II and I regions. MHC molecules are absent in nonvertebrates, whereas jawed vertebrates already have MHC class I/II, T cell receptor and immunoglobulin genes (Klein and Sato, 1998; Kulski *et al*., 2002). There are three class I loci in humans, called HLA-A, B and C; in mice H-2K, H-2D, and H-2L. The class I genes are extremely polymorphic. All MHC locus products are codominantly expressed, so that an individual may express up to six different MHC class I molecules.

The MHC has a three features; first, its strong effect on graft survival, second, its genetic complexity, and third , the extraordinary polymorphism of its loci.

1.1.5 Structure of MHC molecules

The MHC class I molecule is heterodimeric protein containing of a membrane-spanning, heavy α chain (~45 kDa) which is non-covalently linked to the non-MHC encoded molecule, light chain β microglobulin (β_2m) (~12 kDa), which does not span the membrane. The heavy chain is a type I glycoprotein with extra-cytoplasmic domains

called α_1, α_2 and α_3 connecting to the C-terminal cytoplasmic tail via a transmembrane domain. The extracellular portion of MHC I molecules contains one to three N-linked glycosylation sites (see section 1.3.2). MHC class II molecules consist of two types I membrane–spanning polypeptide chains (α and β chain). In case of MHC class I, the peptide-binding groove is made up of the α_1 and α_2 domains of the α chain (figure 1.1) while in case of MHC class II both the α and β chain contribute to the peptide binding groove. One of the main differences between these two molecules, beside their different cellular distribution and mechanisms of peptide loading, is the structure of the peptide binding groove. In both cases, the peptide binding groove is made of a "floor" of β sheet structures (Saper *et al*., 1991) and two lining walls of α-helices. However, the peptide binding groove is open at both sides in MHC class II and due to that they can hold peptides up to 15-25 amino acids. It is closed in MHC I molecules and as a result, MHC class I can accommodate peptides of only 8-11 amino acids in length. In any case, the antigenic peptide interacts with the surface of the peptide binding groove only over few amino acids. Non-covalent (hydrophobic) interactions, electrostatic forces (hydrogen bonds) and salt bridges stabilize the peptide in the MHC binding groove (Madden, 1995). This is accomplished by means of particular amino acids of the peptide, termed anchor residues (Fremont *et al*., 1995), that fit snugly into complementary pockets in the core of peptide binding groove (Deres *et al*., 1993; Guo *et al*., 1992; Jaulin *et al*., 1992).

In MHC class I molecules, the peptide binding groove is subdivided into 6 pockets, named A, B, C, D, E, and F. The A and F pockets interact with the amino and carboxyl groups of the peptide. The F pocket harbors the C-terminal anchor residue while the position of the N-terminal anchor residue varies.

The MHC class I gene contains 8 exons. The first and second exons encode the signal sequence as well as the α1 domain, which is about 90 amino acids in length, the third exon encodes the second domain (α_2), the fourth exon encodes for the third membrane proximal immunoglobulin like domain (α_3), and the transmembrane domain is encoded by the fifth exon. The remaining small three exons that can be alternatively spliced containing a potential phosphorylation site, and they might play a role in the recycling of the molecules between endosomes and the cell surface (Zuniga *et al*., 1999).

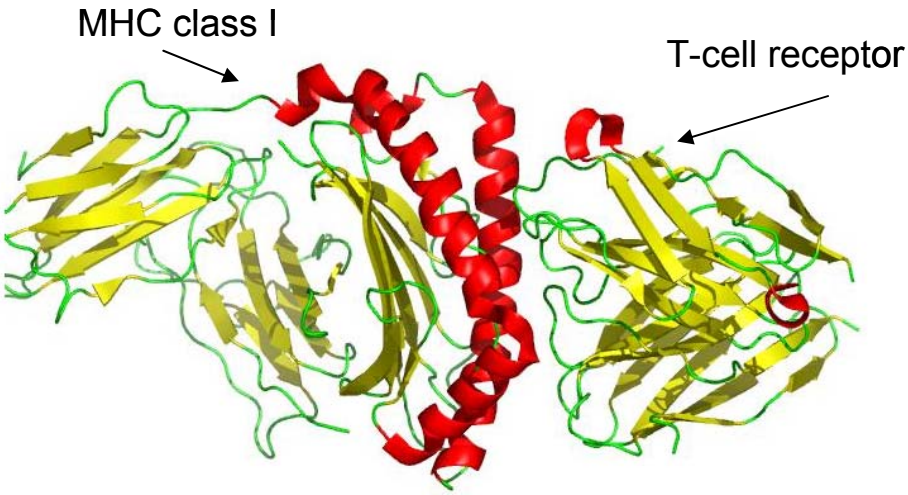

Figure 1.1a Crystal structure of a peptide occupied MHC class I (H-2K^b) complex and T- cell receptor.

The image was generated through the PyMOL software via accession number 1NAM

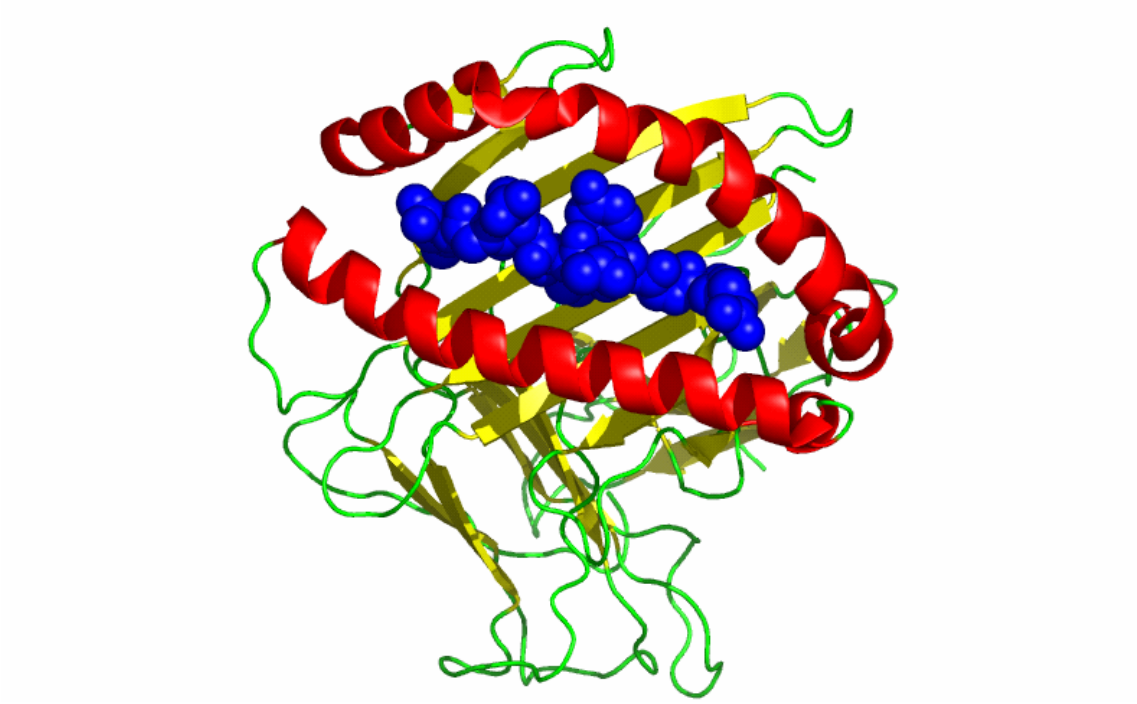

Figure 1.1b Crystal structure of a peptide occupied MHC class I (H-2K^b) complex.

The mouse MHC class I heavy chain is shown as peptide occupied form. Peptide is shown in blue color. Heavy chain β sheet is colored yellow and α helix is colored red. The image was generated through the PyMOL software via accession number 1NAM.

MHC class I molecules are very polymorphic with the polymorphic residues clustering around the peptide binding groove. Different MHC alleles therefore vary in the chemical characteristics of their pockets and require different peptide binding motifs (Rammensee *et al*., 1995). Most MHC I binding motifs require hydrophobic amino acid such as A, I, L, M, F and V at the C-terminal end of the peptide while other prefer aromatic or basic residues.

1.2 Antigen presentation

1.2.1 Outline of the conventional MHC class I pathway

The class I pathway of antigen processing leads to the loading of MHC class I molecules by peptides mostly derived from cytosolic proteins (Momburg *et al*., 1994c; Niedermann *et al*., 1995; Shastri *et al*., 2002). The first step in this pathway is the generation of peptide fragments in the cytoplasm, which is mainly done by barrel-shaped, multicatalytic protease complexes, known as the proteasomes (Brown et al., 1991; Niedermann et al., 1996; Peters, 1994). The proteasomes chops up proteins into small peptides (8-15 amino acids in length), some of which will make their way to the transporter associated with antigen processing (TAP) (Momburg *et al*., 1994c) in the ER membrane while others are destroyed by cytosolic peptidases (Reits *et al*., 2003). TAP preferentially translocates peptides of 8-16 a.a. with hydrophobic or basic C-termini into the ER (Momburg *et al*., 1994a; Momburg *et al*., 1994b; Van Endert *et al*., 1995). After that, these peptides are either further cleaved by ER resident aminopeptidase(s) (Serwold *et al*., 2002) or directly loaded onto available MHC class I molecules and exported to the cell surface if they are optimal in length.

The MHC class I heavy chain and β_2–microglobulin are synthesized separately on the rough ER and are co-translationally transported into the ER. During translocation into the ER, signal sequences are cleaved by the ER-resident signal sequence peptidase. MHC class I heavy chains first interact with BiP and the lectin-like chaperone calnexin followed by assembly with β_2m (for more details see section 1.3.2).

It was reported that the oxidoreductase ER60 also associates with class I heavy chains during early stage of maturation (see section 1.3.4). As soon as heavy chains get associated with β_2m, calreticulin either replaces calnexin (human cells) or additionally associates with heavy chain (mouse cells). At this step, class I heavy chain/β_2-

microglobulins associate with TAP and tapasin in the TAP-associated complex and they acquire the peptide ligand. Peptide occupancy leads to conformational changes in MHC class I and properly folded MHC class I molecules leave the ER via the Golgi complex to the cell surface. In the *trans*-Golgi, carbohydrates are modified into the complex type and sialic acids are added, converting them into mature MHC I molecules.

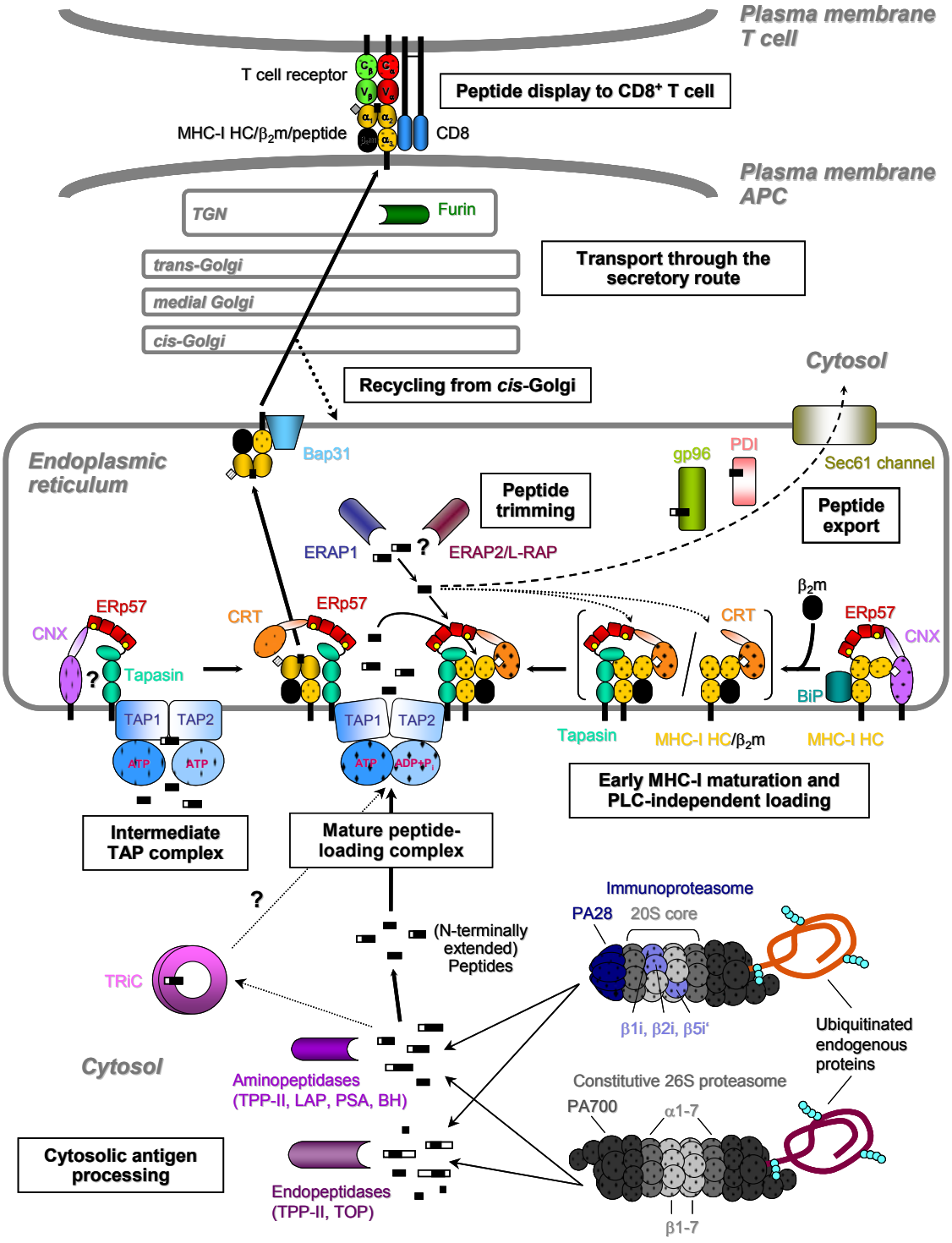

Figure 1.2.1 Outline of the conventional MHC class I antigen presentation pathway

1.3 The components of the peptide loading complex

1.3.1 Transporter associated with antigen presentation (TAP)

TAP is a member of the ATP binding cassette (ABC) transporter family whose members translocate molecules across the membranes utilizing energy from ATP hydrolysis. ABC transporters have a modular structure comprising two nucleotide-binding domains (NBD) and two polytypic membrane domains. Functional TAP is composed of two subunits known as TAP1 and TAP2 whose genes are encoded in the MHC II region. The two subunits TAP1 and TAP2 combine noncovalently to form a heterodimer and each has an N-terminal membrane domain and a C-terminal cytoplasmic nucleotide-binding domain **(Figure 1.3.1)**. The NBD has a highly conserved sequence motif (Walker A and B) that allows ATP binding and subsequently their hydrolysis. Peptide transport requires ATP (Neefjes *et al*., 1993) while binding of the peptide to TAP is independent of ATP. TAP is localized in the ER and *cis*-Golgi.

The first indication that MHC class I molecules require a transfer of peptides from the cytosol to the ER came from mutant cell lines, whose surface expression of MHC I was severely impaired (Townsend *et al*., 1989). Peptides directed into the ER by a signal sequence could rescue the defective presentation in a TAP-deficient mutant cell line (Anderson *et al*., 1991). Transfection of TAP1 and TAP2 cDNAs restored MHC class I cell surface expression (Spies *et al*., 1990; Trowsdale *et al*., 1990).

The major role of TAP is to transport peptide from the cytosol to the endoplasmic reticulum, where they bind to empty MHC class I. TAP most efficiently binds and transport peptides with a length of 8-16 amino acids (Momburg *et al*., 1994c; Uebel *et al*., 1995). However, TAP can even transport peptides up to length of 40 amino acids (Gromme and Neefjes, 2002; Koopmann *et al*., 1996; Uebel *et al*., 1995). Murine TAP selectively transport peptides with hydrophobic C-terminal residue whereas human TAP prefers both hydrophobic as well as basic C-terminal residue peptide (Momburg *et al*., 1994b). Upon treatment with cytokines like IFN-γ and TNF-α, TAP subunits get upregulated causing an increased peptide supply to the ER. These cytokines also increase MHC class I expression. In case of IL-10, TAP expression gets downregulated at the transcriptional level, resulting in reduced MHC class I cell surface expression

(Lautscham *et al*., 2003; Petersson *et al*., 1998; Salazar-Onfray *et al*., 1997; Zeidler *et al*., 1997).

Using a chemical cross linker approach, Lacaille and Androlewicz (Lacaille and Androlewicz, 1998) found that subtle conformational changes occur in the TAP heterodimer upon the binding of peptides. The viral inhibitor ICP47 also has a deleterious effect on the heterodimer structure of the TAP, in addition to its role in blocking the peptide transport from the cytoplasmic side. Moreover, TAP association influenced the conformation of MHC class I molecules in the ER (Owen and Pease, 1999). TAP may also serve as relay to transmit a signal for dissociation of peptide-loaded MHC I. Reits and colleagues have shown that the lateral mobility of TAP is strongly influenced by the peptide transport activity (Reits *et al*., 2000). The mobility increases when TAP is inactive and in the presence of transportable peptide and ATP it decreases, reflecting a different conformation of the heterodimer. TAP requires the ER chaperone tapasin for stabilization of its structure (Garbi *et al*., 2003).

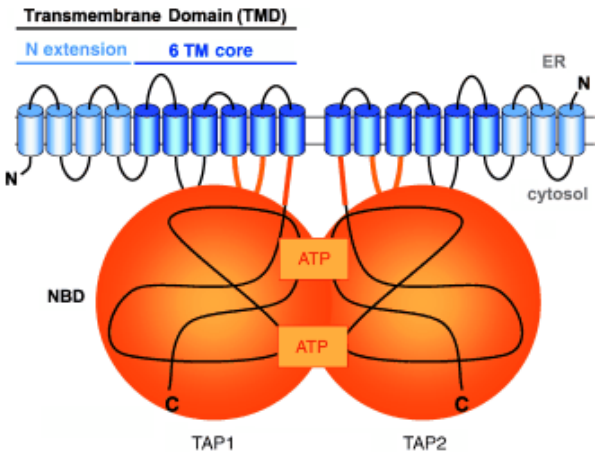

Figure1.3.1 Structural organization of the TAP complex.
Putative TMs of the N-terminal extensions are shown in light blue, while the six canonical TMs proposed to form the translocation pore (TM1-6) are shown in blue. The peptide-binding region is indicated in orange

(Adopted from Beismann-Driemeyer and Tampe, 2004)

1.3.2 Calreticulin and calnexin

Calreticulin and calnexin are Ca^{2+} binding lectin-like chaperones that assist in the folding of newly synthesized glycoproteins in the ER.

Calreticulin was first isolated by Ostwald and MacLennan in 1974. It is a 46-kDa soluble protein located in the lumen of the ER. It has N-terminal signal sequence and at the C-terminal end carries a KDEL ER-retrieval signal. It has three structural and functional domains: N, P and C.

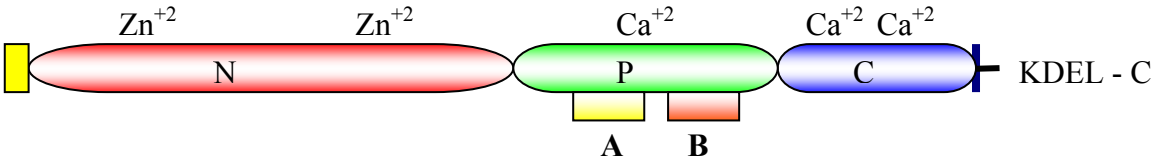

The N and P terminal domains are responsible for its chaperone activity (protein folding) whereas the C-terminal acidic region plays a crucial role in Ca^{+2} homeostasis within the ER.

Efforts to make a knockout mouse for this protein were unfruitful because the homozygous calreticulin knockout is embryonically lethal due to defects in heart development and function (Mesaeli *et al*., 1999). In a calreticulin-deficient embryonic cell line, protein folding was compromised, resulting in the accumulation of mis-folded protein and activation of the unfolded protein response (UPR) (Molinari *et al*., 2004).

Calnexin was characterized as a glycoprotein-specific ER-resident chaperone (David *et al*., 1993; Hochstenbach *et al*., 1992). It is a membrane bound protein of 88 kDa (Galvin *et al*., 1992). It interacts early with nascent MHC I heavy chain and also independently with TAP (Diedrich *et al*., 2001; Jackson *et al*., 1994). Calnexin has an important role in the glycoprotein folding and it works with calreticulin in a co-operative manner during the ER quality control (see figure 1.2).

During the ER translocation, a core unit of N-linked glycans (Glc_3-Man_9-$GlcNAc_2$) is added to the asparagine side chain in Asn-X-Ser/Thr consensus sequences (Kornfeld and Kornfeld, 1985). Sequential action of glucosidase I, an integral membrane protein, and the soluble luminal glucosidase II remove the two terminal glucose residues from the N-linked glycoprotein, resulting in a Glc_1-Man_9-$GlcNAc_2$-carbohydrate. At this stage calnexin or calreticulin recognizes specifically this single terminal glucose (Zapun

et al., 1997). Binding by calnexin or calreticulin retains the unfolded glycoprotein in the ER and assists disulfide isomerases (e.g., PDI or ERp57) to facilitate folding of the protein into correct arrangement. As soon as glycoproteins are correctly folded, they are no more reglycoslyated and thus ready for export from the ER.

Murine class I histocompatibility molecules synthesized in the absence of calnexin assemble inefficiently due to heavy chain misfolding and aggregation (Vassilakos *et al*., 1996). In human cells calnexin can promote disulfide bond formation in class I heavy chains but does not directly facilitate subsequent binding of β_2m (Tector and Salter, 1995). Binding of human MHC class I molecules to either calnexin or calreticulin appears to be dictated by the assembly state of these molecules. Calnexin binds exclusively to the free heavy chain subunits, whereas calreticulin appears to bind only after following assembly of the heavy chain with β_2-microglobulin (Sadasivan et al., 1996; Van et al., 1996). Murine class I molecules differ in that calnexin appears to be the main chaperone associated with both free and β_2-microglobulin-associated heavy chains (Degen and Williams, 1991; Suh *et al*., 1996). Human MHC I heavy chain contains one glycosylation site (Asn 86) (Orr *et al*., 1979) while mouse heavy chains have two glycosylation binding sites in α1 and α2 domains (Asn 86 and Asn 176) (Evans *et al*., 1982; Harris *et al*., 1998; Maloy and Coligan, 1982) and sometimes, a third glycan (Asn227) in the α3 domain. Removal of the L^d α1 domain glycosylation site by site-directed mutagenesis (L^dN86K) prevents association of calreticulin and TAP with the class I molecule. However, mutation of the glycosylation site in the α2 domain (L^dN176Q) has no effect on calreticulin or TAP binding. Calnexin still binds strongly to both mutants (Harris *et al*., 1998).

1.3.4 ERp 57/ER60

In 1998, three labs including our group (Hughes and Cresswell, 1998; Lindquist *et al*., 1998; Morrice and Powis, 1998), simultaneously discovered that ER60/ERp57 is a member of the TAP-associated peptide loading complex.

ERp57 is a thiol-dependent oxido-reductase, which belongs to the protein disulfide isomerase (PDI) family and contains 2 thioredoxin motifs. It mediates disulfide bond rearrangement in nascent monoglucosylated glycoproteins to which it is recruited by either calreticulin or calnexin (Cnx). It was reported that ERp57 interacts with

incompletely oxidized, free class I heavy chain in the early Cnx-associated stage which is sensitive to the glucosidase inhibitor castanospermine (Lindquist *et al*., 1998). In Cnx-deficient human CEM-NKR cells class I heavy chain (HC) assemble, however, with ERp72 instead to ERp57 (Lindquist *et al*., 2001). ERp57 has also been found in the peptide loading complex of a Crt deficient cell line (Gao *et al* 2002). *In vitro*, ERp57 enhanced oxidative refolding of RNase B, the glycosylated variant of RNase A, in where it is critically dependent on its interaction with calnexin and calreticulin (Zapun *et al*., 1998)

There are reports that ERp57 can also act as ER protease (Urade *et al*., 1993), because it contains CGHC motifs characteristic of cysteine proteases (Okudo *et al*., 2000). However, evidence for ERp57 as protease has been rather indirect and inconsistent.

The specific function of ERp57 within the peptide-loading complex, however, remains elusive and deletion of the ERp57 gene in mice is embryonically lethal (Garbi *et al*., unpublished observation). Only an approximately two-fold downregulation of surface MHC class I molecules was observed in siRNA-directed ERp57-silenced cell lines (Tiwari *et al*., unpublished observation).

1.3.5 Tapasin (Tpn)

Tapasin is a 48 kDa type I glycoprotein located in the ER. Tpn is broadly expressed and high mRNA levels were detected in T cells, bone marrow, thymus, intestine, lung, and kidney. Tapasin expression is frequently downregulated in carcinoma and melanoma lines, but could be rescued by IFN-γ treatment, or a combination of IFN-β and TNF-α (Ritz *et al*., 2001; Seliger *et al*., 2001).

It was discovered by Cresswell and coworkers that this protein is also a part of peptide loading complex and is associated with the TAP1 subunit (Ortmann *et al*., 1994). Later they also found that tapasin interacts with MHC I heavy chain which is associated with β_2m (Sadasivan *et al*., 1996). Expression of tapasin in a Tpn$^-$ mutant human cell line (LCL .220) restored class I-TAP association and normal class I cell surface expression (Ortmann *et al*., 1997), revealing that it is a connecting bridge between TAP subunits and MHC I. Up to four MHC class I-tapasin complexes were found to bind to each TAP molecule.

Tapasin is a member of the immunoglobulin superfamily with a putative cytoplasmic ER KKXX retention signal (Grandea *et al*., 1998). Tpn contains a highly conserved pair of cysteines in the N-terminal domain (Cys-7 and Cys-71 in human Tpn) that presumably form a intramolecular disulfide bridge (Dick *et al*., 2002).

MHC class I molecules that fail to interact correctly with the peptide loading complex (PLC) often exit the ER prematurely in a peptide-receptive state (Lewis and Elliott, 1998; Williams *et al*., 2002). Thus, a two-steps model for MHC class I peptide binding has been proposed. Initially, MHC class I molecules may bind low-affinity, suboptimal peptides. Within the PLC, the suboptimal peptides are replaced with high-affinity optimal peptides, which stabilize the MHC class I–β2m heterodimer. Peptide binding and exchange within the PLC is probably mediated by the luminal domain of tapasin. Tapasin may also play a crucial role in reshaping of the peptide repertoire (Howarth et al., 2004; Lybarger et al., 2001; Morrice and Powis, 1998; Purcell et al., 2001).

The analysis of Tpn knockout mice further substantiated the crucial role of tapasin in the class I antigen presentation pathway (Garbi *et al*., 2000; Grandea *et al*., 2000). In our lab, Garbi *et al.* discovered that in Tpn deficient mice the repertoire of class I-bound peptides is altered towards less stably binding ones and the MHC class I cell surface expression is also impaired. During my thesis I have explored the role of tapasin in a different approach. I have looked whether peptide trimming is altered in absence of tapasin or not.

1.4 (a) The proteasomes

Proteasomes are the key proteases for non-lysosomal proteolysis in eukaryotic cells. Recent evidences suggest that approximately one third of newly synthesized proteins are degraded by proteasomes within minutes of their synthesis (Schubert *et al*., 2000; Yewdell *et al*., 2001). Proteasomes are the major source for MHC class I antigenic peptide. They are abundant in the cytosol and in the nucleus (Reits *et al*., 1997) and account for upto 1% of cellular protein. Most of the proteins, in order to be recognized and further degraded by proteasomes, have to be tagged by ubiquitin, a small 5 kDa protein (figure 1.4 a). Covalent attachment of multi-ubiquitin chains to lysine residues of the misfolded protein or short-lived protein targets them to proteasomes.

The **26S** proteasome (named after its sedimentation coefficient) is a 2,000 kDa multisubunit cylindrical complex comprised of a barrel-shaped **20S** core catalytic component (the **20S** proteasome) capped at one or both ends by a **19S** regulatory component (**19S cap, PA700**) (Adams, 2003). The base of each regulator subunit is composed of 6 ATPases of the AAA family, which allows entry of the protein in an ATP-dependent manner. The **19S** regulatory component recognizes and binds the polyubiquitinated protein and cleaves the ubiquitin chain from the protein substrate. The protein is then unfolded, fed into the 20S core, and the ubiquitin molecules are recycled back to the cytosol. The 20S core is composed of 4-stacked rings: 2 outer rings (α rings) and 2 inner rings, termed as β rings, in which the proteolysis occurs. Each β ring consists of 7 subunits containing 3 active enzymatic sites termed trypsin-like β2 (which cleaves after basic residues Arg and Lys), chymotrypsin-like β5 (which prefer hydrophobic residues both branched chain and aromatic) and post-glutamyl peptide hydrolase-like β1 (caspase-like), after enzymes that show similar activity or specificity (Adams, 2003; Almond and Cohen, 2002). Within the 20S core, proteins are degraded to oligopeptides of 3 to 25 amino acids and released to the cytosol.

The expression of 3 proteasome β-subunits is induced by interferon-γ. After interferon treatment additional subunits termed LMP2, LMP7 and MECL1 are expressed. They are incorporated into the β-rings of the 20S core particles in place of the constitutively expressed β1, β2 and β5 subunits and thereby form immunoproteasomes. These six subunits have N-terminal threonine residues (the nucleophile of the proteasome's active sites) and only these are catalytically active. It was shown by several groups that immunoproteasomes stimulated cleavage of small fluorogenic peptides after hydrophobic, basic, and branched chain residues while suppressing cleavages after acidic residues. The new pattern of peptides that are produced by immunoproteasomes has been suggested to be more favorable for antigen presentation, because TAP and MHC I molecules prefer hydrophobic and basic C-terminal peptide residue (ref).

It has been shown that a large proportion of the substrates for ubiquitin-dependent proteasomal degradation are newly synthesized proteins, the so-called **DRiPs** (for Defective Ribosomal Products) (Yewdell *et al*., 2001). Some of the substrates, however, are degraded by the proteasomes in a ubiquitin-independent manner for, example, ornithine decarboxylase, p21/Cip1, TCRα, IκBα, c-Jun, calmodulin and thymidylate

synthase (Hoyt and Coffino, 2004). This might reflect a more ancient mode of recognition by proteasomes governed by sequence signals (Verma and Deshaies, 2000), but still it can be assume that the main part of eukaryotic protein turnover is by ubiquitin dependent.

The importance of ubiquitin-dependent protein degradation in MHC I antigen presentation was suggested by the fact that enhanced protein degradation rescued the defective presentation of viral epitopes in vaccinia-infected cells (Townsend *et al*., 1988).

The fundamental role of proteasomes for the supply of MHC class I ligands were confirmed by the use of proteasomal inhibitors**.** In living cells, peptide aldehyde-like inhibitors, such as MG-132, and a specific streptomyces compound, lactacystin-β-lactone completely blocked the presentation of peptide from several proteins including ovalbumin, influenza virus nucleoprotein and β−galactosidase (Anton *et al*., 1998; Cerundolo *et al*., 1997; Grant *et al*., 1995; Rock *et al*., 1994).

There were speculations of how peptides can survive in the cytosol after proteasomal generation in the presence of abundant peptidase, before they are imported *via* TAP into the ER. Some groups claimed that proteasomes are closely connected with the endoplasmic reticulum (Brooks *et al*., 2000; Enenkel *et al*., 1998; Newman *et al*., 1996), however, other investigators have failed to demonstrate an association of TAP and proteasomes.

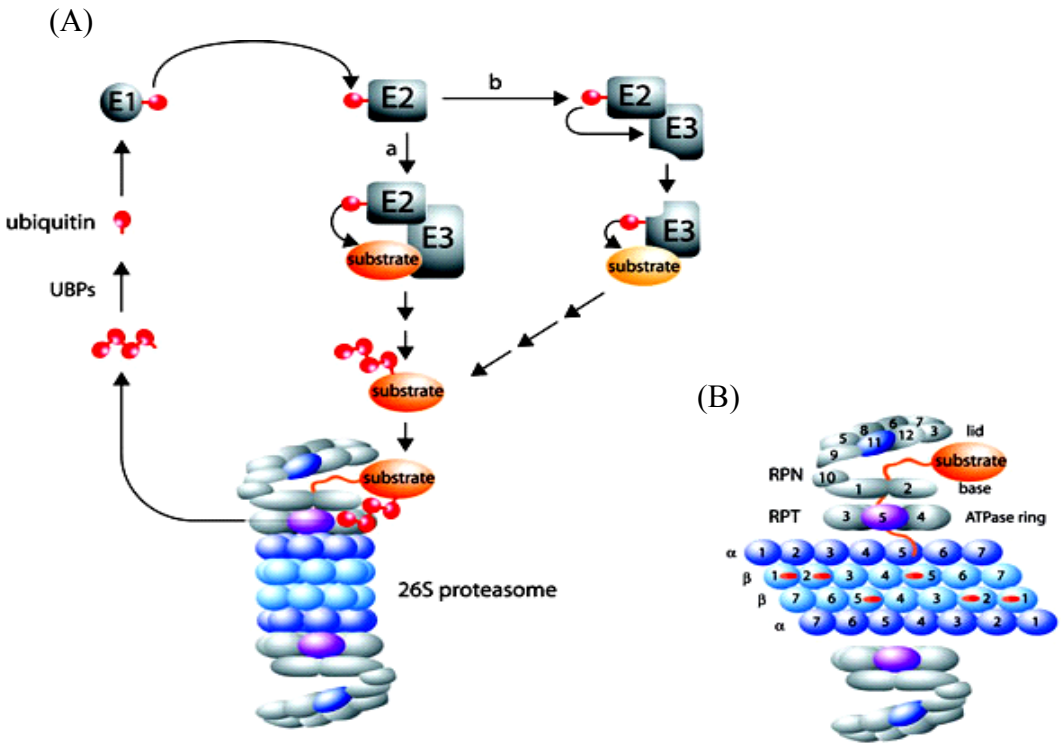

Figure 1.4 (a) The ubiquitin–proteasome pathway (schematic).

(A) Attachment of ubiquitin (Ub) to the target protein requires three major enzymatic steps. Ubiquitin-activating enzyme (E1) activates ubiquitin by forming a thiol esther linkage leading to an E1-ubiquitin bond. This reaction requires energy provided by ATP and forms an activated ubiquitin moiety that is transferred and bound by an additional thiol ester linkage to ubiquitin-conjugating enzyme (E2), which serves as a carrier protein. Ubiquitin–protein ligase (E3) catalyzes the covalent attachment of ubiquitin to the target protein by the formation of isopeptide bonds. Multiple cycles of ubiquitination finally result in the synthesis and the attachment of polyubiquitin chains to the target protein. (B) The 26S proteasome consists of the 20S cylindric catalytic core complex and two 19S cap regulatory complexes. The polyubiquitinated target protein enters the 19S regulatory complex, is recognized, deubiquitinated, unfolded and translocated into the central cavity of the 20S catalytic core complex, where it is degraded by different hydrolytic activities. Ubiquitin is recycled by the ubiquitin carboxy terminal hydrolase (UCH). Peptides as a product of degradation are released by diffusion.

(Adopted from Kostova *et al.*, (2003) *The EMBO Journal* **22,** 2309–2231)

1.4 (b) Cytosolic peptidase

Although proteasomes play a major role in the generation of MHC class I antigenic peptides, other cytosolic peptidases can contribute to the generation of antigenic peptides. The cytosolic proteolytic pathway rapidly converts intracellular proteins to

free amino acid without the buildup of polypeptide or small peptide intermediates (Rock *et al*., 2004). Cytosolic peptidases are mostly metallopeptidases that can be blocked by o-phenanthroline. Thimet oligopeptidase (TOP) has been shown to cleave peptides of 6-17 amino acid residues and upon overexpression it destroys antigenic peptides (Saric *et al*., 2001). Using the RNAi approach it was shown that downregulation of TOP can improve the presentation of antigenic peptides (York *et al*., 2003). Leucine aminopeptidase was reported to trim the N-terminally extended antigenic peptides. This enzyme is inducible by INF-γ treatment (Beninga *et al*., 1998).

TPPII is a ubiquitous serine protease that exists as a cytosolic and membrane bound form. It cleaves aminoterminal tripeptides in a chymotrypsin-like manner (Kloetzel, 2004).

1.5 Endoplasmic Reticulum Associated Peptidase/s

The TAP associated peptide loading complexes comprise MHC class I heavy chain/β_2-microglobulin and at least three known chaperones: tapasin, ERp57 and calreticulin.

It was suggested that MHC I molecules themselves play an instructive role in the ER-associated N-terminal trimming of peptides (Paz *et al*., 1999; Shastri *et al*., 2002). At least four distinct modes of class I implication can be taken into consideration:

1. One component of the loading complex (ER60) may possess a proteolytic activity (Okudo *et al*., 2000).

2. Loading complexes are stabilized by cooperative interaction between individual proteins. Peptidase activity of a complex component other then MHC class I may depend upon class I-mediated stabilization of the loading complex.

3. A distinct peptidase may act only on precursor peptides correctly positioned for a cleavage in the binding site of a class I molecule (Brouwenstijn *et al*., 2001).

4. A peptidase may act on free N-terminal peptide which were imported by TAP but not attached to the MHC class I binding groove (Fruci *et al*., 2001).

Studies have shown that many peptides, which are generated by proteasomes or immunoproteasome and translocated by TAP into the ER, carry N-terminal extensions

(Lauvau *et al.*, 1999; Neisig *et al.*, 1995). Peptides eluted from the cell surface have an optimal length suggesting that there must be an aminopeptidase activity**,** which further cleaves this N-terminal extension. Using ER-targeted precursor peptides, a number of groups have shown that N-terminal but not C-terminal flanking residues can be efficiently cleaved from antigenic peptides in the ER. Shastri and colleagues have used an elegant method to show that in presence of appropriate MHC class I, the N-terminally extended precursor can be efficiently trimmed in ER to produce a high level of MHC I-peptide complex on the cell surface (Paz *et al*., 1999). They defined the specificity of the ER aminopeptidase using a series of ER-targeted precursors with N-terminally extensions (Serwold *et al*., 2002). They found that except X-Proline-Xn, where X is any amino acid, all other peptides can be efficiently cleaved by a leucinethiol-sensitive aminopeptidase. Recently two groups identified the ER-associated peptide trimming aminopeptidase (Saric et al., 2002; Serwold et al., 2002). The previously known aminopeptidase is now termed ERAP-1 or ERAAP. The ER-associated aminopeptidase was upregulated by interferon treatment and the activity can be suppressed by leucinethiol.

In contrast to aminopeptidase activity, there is no evidence for carboxypeptidase activity in the ER (Eisenlohr et al., 1992; Snyder et al., 1994). The other recognized peptidase activity that has been shown to influence MHC I assembly within the ER relates to signal peptidase (SP) and signal sequence peptidase (SPP) (Martoglio and Dobberstein, 1998). SP is known to trim the signal sequence from ER translocated proteins and was initially shown to be important in providing hydrophobic peptides in a TAP-independent manner to alleles such as HLA-A2 (Hughes *et al*., 1996). Later**,** it was shown that signal sequence-derived peptides released into the cytosol are the major peptide source for the non-classical class I molecules HLA-E (Lemberg *et al*., 2001).

1.6 Protein sorting

Like many other glycoproteins synthesized in the ER, MHC class I molecules follow the route ER→cis-Golgi→trans-Golgi→ cell surface. This was concluded from studies using inhibitors, which either prevent MHC I maturation or stop the vesicular budding in the secretory pathway. MHC class I molecules**,** which do not attain a proper conformation in the ER are routed back to the cytosol probably via Sec61 channel where they get degraded by proteasomes (see section 1.4a).

1.6.1 ER to Golgi protein export/import

Vesicular transport of proteins between intracellular compartments is coordinated by the activity of coat complexes, that direct the selection of cargo through cytoplasmic signals and the budding from membranes (Lippincott-Schwartz, 1993).

Some coat complexes include clathrin, which mediates sorting of receptors containing Tyr-based motifs from the trans-Golgi network and the cell surface (Schmid, 1997). The COPI complex binds cytoplasmic carboxy-terminal di-lysine motifs (KKXX) in trans-membrane proteins and functions to direct retrograde transport of proteins from the *cis*-Golgi (Doms *et al*., 1987). The COPII complex participates in protein export from the ER (Aridor *et al*., 1995; Stephens *et al*., 2000). Tapasin**,** which also contains a di-lysine signal was shown to bind a subpopulation of MHC1 molecules and prevents anterograde transport of immature MHC class I molecules via COPI mediated retrieval (Paulsson *et al*., 2002)

A coat assembly protomer (coatomer) is a complex**,** which consist of seven subunits that appear in the cytosol en bloc. ADP-ribosylation factor (ARF), a small GTP-binding protein belonging to the *ras* superfamily, activates the binding of coatomer to Golgi-enriched membranes and subsequentially**,** the formation of coatomer-coated vesicles. ARF is known to cycle between the cytosol (GDP form) and the membrane (GTP form) under the regulation of a specific GDP-GTP exchange factor (ARF-GEF) and a GTPase activating protein (ARF-GAP) (Nie *et al*., 2003). Thus ARF is activated by ARF-GEF, and returned to its GDP form by ARF-GAP. The ARF-GEFs are all peripherally associated membrane proteins.

Brefeldin A (BFA), a fungal toxin, inhibits ARF-GEF and thus coatomer binding to the membrane and vesicle formation is inhibited (Nebenfuhr *et al*., 2002). Recently, it was shown that BFA inhibits the formation of an ARF-GEF-GBF1 complex and consequently COPI formation (Niu *et al*., 2004). GBF1 is a GEF family member protein and at steady state it is localized in early Golgi compartments of mammalian cells (Garcia-Mata *et al*., 2003; Kawamoto *et al*., 2002).

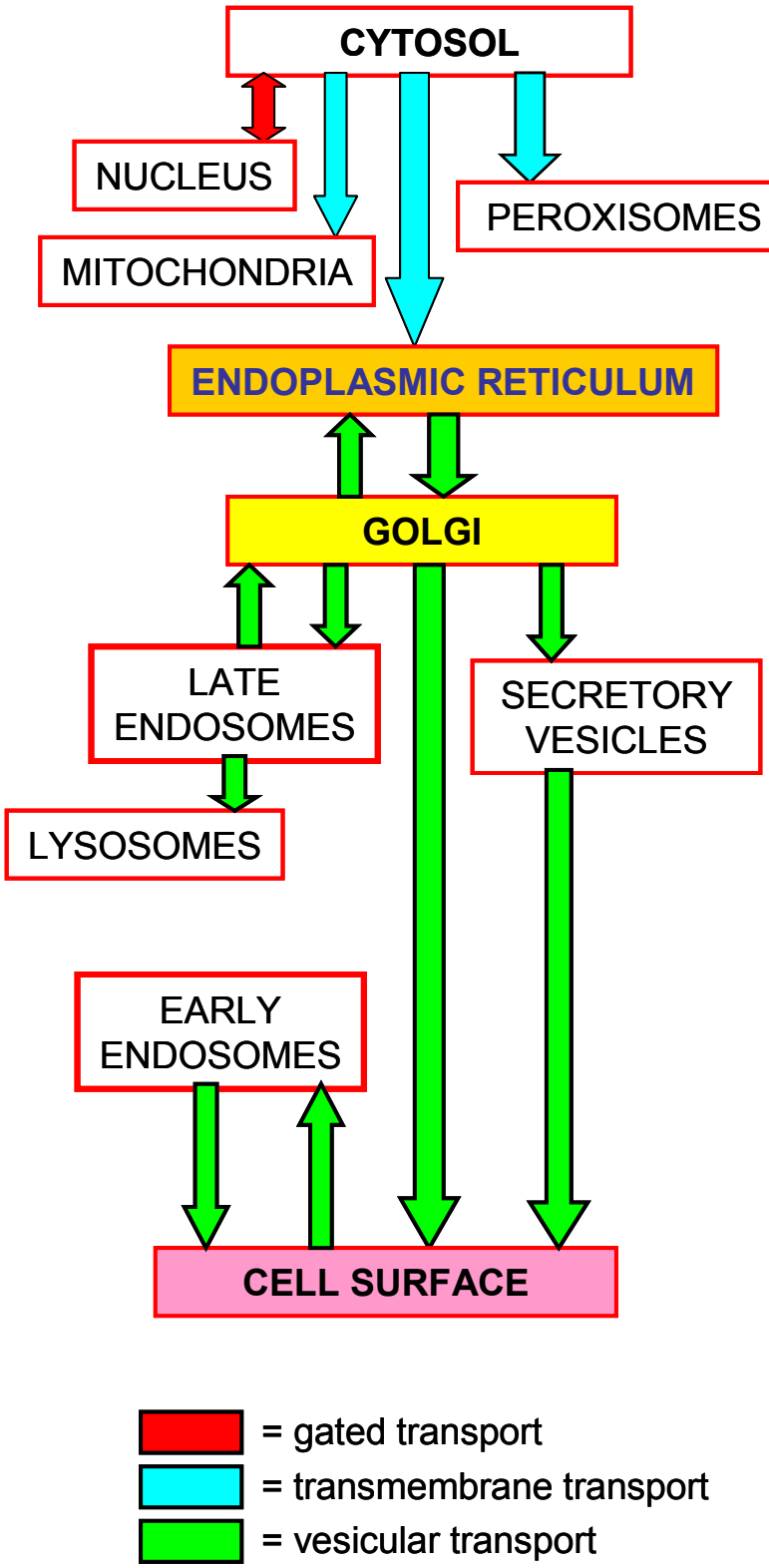

Figure 1.6 Intracellular protein trafficking/sorting pathways.

1.6.2 Vesicular transport in the Golgi apparatus

The Golgi consists of a stack of membrane-bounded ***cisternae*** located between the endoplasmic reticulum and the cell surface. It is mainly devoted to the processing/modifying of proteins synthesized in the ER. In addition to the Golgi-based modification of sugar moieties in glycoproteins, there is also report of proteolysis of peptide molecules by the subtilisin protease family member furin (Garred *et al*., 1995). Furin endopeptidase was reported to be involved in the generation of MHC class I ligands in the *trans*-Golgi network (Gil-Torregrosa *et al*., 2000; Gil-Torregrosa *et al*., 1998). The Golgi complex is also a site for the synthesis of glycolipids. From the *trans*-Golgi network, proteins either migrate to the cell surface or are targeted to endosomes.

The Golgi is divided into three functionally separated areas.

1. The *cis*-Golgi (closest to the ER) receives transport vesicles from the smooth ER.

2. The *medial* Golgi**,** which adds sugars to both lipids and polypeptides.

3. The *trans*-Golgi network (closest to the cell membrane)**,** which also performs proteolysis and sorts molecules to their final destinations.

The *trans*-Golgi network (TGN), where transport can be blocked by incubating cells at 20^0C temperature (Matlin and Simons, 1983), is responsible for the sorting and packing of unretained proteins for delivery to various cellular destinations (Keller and Simons, 1997; Traub and Kornfeld, 1997). At the TGN, lysosomal enzymes bound to mannose-6-phosphate receptors (M6PRs), as well as late endosomal/lysosomal membrane proteins and are sequestrated into clathrin-coated vesicles, for transport to the endocytic organelles (Bonifacino and Traub, 2003; Mellman, 1996). Sorting of proteins into secretory granules may be facilitated by pH- and Ca^{2+}-dependent aggregation and/or specific sorting receptors (Bonifacino and Traub, 2003)

1.6.3 Endocytic pathway

Observation of the flow material along the endocytic pathway has lead to the basic description of the architecture of the pathway. Various activities in eukaryotic cells, such as antigen presentation, the transmission of neuronal and proliferative signals, the uptake of essential nutrients, and the maintenance of cell polarity, are based on

endocytosis. Endocytosis can be divided into clathrin-dependent and clathrin-independent processes. Clathrin-dependent endocytosis is well characterized and involves the selective uptake of plasma membrane proteins containing cytoplasmic sorting sequences. The main building blocks of the clathrin coats are clathrin and the adaptor protein AP-2. Coat assembly starts with the oligomerization of AP-2 and the subsequent recruitment of clathrin. As the coat expands, the curvature of the membrane becomes more pronounced until it undergoes fission. The newly formed vesicle rapidly sheds its coat.

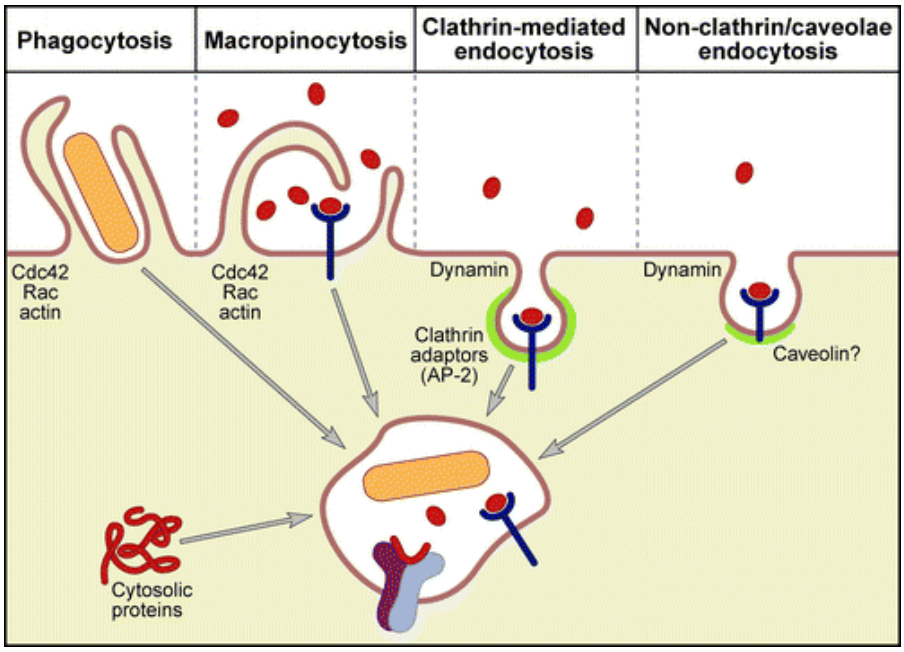

Figure:1.6.3 Types of endocytosis used for antigen accumulation.

APCs internalize exogenous antigens using, to variable extents, the same mechanisms of endocytosis found in other cell types and organisms. Phagocytosis involves the ingestion of large particles or cells >1 m in diameter. Particle binding to specific receptors signals actin assembly and drives pseudopod extension and particle engulfment. It has recently been proposed that the ER fuses with the cell surface to supply the extra membrane for this event, although this suggestion still awaits direct support. Macropinocytosis is constitutive in MØ and immature DCs, but it can also be triggered by growth factors or certain pathogenic bacteria (e.g., Salmonella). Macropinocytosis is also actin-dependent and can account for the uptake of large quantities of extracellular fluid and fluid-dissolved antigens. Soluble receptor-ligand complexes are typically internalized by clathrin-coated vesicles or (to a lesser extent) by caveolin-containing invaginations designated "caveolae." Proteins internalized by any of these mechanisms eventually reach endosomal/lysosomal compartments. Endogenous proteins in the cytosol or other organelles can also be imported into lysosomes by autophagy.

(Adopted from Trombetta and Mellman, 2005)

Clathrin-independent mechanisms encompass pinocytosis, macropinocytosis, and phagocytosis. Despite the growing list of ligands and receptors that utilize clathrin-independent uptake pathways, we still know little about the molecular mechanisms that underlie uptake by these pathways, or exactly where these pathways lead inside the cell (Nichols and Lippincott-Schwartz, 2001). MHC class I molecules have been reported to undergo endocytosis *via* clathrin-independent mechanisms (Naslavsky *et al*., 2004; Nichols and Lippincott-Schwartz, 2001; Pelkmans *et al*., 2001). The pathway is regulated by the small GTP-binding protein ADP-ribosylation factor 6 (Arf6) (Brown *et al*., 2001; Radhakrishna and Donaldson, 1997).

Similar to the secretory pathway, the endocytic pathway consists of physically and functionally distinct compartments (Table 1).

TABLE 1: Characteristics of organelles on the endocytic pathway

	Morphology	pH	Characteristic proteins
Early endosomes/Sorting endosomes	tubulo-vesicular, cisternal (internal membranes)	6.0-6.5	rab4, rab5, transferrin receptor
Recycling endosomes	tubular	6.0-6.5	rab11, transferrin receptor
Endocytic carrier vesicles	spherical with internal membranes	< 6.0	
Late endosomes	complex structure with internal membranes	5.5 -6.0	rab7, rab9, lgp120, M6PRs, LAMPs
Lysosomes	variable: tubular or similar to late endosomes	5.0-5.5	LAMPs

Uncoated endocytic vesicles (Greener *et al*., 2000) fuse with early endosomes, a network of tubules and vesicles distributed around the cytoplasm. The fusion is regulated by rab5 GTPase (Bucci *et al*., 1992; Gorvel *et al*., 1991). The ability of early endosomes to host multiple sorting events is crucial for cells. The majority (>95 %) of internalized lipid is recycled from early (sorting) endosomes back to the plasma membrane. Some endocytosed receptors, such as low-density lipoprotein (LDL) and transferrin receptors, are efficiently recycled from the sorting endosomes along with the bulk membrane lipids. The process is well coordinated, e.g. transferrin receptor recycling is regulated by ARF4L (Katayama *et al*., 2004), which is a member of ARF family proteins.

The slightly acidic pH of the sorting endosomes allows dissociation of ligands destined to lysosomes, e.g. LDL, from their recycling receptors (Mukherjee *et al*., 1997). Apparently, recycled receptors are segregated from the soluble contents into the narrow tubular extensions of sorting endosomes (Dunn and Maxfield, 1992; Hubbard *et al*., 1989). These tubular extensions will then give rise to tubular/vesicular carriers mediating recycling to the plasma membrane. Some recycling cargo also accumulates in a pericentriolar cluster of tubules and vesicles (recycling endosomes) (Hopkins and Trowbridge, 1983; Hopkins, 1983; Yamashiro *et al*., 1984). The role of this distinct pool of early endosomes is currently unclear. The recycling through sorting and recycling endosomes appears to be regulated by the resident GTPases, rab4 (Van der Sluijs et al., 1992) and rab11 (Ullrich *et al*., 1996), respectively.

Sorting endosomes can also generate a variety of cell type-specific recycling vesicles, e.g. synaptic vesicles in neurons and neuroendocrine cells, insulin-responsive glucose transporter (Glut-4)-containing vesicles in adipocytes, and major histocompatibility (MHC) class II-containing vesicles in antigen-presenting cells (Mellman, 1996).

Many signaling receptors, e.g. epidermal growth factor (EGF) receptors, are targeted to lysosomes for degradation. Also, a pool of newly synthesized lysosomal proteins and mannose-6-phosphate receptor (M6PR)-ligand complexes, harvested to clathrin-coated vesicles in the TGN, reach the endocytic pathway in sorting endosomes to be further transported to late endosomes and lysosomes. While the lumenal content of early endosomes is passively delivered to late endosomes and, finally, to lysosomes, membrane proteins seem to be actively sorted for transport to late endosomes. This

sorting may involve specific retention signals or phosphorylation-induced changes in the oligomeric structure of the proteins (Mellman, 1996). Two models for the transport from early to late endosomes have been proposed. One model assumes that early endosomes gradually mature to give rise to late endosomes (Dunn and Maxfield, 1992; Stoorvogel *et al*., 1991). According to the other model, transport requires specific carrier vesicles pinching off early endosomes and fusing with late endosomes (Aniento *et al*., 1993; Gruenberg and Howell, 1989). Transport to late endosomes is dependent on intact microtubules (Gruenberg and Howell, 1989) and dynein (Aniento *et al*., 1993) and appears to be controlled by rab7, a small GTPase localized to late endosomes (Feng *et al*., 1995). Rab7 has also been implicated for the maintenance of a functional lysosomes (Bucci *et al*., 2000).

Endosomes are in close interrelation with the secretory pathway. TGN38, a protein of unknown function enriched in the TGN, continuously cycles between the TGN and the plasma membrane, apparently via early endosomes (Stanley and Howell, 1993). Some protein toxins, such as ricin and Shiga toxin (Sandvig and van Deurs, 2002) are endocytosed, enter the TGN and may also reach the ER by retrograde transport for the intoxication of cells. M6PRs cycle between the TGN and late endosomes releasing their ligands at an acidic milieu of the latter (Dittie *et al*., 1999) and transport between late endosomes and the TGN is controlled by rab9. GTPase TIP47/Rab9 prevents the MPRs from reaching the lysosomes, in which they would otherwise be degraded (Ghosh *et al*., 2003).

1.6.4 Endocytic proteases

The proteases contained in the endocytic pathway are classified into four main groups based on the active amino acid site used by the respective enzyme to hydrolyze amide bonds of protein. They are cysteine, aspartyl, serine and metalloproteases (Riese and Chapman, 2000). More than 16 defined intracellular acidic proteases are referred as the cathepsins**,** which fall into four groups. Cathepsin B, C, F, H, L and S belong to the papain family and are cysteine proteases. Based on chromosomes location and sequence homology, cysteine proteases are subdivided into Cat B-like and Cat L-like subgroups (Cyglera and Mort, 1997; McGrath, 1999).

Cathepsin D and E are aspartyl proteases. Cathepsin A and G are serine proteases. The structures of cathepsins B, L, K, H and S have been determined. The mature cathepsins range between 20 and 30 kDa and are composed of two equivalent sized domains, stabilized by the presence of disulfide bonds. The two domains are separated by the catalytic center that contains the active site nucleophile used to cleave the bound substrates. The specificity of an enzyme is determined by the architecture of its active site. Cathepsins K, L, S, and F are endopeptidases as they hydrolyze internal amide bonds of proteins (Chapman *et al*., 1997; McGrath, 1999; Turk *et al*., 1997). Catalysis by endoproteases relies on the triad composed of a cysteine, a histidine, and an asparagine residue. The histidine and asparagine residues polarize the cysteine residue to generate the nucleophile that attacks the carbonyl carbon of the targeted amide bond of the substrate proteins (Chapman *et al*., 1997; Turk *et al*., 1997). In contrast, the amino-exopeptidase activities of Cat H and Cat C, and the carboxyl-exopeptidase activities of Cat B and Cat Z are generated by obstructing part of the active site with side chains that stabilize either the N terminus or C terminus of the bound substrate (Turk *et al*., 2000). The result is the hydrolysis of one or two amino acid from either side. At lower pH the occluding loop of Cat B is flexible, allowing the enzymes to function also as an endopeptidase (Nagler *et al*., 1997).

Cathepsin S is highly expressed in B cells and DC and its expression can be induced by IFN–γ treatment. This is the only known cathepsin**,** which has broad optimum pH and maintains the enzymatic activity at neutral pH. Cathepsin L is expressed in thymic epithelial cells and F and L expression is profound in macrophages.

1.6.4.1 Biosynthesis and transport of cathepsins

Endosomal proteases are synthesized in the ER as inactive zymogens or proenzymes (McGrath, 1999). The propiece can vary in length and it is located at the N terminus of the mature enzyme. In the ER, the inactive protease requires its propiece for efficient folding as well as to maintain the enzymes in an inactive state. This propiece occupies the active site of the enzyme resulting in the prevention of premature activation while traveling through the Golgi on its way to endocytic vesicles (Coulombe *et al*., 1996). The cathepsins exit the ER and travel through the Golgi, where they acquire post-translational modification including glycosylation (Lingeman *et al*., 1998) and phosphorylation, which is essential for their sorting. The enzymes are carried to

endosomes/lysosomes by the mannose-6-phosphate (M6PR) receptor, requiring phosphomannosyl residue of cathepsins. M6PR shuttles between trans-Golgi network and late endosomes.

1.6.4.2 Activation of cathepsins

The ATP-dependent proton pump known as vacuolar H^+-ATPase maintains the pH in each vacuolar organelle of eukaryotic cells, which include endosomes, lysosomes, and the TGN. Neutralization of these compartments with acidotropic drugs, such as chloroquine and ammonium chloride, and carboxylic ionophores such as monensin or nigericin, prevents lysosomal protease activation. Selective inhibitors of the vacuolar H^+-ATPase include macrolide antibiotics such as bafilomycin A_1 and concanamycin B or folimycin.

Inactivation of the vacuolar H^+-ATPase with these agents affects not only pH but also the formation of endosomal cargo vesicles as well as sorting events in the TGN. The pH is thus not only important for enzyme activation but also for the intracellular transport of protein such as M6PR, including sorting and recycling of various proteins.

1.6.4.3 Inhibitors of endosomal proteases.

Regulation of endosomal protease activity plays an important role in modulating the endosomal environment. Cystatin and related molecules comprise a large group of naturally occurring cysteine protease inhibitors that tightly regulate enzyme activity (Turk and Bode, 1991). They play an essential role in protecting cells and tissues from appropriate proteolysis by enzymes that overexpressed or escape the endocytic pathways (Turk *et al*., 1997).

The enzymatic mechanism utilized by cysteine proteases is quite conserved and well defined. This has enabled the development of a wide range of electrophilic substrate analogs that are reactive only with the conserved active site of cysteine proteases. These inhibitors consist of a peptide specificity determinant attached to an electrophile that become irreversibly alkylated when bound in close proximity to an attacking nucleophile (Bogyo *et al*., 2000). Peptide analogues also can inhibit the endopeptidase activity to some extent.

1.7 Antigen processing by alternative pathways

Endo-lysosomal pathways of antigen processing operate to present peptides on the cell surface to MHC II-restricted $CD4^+$ T cells. Protein antigens taken up from the extracellular fluid or internalized from the cell membrane usually enter the exogenous processing pathways where they get partially digested by various endopeptidase/exopeptidases. Weak bases such as chloroquine, NH_4Cl, and primaquine which increase the pH of these compartments inhibit processing and peptide loading in these compartments.

There is a growing number of reports demonstrating that MHC class I can also present peptides derived from exogenous protein sources in absence of TAP and cytosolic proteases (Carbonetti *et al*., 1999; Liu *et al*., 1995). How MHC class I molecules acquire such exogenous peptides and which cell organelles play the more important role in alternative MHC I presentation is still not completely resolved. Recycling of the MHC class I from the cell surface to endosomes has been observed. This permits an exchange of peptides within acidic vesicles. Its has been shown that such recycling may also refine the peptide repertoire by destabilizing certain pH-sensitive cargo and preventing these from returning to the cell surface (Chefalo and Harding, 2001).

The alternative pathway was first demonstrated nearly 20 years ago as the ability to prime a minor transplantation CTL response using cells mismatched at the MHC and was termed cross-priming (Bevan, 1976; Gordon *et al*., 1976). Cross-presentation is thought to be mostly restricted to DC (Brossart and Bevan, 1997) and macrophages. Both are professional antigen presenting cells (pAPC) and have the capacity to engulf particulate antigens, cell debris as well antigen conjugated with latex beads.

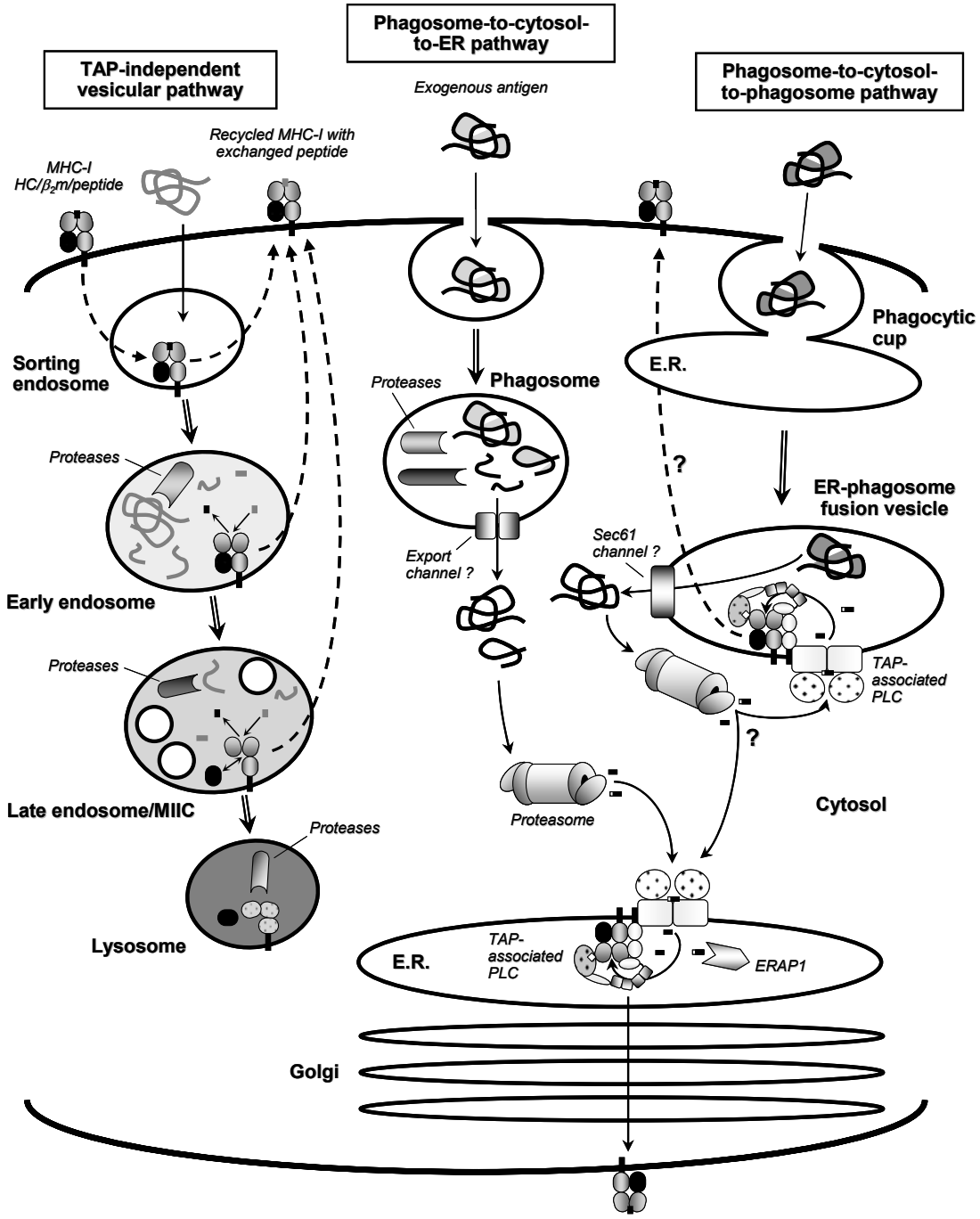

Figure 1.7 Alternative pathways of antigen processing for MHC class I presentation.

How MHC class I molecules are loaded with peptides in the alternative route is a matter of debate. In one pathway, proteins or particulate antigens can enter the cell via plasma membrane invaginations (phagocytic cups). These Phagosomes can further fuse with ER membranes to generate vesicles, which contain MHC molecules, TAP and tapasin. These ER-derived phagosomes like structure were mostly found in pAPC like dendritic cells and macrophages and they may play a major role in cross-presentation (Guermonprez *et al.*, 2003; Houde *et al*., 2003) .

Several mechanisms for the processing of exogenous proteins and MHC I presentation have been proposed (**Figure 1.7**). Studies suggest an alternative mechanism in which endocytosed exogenous antigen/proteins are degraded in endosomal compartments followed by MHC I peptide loading in same compartments (Gromme *et al*., 1999; Kleijmeer *et al*., 2001).

It was shown recently that TAP-independent alternative pathways work along with the classical pathway and generation of peptides in endosomes is facilitated by cathepsin S (Shen *et al*., 2004).

It has been shown that macrophages as well DC can process a vast diversity of exogenous antigen, including particulate antigens such as bacteria, bead coupled antigens, cell debris, inactivated viruses, and antigen incorporated into liposomes for MHC I presentation (Gromme and Neefjes, 2002; Roberts *et al*., 2002; Yewdell *et al*., 1999).

1.8 Aim of the thesis

The aim of my thesis was to analyze antigen presentation by using single-chain peptide-MHC conjugates containing either N-terminally extended or definitive epitopes. It has been reported that peptide-linked MHC class I molecules expressed by cells can present peptides to T-cells and effectively induce T-cell responses. So far, these peptide-linked MHC class I molecules have never been applied to explore peptide trimming and protein processing in the secretory pathway and endolysosomal compartments.

By using this model system, I studied the processing and presentation of such peptide linked-MHC class I conjugates in the classical as well as the alternative MHC class I antigen presentation pathways. I investigated whether ER-associated N-terminal trimming was influenced by peptide loading complex components such as TAP, tapasin, ERp57 etc. Furthermore, I wanted to explore if peptide contained in these conjugates were processed at C-terminus where the processing and presentation occurs.

2. Materials and methods

2.1 Materials

2.1.1 Bacterial strains

The bacterial strains used in our studies for molecular cloning was XL-1 blue (Stratagene, Heidelberg germany). *Escherichia coli* was grown in LB (Luria Bertani) medium and maintained on LB agar plates supplemented with suitable antibiotics wherever necessary. All bacteria were grown at 37°C (with shaking at 220 rpm for liquid cultures). For routine storage, plates were maintained at 4°C.

2.1.2 Plasmids

Plasmids containing K^b cDNA (pSP72.K^b), K^d cDNA (pB4) and OVA cDNA (BS CR-OVA) have been provided by Dr. H. Ploegh, Harvard Medical School, Boston, Dr. B. Arnold, DKFZ, Heidelberg, and Dr. Y. Reiss, Tel Aviv, respectively.

2.1.2.1 Construction of plasmids

cDNAs coding for peptide class I fusion proteins were assembled stepwise in pBluescript II KS+ (Stratagene, Heidelberg, Germany) and after completion subcloned into pcDNA3.1+ (Invitrogen, Karlsruhe, Germany), for expression in mouse cells, using *Nhe*I and *Xho*I (present in primers #9 and #2-5). K^b and K^d cDNAs lacking the ER leader sequence were generated by PCR using the forward primer #1 and reverse primer #2 and subcloned using the underlined *Bam*HI and *Xho*I sites. Primer #1 was used together with reverse primer #3 to produce K^b and K^d cDNAs with truncated cytoplasmic tail. Primer #1 was used together with reverse primer #4 to produce the same constructs without stop codon. The underlined *Eco*RI site was later used for ligation of peptide-Kb/Kd fusion cDNAs into pEGFP-N1. Leader-free K^b and K^d cDNAs containing the ER retrieval signal Lys-Lys-Tyr-Leu instead of the C-terminal 4 residues were generated by PCR using forward primer #1 and the reverse primer #5. Together with reverse primer #2 the forward primers #6, #7 and #8 were used to mutate Tyr321 K^b and Tyr320 in K^d into Pro as well as residues Thr329, Ser330 and Ser333 in exon 7 of K^b (and K^d) into Ala. The products of the latter PCR reactions were purified and used as reverse primers in a second PCR reaction with forward primer #1 and pSP72.Kb and pB4 as templates.

A modified influenza virus HA1 leader sequence (MAKANLLVLLCALAAADA (Elliott *et al*., 1995) and the peptide sequence SIINFEKL were assembled by oligonucleotides #9 and #10. The second strand of oligonucleotides #9 and #10 was synthesized by T4 DNA polymerase the reverse primer #11 5'-GCGCGGATCC-3' and double-stranded oligos assembled in pBluescript II KS+ using the underlined *Sac*II, *Not*I and *Bam*HI sites. In this HA1-S8L encoding sequence, LESIINFEKL replaced SIINFEKL by cloning oligonucleotide #12 into the *Not*I and *Bam*HI sites. *Not*I and *Bsu*15I sites in sequence #12 were used to insert oligonucleotides #13, #14 and #15 coding for the extensions DYKDDDDKA, GPDYKDDDDKA and VSGLEQLE of S8L. The 137-residue extension from the OVA sequence was generated in a PCR reaction using the forward primer #16 and the reverse primer #17 and subcloned into the HA1-S8L construct using NotI and *Hind*III. The extended peptides RKKRSIINFEKL and RKNKTRSIINFEKL were generated by cloning the double-stranded oligonucleotides #16 and #17 between NotI and *Bam*HI of the HA1-S8L construct. The LCRKKR extension of S8L was made by cloning the oligonucleotide #18 between the *Not*I and *Bgl*II sites of the HA1-RKKRSIINFEKL construct. The linker sequence $FLG_4SG_4APGSG_3S$ (sp19) was created by cloning the oligonucleotide #19 between *Hind*III of HA1-LE- S8L (see #10, #12) and of *Bam*HI of leader-free K^b/K^d (see #1). Various LX extensions of S8L were produced by cloning oligonucleotides or between the *Not*I and *Bsu*15I sites or *Not*I and *Hind*III sites of the construct HA1-LESIINFEKL-sp19-Kb, respectively. Various C-terminal flanks of S8L were generated by cloning oligonucleotides and between the HindIII and Kpn2I sites of the linker (see #19).

Mouse ERAP1 cDNA in pCMV·SPORT6 was obtained from the German Resource Center for Genome Research, Berlin (clone IRAKp961H13100Q2) and subcloned into pcDNA3.1/HisA. In-frame ligation of the N-terminal His-tag (blunted *Kpn*I site) with residue 3 of the ERAP1 open reading frame (blunted *Sph*I site) was confirmed by sequencing.

A plasmid containing N-terminally His-tagged, human ERAP2/MAMS cDNA was kindly provided by Dr. Luz Shomburg, Charite, Berlin, Germany.

2.1.3 Primer list

Primer No.	Primer sequence 5'-3'
#1	*GGCCGGATCCGGCCCACACTCGCTGAGGTATTTC*
#2	*GGCCCTCGAGATCTTCACGCTAGAGAATGAGGGTCATG*
#3	*GGCCCTCGAGTCATCCACCTGTGTTTCTCCTTCTCATCTTC ATCACAAA*
#4	*GGCCCTCGAGTCACTGAATTCGTCCACCTGTGTTTCTCCTT CTCATCTTCATCACAAA*
#5	*GGGCCTCGAGTCACAGATACTTTTTAGGGTCATGAACCAT CACTTTAC*
#6	*GGAAAAGGAGGGGACCCTGCTCTGGCTCCAGGC*
#7	*GGAAAAGGAGTGAACCCTGCTCTGGCTCCAGGC*
#8	*GCTCCAGGCTCCCAGGCCGCTGATCTGGCTCTCCCAGAT GGTAAAGTGATGGTTCAT*
#9	*GCTCCCGCGGCTAGCATGGCCAAGGCCAACCTGCTGGTG CTGCTCTGCGCCCTGGCGGCCGCTGGATCCGCGC*
#10	*GCCCTGGCGGCCGCTGACGCCAGCATCATTAATTTCGAAA AGCTTTAGGATCCGCGC*
#11	*GCGCGGATCC*
#12	*GCCCTAGCGGCCGCTGACGCTCTAGAATCGATAATTAATT TCGAAAAGCTTTAGGATCCGCGC*
#13	*GCCCTAGCGGCCGCTGACGCTGATTACAAGGACGACGAT GACAAGGCATCGATAGGATCCGCGC*
#14	*TGCGCCCTAGCGGCCGCTGACGCAGGTCCAGATTACAAG GACGACGATGACAAGGCATCGATAGGATCCGCG*
#15	*TGCGCCCTAGCGGCCGCTGACGCAGTCTCAGGCCTTGAG CAGCTAGAATCGATAGGATCCGCGG*
#16	*GCCCTGGCGGCCGCTGACGCCGTGAAGGAACTGTATAGA GGAGGC*
#17	*CTAACTGGTCCATTCAGTAAGCTTTTCAAAGTTGATTATACT*
#18	*TGCGCCCTAGCGGCCGCTGACGCACTATGCCGCAAAAAG AGATCTGGATCCGCGC*
#19	*TTCGAAAAGCTTTTTCTAGGAGGGGGCGGATCCGGAGGA GGCGGCGCGCCGGGGTCTGGAGGTGGATCCGCGC*
LX	*TGCGCCCTGGCGGCCGCTGACGCANNATCGATAGGATCC GCGC*
LX	*TGCGCCCTGGCGGCCGCTGACGCANNNTCGATAATTAAT TTCGAAAAGCTTTAGGATCCGCGC*

2.1.4 PCR conditions

PCR amplification was done using a touch-down protocol. Reactions were carried out in 200 µl PCR tubes using PTC200 (MJ Research), USA PCR machine.

The conditions were as follows:

Initially denaturation was achieved at 94^{o} C for 3 minutes, subsequently at 94^{o} C for 30 seconds, followed by annealing at 55^{o} C for 35 seconds and amplification at 72^{o} C for 45 seconds. For the first 10 cycles, annealing temperature was reduced 1^{o} C each cycle in a preprogrammed manner. The next 20 cycles, annealing was achieved at 45^{o} C for 35 seconds. The other conditions (i.e. denaturation and amplification) were as mentioned above. At the end, final elongation was performed at 72^{o} C for 10 minutes.

2.1.5 Antibiotics

Ampicillin and kanamycin used in this study were purchased from commercial sources (Sigma Chemicals, Taufkirchen, Germany) and their stocks were prepared as follows:

Ampicillin: 100 mg/ml in water

Kanamycin: 30 mg/ml in water

Stock solutions of antibiotics were sterilized through 0.22 μm filters (Millipore) and stored in aliquots at –20°C.

2.1.6 Chemicals

All reagents used in this study were of molecular biology grade and obtained from commercial sources. Restriction/modifying enzymes and molecular biological reagents were obtained from Fermentas Life Sciences, St. Leon-Rot, Germany or New England Biolabs, Frankfurt, Germany. Plasmid isolation, gel extraction and PCR purification kits used in this study were obtained from Qiagen, Hilden, Germany.

2.1.7 Media for bacterial cells

LB medium was prepared following the procedure as described in Sambrook *et al.* (Sambrook and Russell, 2001) and using Millipore Elix-3 water and autoclaved for 15 min at 121°C at 15 pounds per square inch pressure.

LB medium

Tryptone	10 g
Yeast extract	5 g
NaCl	10 g

The above contents were dissolved in 900 ml water and pH was adjusted to 7.5 with 10 N NaOH. Final volume was made to 1 l with water.

LB agar contained 1.5% agar in LB medium.

LB medium was cooled down to ~55°C prior to the addition of antibiotics.

2.1.8 Protein Chemicals

1 X TBS (pH 7.4)		1 X Lysis buffer (pH 7.4)	
50 mM	Tris-HCl (pH 7.4)	1 X	TBS
150 mM	NaCl	1 %	Detergent (v/v)
5 mM	$MgCl_2$	1 protease inhibitor tablet/50ml	

(Roche Diagnostics, Mannheim, Germany)

SDS-PAGE components

10% Resolving gel solution component	**volumes (ml) per gel mold**		
	10 ml	30 ml	50ml
H_20	**4.0**	**11.9**	**19.8**
30% acrylamide mix	**3.3**	**10.0**	**16.7**
1.5 M Tris (pH 8.8)	**2.5**	**7.5**	**12.5**
10% SDS	**0.1**	**0.3**	**0.5**
10% ammonium persulphate	**0.1**	**0.3**	**0.5**
TEMED	**0.004**	**0.012**	**0.02**

5% Stacking gel solution component volumes (ml) per gel mold

	2 ml	6 ml	10 ml
H_20	**1.4**	**4.1**	**6.8**
30% acrylamide mix	**0.33**	**1.0**	**1.7**
1.0 M Tris (pH 6.8)	**0.25**	**0.75**	**1.25**
10% SDS	**0.02**	**0.06**	**0.1**
10% ammonium persulphate	**0.02**	**0.06**	**0.1**
TEMED	**0.002**	**0.006**	**0.01**

Modified from Harlow and Lane

6x SDS-PAGE loading dye

150 mM Tris-HCl

12 % SDS

30 % Glycerin

0.015 % Bromophenol blue

5 % β-Mercaptoethanol

SEMI-DRY IMMUNOBLOT

Concentrated anode buffer

300 mM Tris base pH 10.4 (36.3 g Tris in 1000 ml of Milli Q water)

Anode buffer

25 mM Tris base pH 10.4 (3.025 Tris in 1000 ml of Milli Q water)

Cathode buffer

25 mM Tris base pH 9.4 (3.025 g/1000 ml of Milli Q water)

40 mM 6-aminocaproic acid (5.24 g/ 1000 ml of Milli Q water)

2.1.9 Animal cell culture media

Unless otherwise stated, all tissue culture media and PBS used to wash cells were purchased from Invitrogen GmbH, Karlsruhe, Germany, together with the supplements such as MEM, L-Glutamine and pyruvate. Fetal bovine serum (FBS) was purchased from Biochrom AG, Berlin, Germany. Trypsin was purchased from Difco Laboratories, Germany, and was diluted to 0.25% in PBS, which were kept as stocks at -20^0 C.

Composition of RPMI-1640

Media components	Stock solution	Final concentration
RPMI-1640	1 x	**1 x**
L-Glutamine	200 mM	**2 mM**
FBS	100 %	**10 %**

Composition of DMEM

Media components	Stock solution	Final concentration
DMEM	1 x	**1 x**
L-Glutamine	200 mM	**2 mM**
Sodium pyruvate	100 mM	**1 mM**
HEPES (pH 7.4)	1000 mM	**10 mM**
MEM (non essential amino acids)	100 x	**1 x**
FBS	100 %	**10 %**

2.1.10 Cell lines

Mouse as well as human cell lines were used in our studies is described below.

Cell lines	**Origin**	***References***
P815	Mouse Mastocytoma (H-2K^{d})	(American Type Culture Collection, ATCC)
RMA	Mouse T-lymphoma C57BL/6 (H-2^{b})	(Ljunggren and Karre, 1985)
RMA-S	Mouse T-lymphoma TAP2 deleted, low K^{b}	(Ljunggren and Karre, 1985)
Ec7.1	Mouse T-lymphoma TAP2 deleted, K^{b} and D^{b} deleted	(Howell *et al*., 2000)
MC6	Mouse Sarcoma	B6 wild type mouse (Garbi *et al.,* unpublished)
MC4	Mouse Sarcoma	Tapasin knockout mouse (Garbi *et al*., 2003)
MCA	Mouse Sarcoma	TAP1 knockout mouse (Van Kaer *et al*., 1992)
HeLa	Human cervix carcinoma	(ATCC)
Ltk-	Mouse Sarcoma	(ATCC)

2.1.11 Antibodies

The following antibodies were used for immunoprecipitation, flow-cytometry, immunofluorescence and Western blotting.

MHC Class I

Y3.1 a mouse monoclonal antibody which recognizes a conformational epitope within the α1−α2 domain of H-2K^b class I heavy chain complex (Jones and Janeway, 1981)

K10-56 a mouse monoclonal antibody which recognizes a conformational epitope within the α1−α2 domain of H-2K^b class I heavy chain complex (Hammerling *et al*., 1982)

25-D1.16 a mouse IgG1 monoclonal antibody specific for SIINFEKL peptide associated with H-2K^b (Porgador *et al*., 1997)

anti-p8 a rabbit polyclonal antibody raised against H-2K^b cytoplasmic tail (Neefjes *et al*., 1992)

Endosomes specific antibody

LAMP1 a rat IgG$_{2a}$ monoclonal antibody (Clone ID4B) Cat. No. 553792

BD Bioscience, Heidelberg, Germany

EEA1 a rabbit polyclonal antibody raised against synthetic peptide (TPPSSKKPVRVCDACFNDLQG) corresponding to amino acid residues 1391-1410 of human early endosomal antigen 1 (cross reactive to mouse antigen) Cat. no. 324610 Calbiochem, Darmstadt, Germany

M6PR a kind gift from Dr. von figura, Gottingen (von Figura *et al*., 1984)

Secondary antibodies:

Secondary antibody	Working solution	Company
Goat anti Mouse Cy3	**1:200**	Dianova, Hamburg, Germany
Goat anti Mouse Cy5	**1:500**	Dianova, Hamburg, Germany
Goat anti Mouse PE	**1:100**	BD Bioscience,Heidelberg, Germany
Goat anti Rabbit Alexa Fluor® 488	**1:100**	Molecular Probes, Germany
Goat anti Rat FITC	**1:100**	BD Bioscience, Heidelberg, Germany
Goat anti Rat TRITC	**1:200**	Dianova, Hamburg, Germany
Goat anti Mouse Biotin	**1:100**	BD Bioscience, Heidelberg, Germany
Goat anti Rabbit TRITC	**1:200**	Dianova, Hamburg, Germany

2.1.11 siRNA oligonucleotides.

The following siRNAs were used and purchased from Qiagen, Hilden, Germany.

Control siRNA sequence UUCUCCGAACGUGUCACGUdTdT (sense)

ACGUGACACGUUCGGAGAAdTdT (antisense)

ERAAP siRNA sequence AGCUAGUAAUGGAGACUCAdTdT (sense)

UGAGUCUCCAUUACUAGCUdTdT (antisense)

2.1.12 Inhibitor stock solutions

Furin inhibitor

Decanoyl-Arg-Val-Lys-Arg Bachem, Bubendorf, Switzerland

-chloromethylketone (Mw. 744.42)

Stock solution **10 mM**: 5 mg dissolved in 672 µl of DMSO

Proton pump inhibitors

Bafilomycin A_1 (MW: 622.8) Sigma, Taufkirchen, Germany

Stock solution **100 µM**: 2 µg dissolved in 30 µl of DMSO

Foliomycin (MW: 866.1) Calbiochem, Darmstadt, Germany

Stock solution **1 mM**: 10 µg dissolved in 11.5 µl of DMSO

Proteasomal inhibitors

Lactacystin (MW: 376.4) Calbiochem, Darmstadt, Germany

Stock solution **10 mM**: 200 µg dissolved in 52 µl of DMSO

MG132 (Z-Leu-Leu-Leu-al) (MW. 475.6) Sigma, Taufkirchen, Germany

Stock solution **10 mM**: 5 mg dissolved in 1000 µl DMSO

Cathepsin inhibitors:

Leupeptin (Acetyl-Leu-Leu-Arg-al) (MW: 475.6) Sigma, Taufkirchen, Germany

Stock solution **10 mM**: 5 mg dissolved in 1050 µl of DMSO

Pepstatin A (MW: 685.9) MP Biomedicals, Eschwege, Germany

Stock solution **50 mM**: 25 mg dissolved in 729 µl of DMSO

10 mM: 5.0 mg dissolved in 729 µl of DMSO

Other inhibitors:

Chymostatin Sigma, Taufkirchen, Germany

Stock solution 5 µg/µl: 5 mg dissolved in 1 ml of DMSO

Wortmannin (MW: 428.4) Sigma, Taufkirchen, Germany

Stock solution **10 mM**: 1 mg dissolved in 233 µl of DMSO

Butabindide oxalate (MW: 411.46) Tocris, Bristol, UK

Stock solution **10 mM:** 4.11 mg dissolved in 1 ml of PBS

Filipin complex Sigma, Taufkirchen, Germany

Stock solution **25 mg/ml**: 25 mg dissolved in 1000 µl of DMSO

Chlorpromazine Sigma,Taufkirchen, Germany

Stock solution **100 mg/ml**: 0.2 g dissolved in 2000 µl of DMSO

Brefeldin A (MW: 280.4) Sigma, Taufkirchen, Germany

Stock solution **5µg/µl**: 5 mg dissolved in 1 ml of methanol

Cycloheximide (MW:281.4) Sigma, Taufkirchen, Germany

Stock solution **10 mM:** 2.8 mg dissolved in 1 ml of DMSO

2.2 Methods

2.2.1 Plasmid Isolation (Mini Preparation)

The plasmid DNA was isolated from transformed *E. coli* (XL-1 Blue) using the Qiagen mini prep method. In brief, an overnight culture was setup by inoculating a randomly selected colony in 4 ml LB medium with appropriate antibiotics and grown at 37^{o}C at 230 rpm. The next morning, cells were pelleted in Eppendorf tubes for 2 minutes at 12000 rpm. The supernatant was removed and bacterial cells were resuspended in 250 µl buffer P1. 250 µl P2 lysis buffer were added, the tube gently inverted and kept for 5 min. After that 350 µl N3 buffer were added and mixed without vortexing. The Eppendorf tube was centrifuged at 12,000 rpm for 10 min. The supernatant was taken out and applied to a QIAprep spin column by pipetting. The spin column was centrifuged for 1 min at 12,000 rpm. The flow-through was discarded and the column was washed with 750 µl buffer PE. Plasmid DNA was eluted with 200 µl TE buffer.

2.2.2 Plasmid Isolation (Maxi Preparation)

For large scale plasmid DNA preparation, commercially available kits (Qiagen, Germany) based on a modified alkaline lysis procedure were used.

The bacterial colony was grown in 2 ml starter culture for 6 hrs at 37^{o}C at 230 rpm. 150 ml overnight culture was set up by inoculating the above starter culture. The next morning, cells were pelleted down in 500 ml roller bottles for 10 min at 5000 rpm in a Beckman Avanti J-25 centrifuge (rotor JLA 10.500). The supernatant was removed and bacterial cells were resuspended in 10 ml buffer P1 and after that 10 ml P2 alkaline lysis solution were added. The tube was gently inverted and kept for another 5 min. After that 10 ml P3 buffer were added and mixed without vortexing.

The supernatant obtained from the treatment of cell pellet with alkaline lysis solutions was allowed to bind to an anion-exchange resin under appropriate low-salt and pH conditions. RNA, proteins and other impurities were removed by a medium-salt wash. Plasmid DNA was eluted in a high-salt buffer and desalted by isopropanol precipitation.

2.2.3 DNA Sequencing

The DNA sequencing was done by MWG Biotech, Ebersberg, Germany using the dideoxy method. One microgram DNA was precipitated in ethanol and air dried. The DNA was further dissolved in 10 µl of HPLC purified water and sent for sequencing.

2.2.4 Nucleic acid quantification

The DNA was quantitated spectrophotometrically (Ultrospec 2000 UV-Visible spectrophotometer, Pharmacia Biotech) by measuring absorbance at 260 nm. An absorbance unit of 1 at 260 nm was taken to be equivalent to a concentration of 50 µg/ml for a double stranded DNA (Sambrook *et al.,* 1989; Sambrook and Russel, 2001). The purity of DNA was confirmed by measuring the OD_{260}/OD_{280} ratio. Purified DNA had an OD_{260}/OD_{280} ratio of ~1.8.

2.2.5 Agarose gel electrophoresis

DNA fragments were fractionated on 1.0% agarose gels. 6x gel loading buffer was added to DNA samples at a final concentration of 1x prior to loading onto the gel. Electrophoresis was carried out in 1x TAE buffer at 10 V/cm. Ethidium bromide (0.5 µg/ml) was supplemented in the agarose gel for visualizing DNA on an UV transilluminator. Lambda DNA/*Hind* III, or Lambda DNA/*Hind* III+*Eco* R I were used as molecular size markers to assess the size of DNA fragments from their relative mobility.

2.2.6 Purification of DNA fragment(s) from agarose gels

After electrophoresis, DNA was visualized using a UV transilluminator. Agarose blocks containing the desired DNA fragment(s) were excised and weighed. DNA was extracted using a gel extraction kit (Qiagen, Hilden, Germany). Briefly, 3 volumes of solubilization and binding buffer were added to 1 volume of the agarose gel slice. The contents were incubated at 50°C till complete dissolution of the agarose gel. The suspension was then pipetted onto a QIAquick spin column to allow the adsorption of DNA on a silica-gel membrane. Impurities were washed away with ethanol-containing PE buffer. DNA was finally eluted in elution buffer (10 mM Tris-HCl, pH 8.0).

2.2.7 Cell Culture

The given cell lines were maintained in monolayer/suspension cultures in defined medium (RPMI-1640 or DMEM) supplemented with 10% heat inactivated fetal calf serum (FCS) with 2 mM L-glutamine. The cells were grown in a humidified atmosphere with 7% CO_2.

2.2.7.1 Long-term storage

Growing cells were trypsinized, pelleted and washed thoroughly with D-PBS to remove traces of trypsin and medium. Cells were then resuspended in freezing buffer (50% FCS, 40% RPMI, 10% DMS0), at a density of 2-3 million cells/ml, and aliquoted into cryovials. DMSO was purchased from Merck, Germany. Vials were placed in a cell freezing box (Nalgene™) and left at -80°C O/N for gradual freezing. Frozen cell vials were then transferred to liquid nitrogen for long term storage. Repropagation was performed by placing the vial with frozen cells briefly at 37°C and gradually thawing the cells by the addition of complete medium. The cell suspension was transferred to a 15 ml Falcon tube, pelleted and washed with complete medium for the removal of DMSO and was resuspended and added to 20 ml complete medium in a 75 cm^2 tissue culture flask.

2.2. 8 Cell transfections

2.2. 8.1 Transient transfections of adherent cells

The adherent cells were transfected with DNA using Lipofectamine™ 2000 (Invitrogen Life Technologies, Karlsruhe, Germany) according to the manufacturer's instruction, with minor modifications adapted to 96-well plate cultures. Round-bottom 96-well plates were coated with 0.01% (v/v) poly L-lysine (stock 0.1%) in water for 60 min in the tissue culture hood, and after that they were washed extensively with double distilled sterile water and dried under UV light for another 2 hours. The day before transfection, 1 x 10^4 cells/well were seeded in to 96-well round-bottom plate. Next day cells were washed with D-PBS (pH 7.4) to remove the serum, and 50 µl Opti-MEM®I serum free medium were added to each well. DNA-Lipofectamine complexes were made as per instructions and 1:3 ratio of DNA: Lipofectamine™ 2000 was used.

For 96-well plates, 0.4 µg DNA/well was diluted into 25 µl of Opti-MEM®I serum free medium and 1.2 µl/well of lipofectamine was diluted into 25 µl of Opti-MEM®I serum

free medium separately. After 5 min incubation, both were mixed together and incubated again for another 20 min at room temperature. Then the DNA-Lipofectamine complex (50 µl) was dropwise added to the 96-well. Transfection efficiency was checked after 48 hrs and normally it was 20-40% by FACS.

2.2.8.2 Stable transfection for suspension cells.

For suspension cells, the electroporation method was used to transfect plasmid DNAs. $1x10^7$ suspension cells like RMA, RMA-S and EC7.1 were transfected with 10 µg of DNA at 220 V and 960 µF using BIO-RAD Gene Pulser I. The cell lines were selected at 0.8-1.0 mg/ml of G418.

2.2.9 Western blotting

The cells were grown till 70% confluency prior to harvesting. The cells were trypsinized, washed 2 times in D-PBS and counted using the hemocytometer. The cells were lysed in ice-cold lysis buffer (1% NP-40 in 50 mM Tris, 150 mM NaCl, 5 mM $MgCl_2$ buffer) with 1 protease inhibitor tablet added per 50 ml lysis buffer. The cells were normally lysed at a concentration of 10^7 cell/ml. Lysis was done for 60 min at 4^0 C followed by centrifugation at 4,000 rpm for 10 min to remove the nuclei and cell debris. The supernatant was further cleared by another round of centrifugation at 12,000 rpm for 10 min at 4^0 C.

2.2. 9.1 Electrotransfer of proteins from SDS-PAGE gels to membrane

The transfer was performed by the Trans/Blot Cell transfer system (Bio-Rad). The assembly of the immunoblot is shown below. For each gel, 9 sheets of Whatmann paper (16 x16 cm) and one membrane were precut. The PVDF membrane (Immobilon^{TM}-P, Millipore) was activated for 15 seconds in methanol, washed in ddH_2O for 5 min and then placed in anode buffer for 5 min. Meanwhile the gel was removed and soaked in cathode buffer for 10 min. For setting the semidry transfer method, 3 precut sheets of Whatmann paper were soaked in concentrated anode buffer and placed into the transfer chamber. After this step another 3 sheets of Whatmann paper were dipped in anode buffer and then the gel was placed on top of this. Bubbles were removed carefully by rolling a 20 ml glass pipette. Next, the activated membrane was placed on top of the gel, the running start was cut on the edge for orientation and air bubbles were removed by gently rolling a glass pipette.

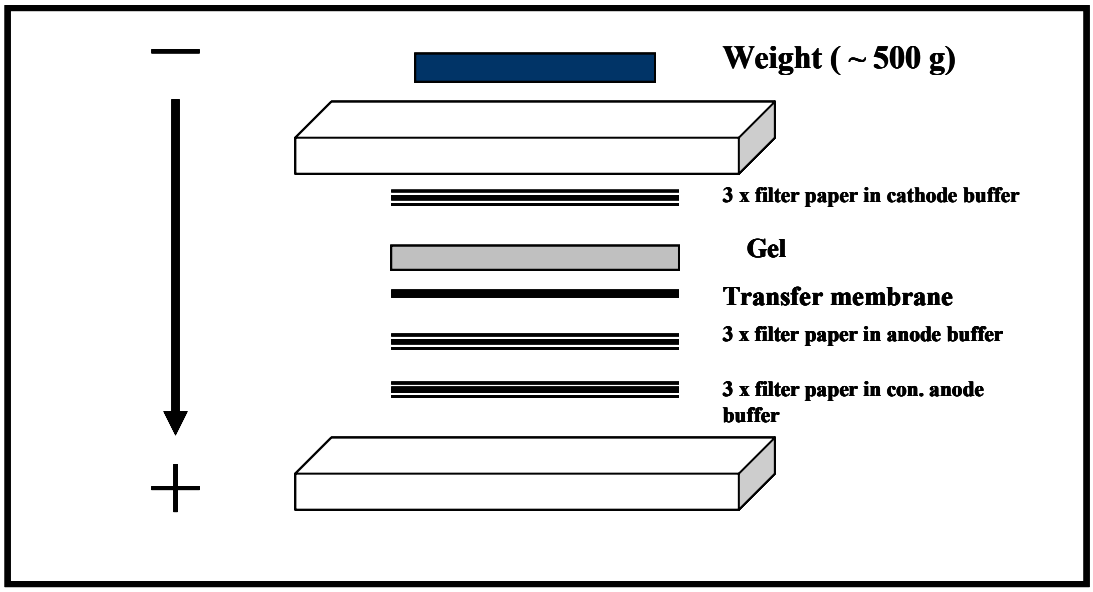

The sandwich was completed by placing 3 sheets of Whatmann papers soaked in cathode buffer and chamber was closed with the lid. Transfers were carried out at 180 mA at RT for 90 min.

2.2.9.2 Immunoblotting

Following transfer, the membrane was placed with the protein side up into a container filled with blocking solution and was blocked either for at least 1 h at RT or overnight at 4^{o}C. Once complete, the membrane was transferred in a plastic box and primary antibody diluted in blocking solution was added. Following 1 h RT incubation, the membrane was rinsed rapidly twice and then washed 3 times, 10 min each, with washing buffer. The membrane then was incubated similarly with appropriate horseradish peroxidase (HRP) conjugated secondary antibody diluted 1: 50,000 for 1 hour at RT. Following washes as described above, chemiluminescence detection was performed using Enhanced Chemiluminescence Supersignal Dura West Extended, (Pierce PerBio, Bonn, Germany) according to the manufacturer's instructions. Blots were visualized on the (LumiImager, Roche, Mannheim, Germany) or exposures were performed on Hyperfilm ECL (Amersham, Freiburg, Germany).

Blocking buffer: 5% skimmed milk powder in 1 x PBS (pH 7.6) with 0.1% Tween 20

Washing buffer: 1 x PBS (pH 7.6) with 0.1% Tween 20 (PBS-T)

2.2.10 FACS Analysis

Flow cytometry was performed using a Becton Dickinson LSR flow cytometer. Monoclonal antibodies (mAbs) used for flow cytometric analysis are listed in section 2.8.

Single cell suspensions were washed twice with FACS buffer (PBS, 2% FCS+ 5mM EDTA). Staining was done as follows: 1x 10^6 cells were incubated in 96-well round bottom plates (TPP, Switzerland) on ice with different combinations of antibodies in FACS buffer for 30 minutes. After the incubation, cells were centrifuged for 2 min at 2000 rpm and were washed two times with FACS buffer. Afterwards, cells were incubated with fluorescent-conjugated secondary antibody for 30 minutes at 4°C in the dark, subsequently washed 3 times in FACS buffer and finally resuspended in 200 µl of FACS buffer containing 1:2000 propidium iodide (stock solution 1 mg/ml).

2.2.11 Acid-wash Recovery Assay

The stably or transiently transfected cell lines were once washed with D-PBS (pH 7.6) and resuspended in isotonic acid-wash buffer (pH 3.0) and incubated for 3 minutes. After this incubation, cells were washed 3 times with full medium. The cells were allowed to recover in the presence or absence of inhibitors at 37°C for the indicated times in complete RPMI-1640 or DMEM medium.

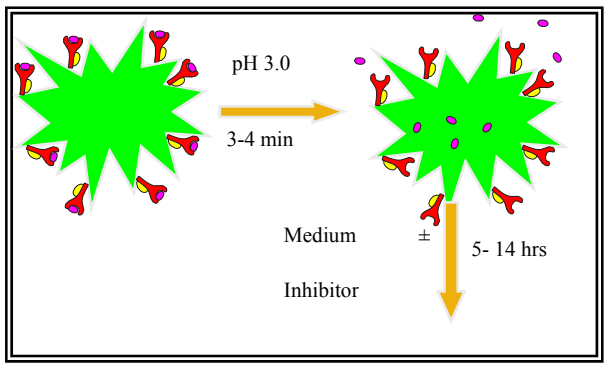

Composition of acid-wash buffer :

Stock solution of **Buffer A**: 0.1 M solution of citric acid (19.21 g in 1000 ml)

Stock solution of **Buffer B**: 0.2 M solution of dibasic sodium phosphate (53.65 g of $Na_2HPO_4.7H_20$ in 1000 ml)

39.8 ml of buffer A + **10.2 ml** of buffer B, diluted to total of 100 ml lead to pH 3.0

2.2.11 Cell Fixation

For T cell activation assays, cells were fixed after the incubations with 0.05% ice-cold glutaraldehyde (Merck, Darmstadt, Germany) in D-PBS for 4 minutes. The fixative was

quenched with 0.2 M glycine in PBS for 30 seconds. Cells were washed 3 times with RPMI-1640 medium.

2.2.12 Peptide synthesis

Purified peptides were obtained as lyophilized powder from Dr. R. Pipkorn (Peptide synthesis lab, DKFZ, Heidelberg). Peptides were dissolved in DMSO at 10 mM concentration and then stored at -20^{0}C. Peptides were diluted to the required final concentrations with either PBS or full medium.

2.2.13 Proteasomal inhibition assay

To assess the role of proteasome, the cells were treated with the proteasomal inhibitor lactacystin. 1 x 10^6 cells were washed with D-PBS followed by 3 min incubation with 250 µl of stripping buffer. The cells were washed 3 times by adding 50 volumes of cold D-PBS followed by spinning at 1500 rpm for 3 minutes. Cells were checked for viability by Trypan Blue dye exclusion method. The cell viability was 90-95%.

1 x 10^6 cells were then treated with 10 µM lactacystin (Calbiochem, Darmstadt, Germany) in 200 µl RPMI complete medium for various time points. After each time point, cells were fixed with 0.05% glutaraldehyde as mentioned in section 2.2.11. The fixed cell samples were stored at 4^{0}C till the last time point.

2.2.14 T-cell proliferation assay (B3Z assay)

Processing and presentation of peptide epitopes derived from N-terminally extended conjugates was assessed using the B3Z T-cell hybridoma (Karttunen *et al*., 1992). B3Z is a lacZ-inducible $CD8^+$ T-cell hybrid specific for OVA peptide 257-264 (SIINFEKL) presented on murine H2-K^b MHC class I molecules and was a kind gift of Dr. N. Shastri (University of California, Berkeley, CA).

The lacZ assay utilizes a reporter construct consisting of the bacterial β-galactosidase gene (lacZ) under the transcriptional control of the nuclear factor of activated T cells (NF-AT) elements of the human interleukin 2 (IL-2) enhancer.

The presentation of the SIINFEKL epitope (S8L) by murine K^b to B3Z cells results in the IL-2 dependent induction of galactosidase (β-gal) synthesis and intracellular accumulation of β-galactosidase by B3Z T cells. The amount of β-gal produced by B3Z

T cells can be measured by the hydrolysis of the chromogenic substrate chlorophenolred-β-D-galactoside (CPRG Calbiochem, Darmstadt, Germany) and is an indication of the amount of S8L/K^b complexes presented on the surface of APCs.

The B3Z assay was performed in 96-well U-bottom plates. The APC were either pulsed with synthetic peptides or expressed SIINFEKL in the context of transfected conjugates/minigenes. APC usually plated at $1x10^4$/well or according to the experimental requirements.

To quantify the T cell stimulation, 5 x 10^4 B3Z cells/well were incubated with either unfixed or fixed APC for 18-20 hrs at 37°C in CO_2 incubator. After this time, cells were pelleted using 2000 rpm for 2 min and the supernatant carefully aspirated. The cells were lysed in Z-buffer containing NP-40 detergents. Due to the detergent, cells release the β-galactosidase, which reacts with the substrate, to produce red-violet color. The absorption was measured at 595 nm in a 96-well plate ELISA reader (Titertek Multiskan Plus, Germany), with 635 nm as the reference wavelength.

Composition of Z buffer:

PBS pH 7.6, 9.0 mM MgCl2, 0.15 mM CPRG, 100 mM 2̃mercaptoethanol and 0.125% NP-40

2.2.15 siRNA mediated gene silencing

For delivery of siRNA duplexes into target cell lines, I have used the oligofectamine transfecting reagent (Invitrogen, Karlsruhe**,** Germany). The cells were transfected according to the manufacturer's standard protocol with slight modifications. The day before transfection, cells were seeded in such a way that they were 50% confluent on the day of transfection. For each 6 cm dish, 20 µl of a 20 µM stock solution of oligonucleotides were added to 350 µl of OPTI-MEM serum free medium. 8 µl of Oligofectamine™ Reagent (Invitrogen) were diluted into 22 µl OPTI-MEM serum free medium to give a final volume 30 µl and were allowed the to stay for 10 minute at room temperature. Following this, diluted the Oligofectamine™ Reagent was mixed with diluted oligonucleotides and the mixture was further incubated at RT for 20 minutes to form complexes. The final oligonucleotides concentration was 200 nM. Now, cells in six well plates were washed once with serum free OPTI-MEM medium. For each plate, 1600 µl serum free OPTI-MEM medium were added and 400 µl of complex

was dropwise added onto the cells. Now cells were incubated for 5 hrs at 37 degree in the CO_2 incubator. After this incubation, the OPTI-MEM medium was replaced by full medium. Gene silencing was assessed after 48-72 hours.

2.2.16 Purification of T cells using magnetically activated cell sorting (MACS) columns

2.2.16.1 Purification of T Cells

Approximately 100 x 10^6 splenocytes were labelled with 20 µl anti-$CD8^+$ mAb coupled MicroBeads (Miltenyi Biotec) in 1 ml of MACS buffer on ice for 30 min and then washed with 10 times excess of MACS buffer by centrifugation at 1300 rpm for 5 min. The cell pellet was resuspended in 1 ml of cold MACS buffer and passed through a cell strainer (70 µm pore size) onto the MACS positive selection column (MS; Miltenyi Biotec) and the T cells purified according to the manufacturer's specifications. An aliquot of cells from each step of purification procedure was used for flow cytometry analysis to check the purity of T cells.

MACS Buffer : 0.5% Bovine serum albumin (BSA) in PBS without Ca^{2+} and Mg^{2+} and 2 mM EDTA.

2.2.17 Confocal microscopy

One day before staining, the transient transfected cells were plated at 30-50% confluency on (0.1% v/v) poly L-lysine coated coverslips. All stainings were setup in 48-well plates.

On the next day, cells were gently washed twice with 400 µl of ice-cold PBS pH 7.6 (without Ca^{+2} and Mg^{+2}). Cells were fixed using fixing buffer for 10 min on ice, followed by addition of 200 mM glycine buffer for 2 min. Cells were again gently washed with 400 µl of quenching buffer. Permeabilization and blocking was done using the mild detergent saponin and performed using blocking buffer for 1 hour in an orbital shaker at room temperature. Primary antibody incubation was always done at 8^oC overnight without shaking and antibody was diluted in 250 µl of blocking buffer. On the next day, cells were gently washed three times with 400 µl of washing buffer for 7 minutes at room temperature on an orbital shaker followed by respective secondary antibodies in 250 µl for 30 minute at room temperature on an orbital shaker. Cells were

again washed twice with 400 µl of washing buffer and the third wash was done in normal PBS. At the end, cells were kept in 10 mM Tris-HCl (pH 8.0) till mounting the slide.

In some cases, after secondary antibody incubation, first washing buffer contained DAPI (1:20,000) for nuclear staining.

Finally, the coverslips were mounted using Mowiol mounting medium followed by overnight incubation at room temperature in the dark and further stored at 4^{o}C.

Fixing buffer: 4% Paraformaldehyde in 200 mM HEPES pH 7.4 containing 0.9 % NaCl

Quenching buffer: 200 mM glycine in PBS pH 7.6

Permeabilization and blocking buffer: 0.1% (w/v) saponin (Sigma, Taufkirchen, Germany**)**, 7% horse serum in PBS pH 7.6 (without Ca^{+2} and Mg^{+2})

Washing buffer: 0.1% (w/v) saponin (Sigma, Taufkirchen, Germany**)**, 5 % horse serum in PBS pH 7.6 (without Ca^{+2} and Mg^{+2})

Mounting medium: 2.4 gm Mowiol + 6 g Glycerol+ 6 ml of DD H_2O+ 0.2 M Tris, pH 8.5

DAPI stock solution: 5 mg/ml in PBS pH 7.4; working solution 1:20,000

Slides were examined using a confocal laser scanning microscope (Leica Microsystems Heidelberg, Germany) equipped with 63× 1.4 Plan-APOCHROMAT oil immersion objectives. GFP, TRITC and Cy5 were excited with the 488nm, 520nm and 670nm lines of Kr–Ar lasers respectively, and individual channels were scanned in series to prevent cross channel bleed through.

3. RESULTS

Part I

3.1. Construction of single-chain mouse MHC I-peptide conjugates.

In MHC class I presentation pathway, optimally trimmed peptides are presented to CD8+ cytotoxic T cells at the cell surface. Proteasomes generate peptides in the cytosol which are subsequently transported through TAP into the ER. These transported peptides may have N-terminal extensions. In the ER, such peptides are further trimmed by aminopeptidases and loaded onto available MHC class I molecules. When I started my thesis, an ER-associated aminopeptidase was not yet discovered. While this work was in progress, two ER-associated aminopeptidases (ERAP1/ERAAP, ERAP2) have been reported (see subsection 3.1.7.1) to be involved in N-terminal trimming of oligopeptides in the ER.

To explore the N-terminal trimming in the endoplasmic reticulum (ER), I have used a model system in which the C-terminal end of the peptide SIINFEKL was covalently linked to the N-terminal end of mouse MHC class I either H2-K^b or H2-K^d. The linkage was achieved by using an 11 (G_3APGSG_3S) or 19 ($FLG_4SG_4APGSG_3S$) amino acid residue spacer sequence.

The main advantage of using peptides tethered to the N-terminus of class I heavy chain by covalent flexible linkers was to avoid confounding effects of peptide retrotranslocation from the ER to cytosol, trimming by cytosolic aminopeptidases and recycling to the ER through TAP. Peptide recycling through TAP can also be avoided using TAP-deficient cells.

The SIINFEKL (S8L) peptide is a K^b-restricted epitope derived from chicken egg ovalbumin (OVA $_{257–264}$).

To target the peptide-linked MHC class I molecules to the ER, all constructs were preceded by the ER signal sequence MKANLLVLLCALAAADA derived from influenza hemagglutinin HA (Elliott *et al*., 1995).

The peptide conjugates either contained the final octamer epitope SIINFEKL, or in addition, had N-terminal extensions derived from the naturally occurring flanks in the

OVA sequence LE, V_{249}-E_{256}, V_{120}-E_{256}. Alternatively, the conjugates contained the artificial sequences *flag*-tag **(DYKDDDDK)** or **RKKR** as N-terminal extensions. The *flag*-tag can be detected by antibody staining on the cell surface. The RKKR tag, which represents a furin cleavage motif, was included to assess potential processing by the *trans*-Golgi endopeptidase furin (Thomas, 2002).

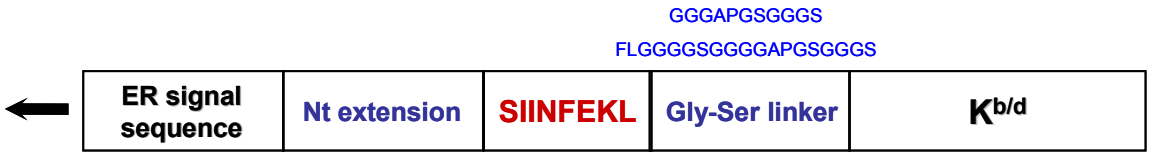

Figure 3.1a Schematic representation of N-terminally extended peptide-linked MHC class I molecules.

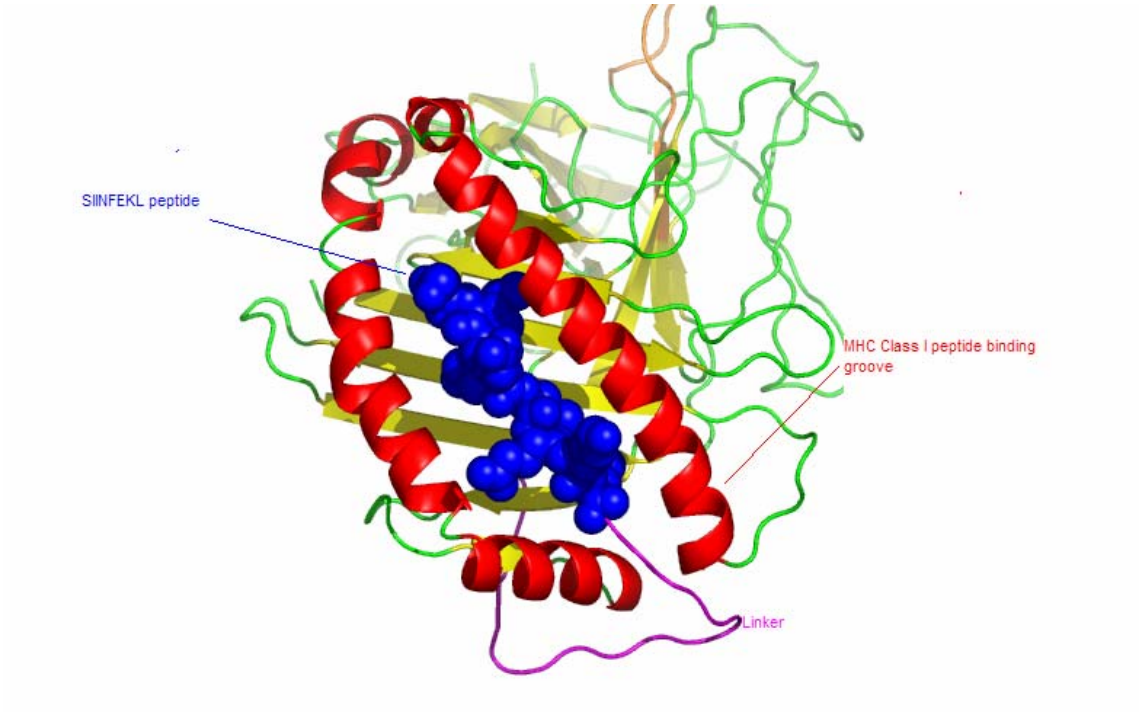

Figure 3.1b Hypothetical modal of C-terminally extend peptide-linked MHC class I molecule.

For the detection of K^b conjugates with SIINFEKL peptide, I have used the well defined B3Z T cell hybridoma (Karttunen *et al*., 1992) and the mAb 25.D1-16 (Porgador *et al*., 1997) which both specifically recognize K^b/SIINFEKL complexes.

3.1.2 Expression of MHC I-peptide conjugates in TAP-proficient cells.

3.1.2.1 Cell surface expression in P815 cells.

To analyze the role of peptide loading complex (PLC) for the expression of SIINFEKL/K^b complexes, I transfected the constructs into the mouse mastocytoma cell line, P815, which expresses all components of the TAP-associated loading complex, but does not express H-$2K^b$. The cells were transfected with peptide conjugates and selected with G418 as a bulk culture.

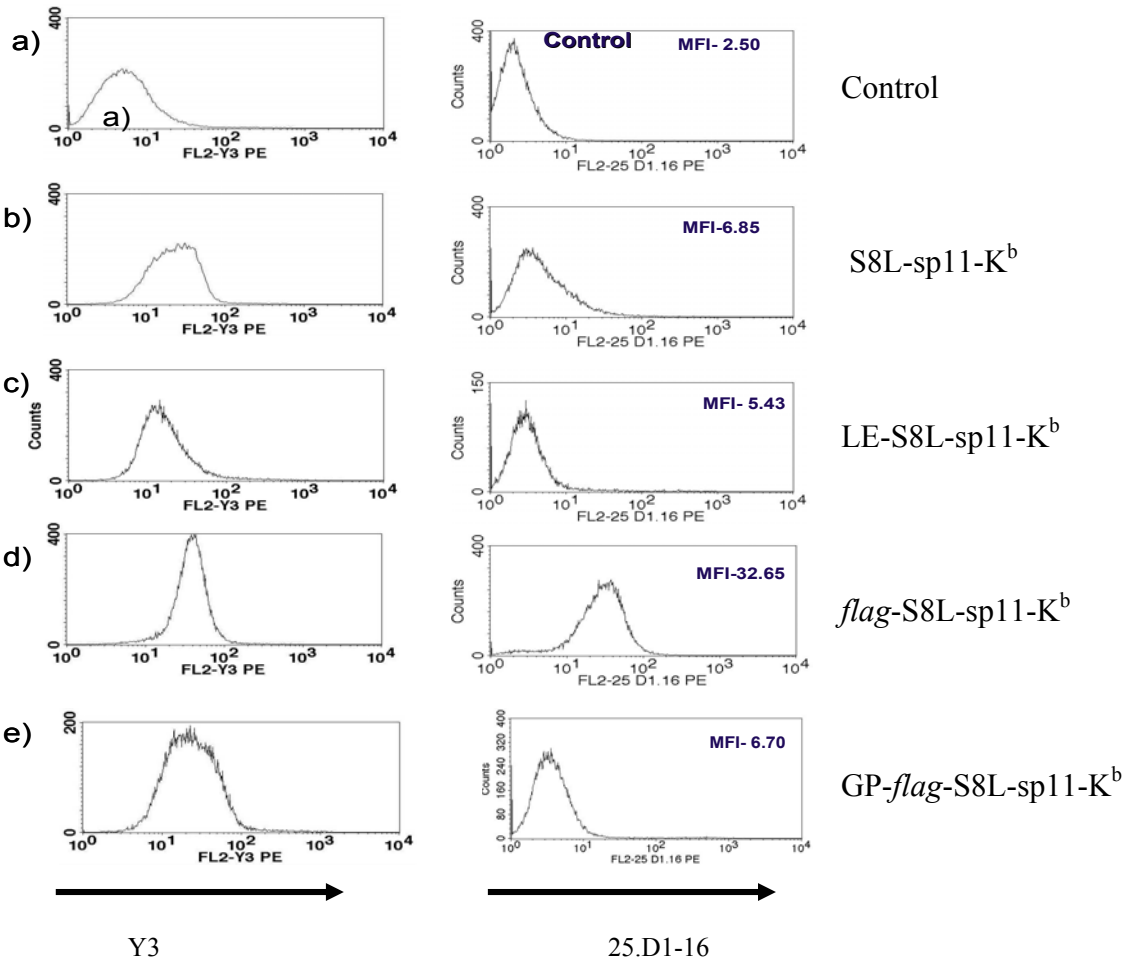

Figure 3.1.2a Cell surface expression of peptide-K^b conjugates in P815 cells
P815 cells were transfected with the indicated constructs and selected with the antibiotic G418. After sorting, the transfectants were stained with the mAb Y3 specifically recognizing peptide loaded H-$2K^b$. The 25.D1-16 antibodies recognizes mouse MHC H-$2K^b$ in conjunction with the OVA peptide SIINFEKL.

The cells were first sorted on the basis of folded K^b molecules using mAb Y3 and later analyzed again for K^b cell surface expression. As shown in figure 3.1.2a, the cell surface K^b expression was more or less equal in all transfectants. Using mAb 25.D1-16, S8L:K^b

complexes could, however only be detected in *flag*-S8L-sp11-K^b and S8L-sp11-K^b.

3.1.2.2 Response of B3Z T cells

P815 cells stably transfected with peptide-K^b conjugates were analyzed by B3Z T cell responses. I titrated the number of APC but left the number of B3Z T-cell hybridoma constant. I expected that the B3Z T cell hybridoma would not tolerate N-terminal SIINFEKL extensions and only recognizes the optimally processed SIINFEKL peptide tethered to H-2K^b. As shown in **figure 3.1.2b**, the responses of B3Z T cells towards our conjugates varied. The *flag*-extended conjugate was presented even better then the finally trimmed conjugate S8L-sp11-K^b.

It was also reported that free peptides containing the residue Gly-Pro at the N-terminus is very slowly trimmed by the ER-resident aminopeptidase ERAAP (Shastri *et al*., 2002). Therefore, I expected, if ERAAP acted upon the GP-*flag*-S8L-sp11-K^b precursor in the ER, it would be unable to generate the final S8L-sp11-K^b. However, our results indicated that the GP-*flag*-S8L-sp11-K^b conjugate was also recognized by B3Z T cells, although less efficiently than other conjugates. This suggested that ERAAP was not solely responsible for the trimming of extended S8L-K^b conjugates. On the other hand, it was possible that these peptide-K^b conjugates might be misfolded, undergo retrotranslocation from the ER and get degraded by proteasomes. Proteasomes may generate the free SIINFEKL peptide which may then recycle back to ER via TAP.

It was an interesting observation that the S8L peptide apparently could be recognized by the B3Z T-cell hybridoma even if the C-terminal end of the peptide was not free. The available literature also suggests that the single-chain peptide MHCI conjugate should be able to load the attached peptide without endoproteolyic cleavage of the spacer (Dela Cruz *et al*., 2000; Mottez *et al*., 1995; Yu *et al*., 2002). Whether S8L indeed bound without additional cleavage could only be revealed by using protease inhibitors and was addressed in subsequent experiments (see part II)

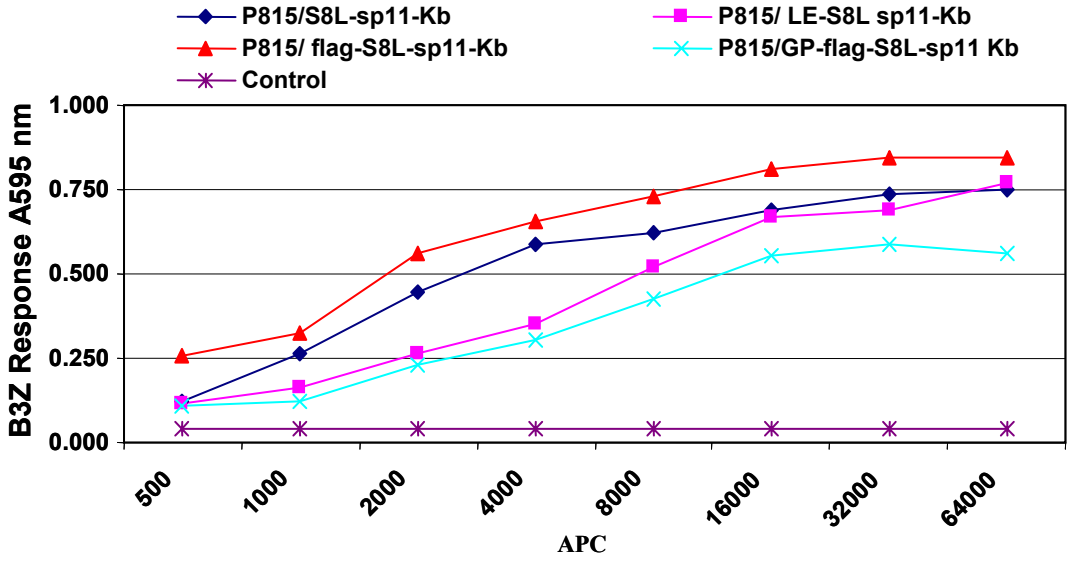

Figure 3.1.2b P815 cells expressing N-terminally extended S8L-sp11-K^b molecules were able to elicit B3Z T cell responses.

The indicated numbers of stably transfected P815 cells with the above mentioned constructs were seeded into a 96-well plate. 5 x 10^4 B3Z cells were added for 18 hrs and the LacZ assay was performed according to the protocol described in Material & Methods

3.1.3 Presentation of exogenous free peptides by P815/K^b cells

To know whether N- or/and C-terminally extended SIINFEKL analogues peptides can in principle bind to MHC class I exogenously and are able to stimulate the B3Z T cell hybridoma, I tested N or/and C-terminally extended SIINFEKL peptides using P815 cells transfected with K^b as APC in the B3Z assay. I pulsed with various concentrations of the indicated peptides either at 4^{o}C or at 37^{o}C for one hour followed by three washes with D-PBS to remove the unbound peptides. Cells were fixed with 0.05% glutaraldehyde followed by the B3Z LacZ assay (**Fig. 3.1.3a**).

After incubation at 4^{o}C, only SIINFEKL peptide was able to induce a strong B3Z T cell response. The 3 N-terminally extended S8L variants and the peptide S8L-FLGG elicited responses at concentrations that were 3 orders of magnitude higher than those needed for equal responses to S8L. The response to the peptide S8L-FLGG was even 5 orders of magnitude less efficient. It was interesting to observe that bi-terminally extended SIINFEKL variants (DYKDDDDKA-S8L-GGGA/ DYKDDDDKA-S8L-FLGG) were unable to give any detectable response even at high concentrations. Thus, the weakly presented peptides were either unable to load onto cell surface K^b molecules and/or B3Z T–cells were not able to recognize extended SIINFEKL variants. It was possible that at

low temperature the loading with extended exogenous peptides was inefficient. Therefore, I have performed the same experiments at 37°C.

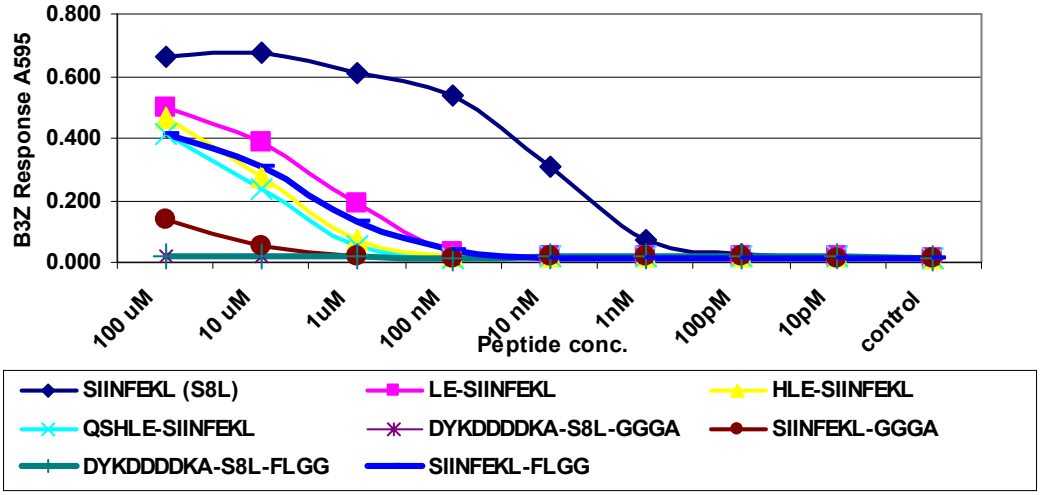

Figure 3.1.3a Exogenous peptide presentation at 4^{0}C

The P815/K^b cells were seeded in a 96-well plate and peptides were added for 60 min at 4^{0}C at the indicated concentrations. After incubation, cells were washed three times with D- PBS followed by fixation and B3Z readout.

Wortmannin, which inhibits recycling of MHC class I, was added to avoid the presentation of processed peptides that might be endocytosed and cleaved by endosomal proteases at room temperature. After incubation at 37°C, presentation of exogenous peptides by P815/K^b cells was 2 orders of magnitude more sensitive in comparison to 4°C, but no change in the hierarchy of peptides was observed **(Figure 3.1.3b)**. B3Z still did not mount a response to the bi-terminally extended SIINFEKL peptide.

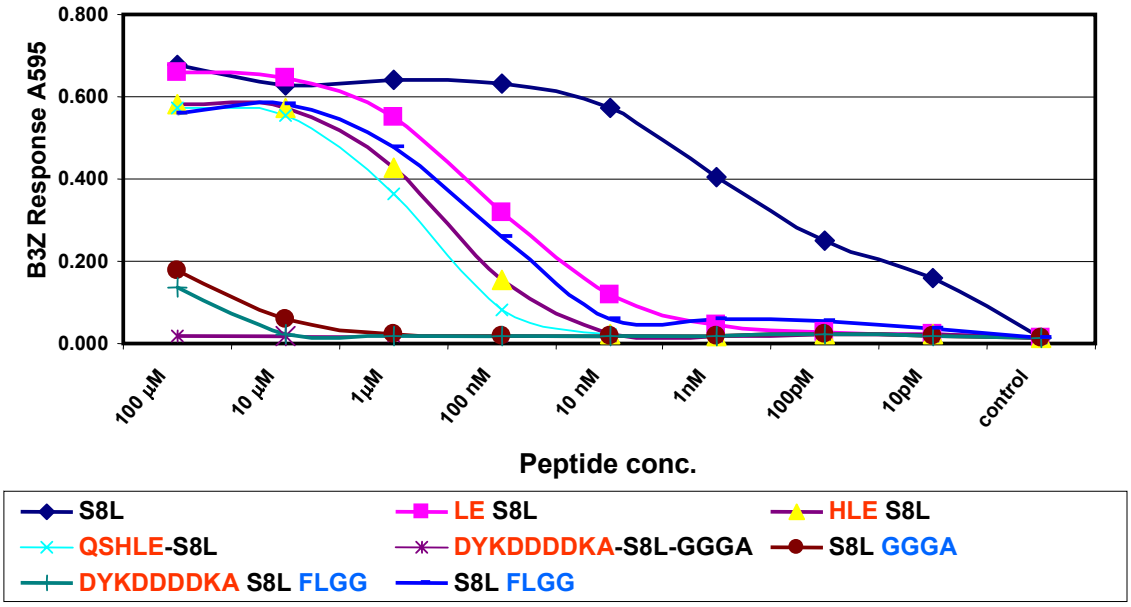

Figure 3.1.3b Exogenous peptide presentation by P815/K^b at 37°C in the presence of 1 mM wortmannin

The P815/K^b cells were seeded in a 96-well plate and peptides were added for 60 min at 37°C at the indicated concentrations. The cells were washed three times with D-PBS followed by fixation and B3Z readout.

Since the bi-terminally extended peptides exactly reflected the sequence context of X-S8L-sp11-K^b and X-S8L-sp19-K^b conjugates, these results strongly suggested that the conjugates had been processed prior to S8L/K^b presentation. This processing almost certainly involved N-terminal trimming. Regarding the relatively poor presentation of S8L variants extended at the C-terminus, also C-terminal processing appeared to be a possibility.

3.1.4 Expression of peptide-K^b conjugates in cells lacking components of the peptide loading complex

3.1.4.1 Role of TAP in peptide-K^b conjugates presentation

Immortalized TAP-deficient MCA fibroblasts, derived from the TAP1 knockout mouse (Van Kaer *et al*., 1992), were chosen to analyze the effect of peptide loading components on peptide-K^b conjugate presentation.

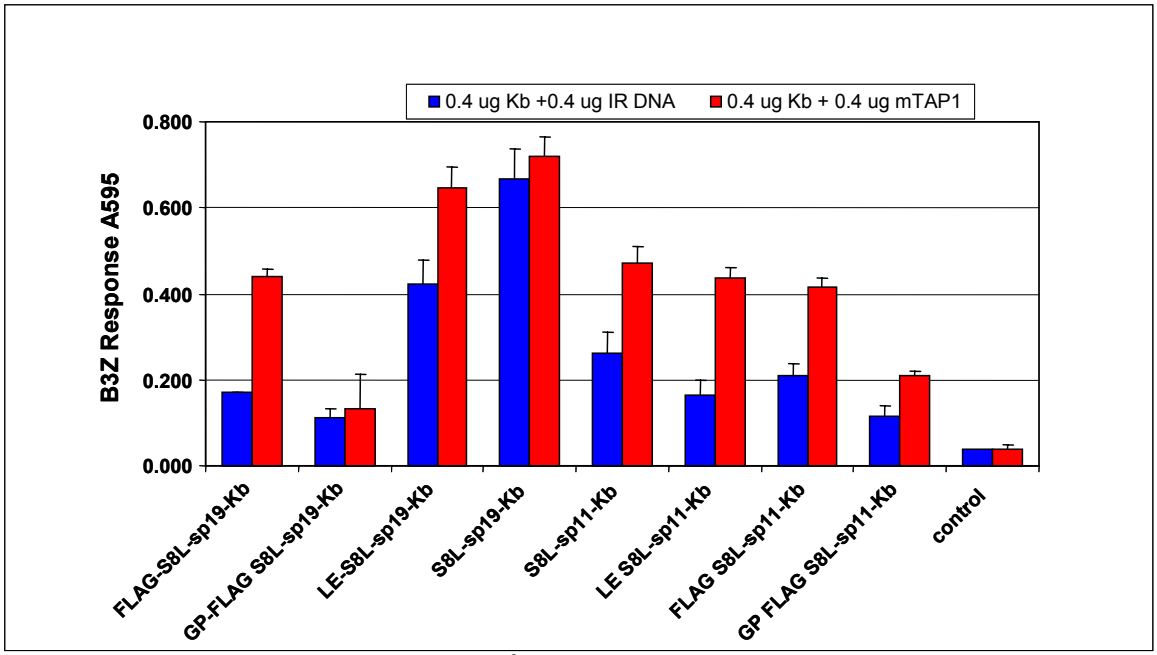

Figure 3.1.4a Influence of TAP on peptide-K^b conjugates presentation

1 x 10^4 cells were seeded in a 96-well plate one day prior to transfection. 48 hrs after transfection with the indicated S8L-K^b conjugates, cells were fixed followed by the B3Z T cell activation assay. Blue bars represent TAP1 knockout mouse cells (MCA) and red bars representing MCA cells reconstituted with mouse TAP1 cDNA.

As shown in **figure 3.1.4a**, all peptide-K^b conjugates were able to stimulate the B3Z T cell hybridoma which recognizes S8L:K^b complexes (Shastri *et al*., 1995). Longer extensions elicited lower responses and restoration of TAP complexes enhanced the presentation of K^b-peptide conjugates with long extensions. Extension of the *flag* sequence by Gly-Pro significantly reduced the T cell response.

Next, I modified the N-terminal extensions. As shown in figure **3.1.4b**, the RKKR-S8L-K^b conjugate was presented as efficiently as S8L-K^b, while the other N-terminally extended constructs elicited lower responses, with longer extensions producing gradually reduced B3Z responses. Presentation of the construct containing a 137 amino

acids residue N-terminal flank from the OVA sequence was, however, still detectable.

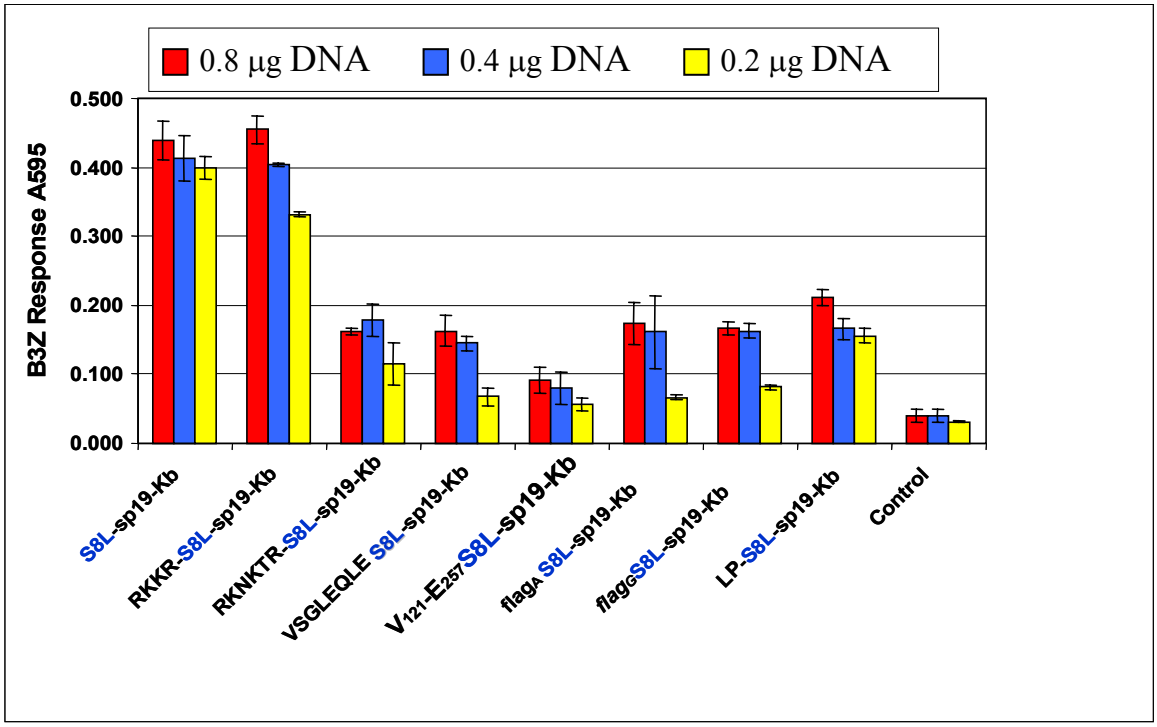

Figure 3.1.4b N-terminally extended peptide MHC conjugate presentation in TAP1-deficient cells.
1 x 10^4 TAP1-deficient MCA cells were seeded in a 96-well plate one day prior to transfection and various N-terminally extended conjugates DNA were analyzed using titrated amounts of DNA by transfection.

I have also investigated another TAP-deficient cell line, Ec7.1 cells (Howell et al., 2000). Ec7.1 cells were derived from the TAP2-deficient RMA-S cell line and due to mutagenesis they have also lost the expression of MHC-I (both K^b and D^b). Western blot analysis showed that it has also a reduced level of tapasin expression. Ec7.1 cells in which various K^b-peptide conjugates constructs were stably expressed showed a significant level of Y3 staining which shows that peptide-K^b conjugates were expressed on the cell surface. None of the constructs were, however, able to give the positive staining with 25.D1-16 recognizing S8L:K^b complexes. In these loading complex-deficient cells, the processing and loading of the S8L epitopes appeared to be impaired and in contrast to TAP-deficient MCA cells, these cells were unable to elicit B3Z response (**Fig. 3.1.4 c**)

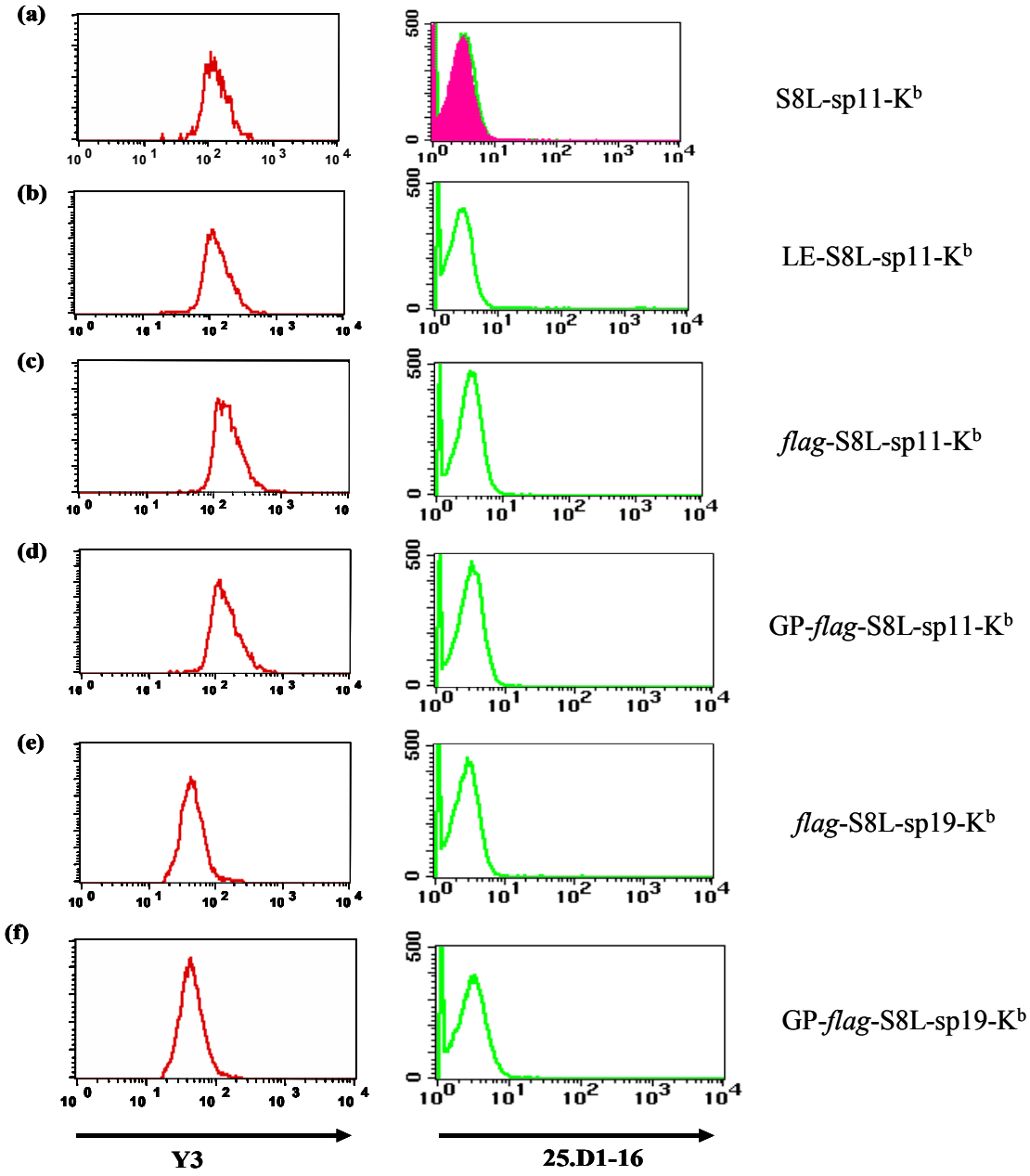

Figure 3.1.4c Cell surface expression of the peptide-K^b conjugates in TAP-deficient Ec7.1 cells. Ec7.1 cells were stably transfected with the indicated DNA constructs of peptide-Kb conjugates. Cells were stained with mAb Y3 recognizing folded H-2K^b and 25.D1-16 antibody which recognizes mouse MHC H-2K^b in conjunction with the OVA peptide SIINFEKL. The shaded area in the top panel indicates control antibody staining.

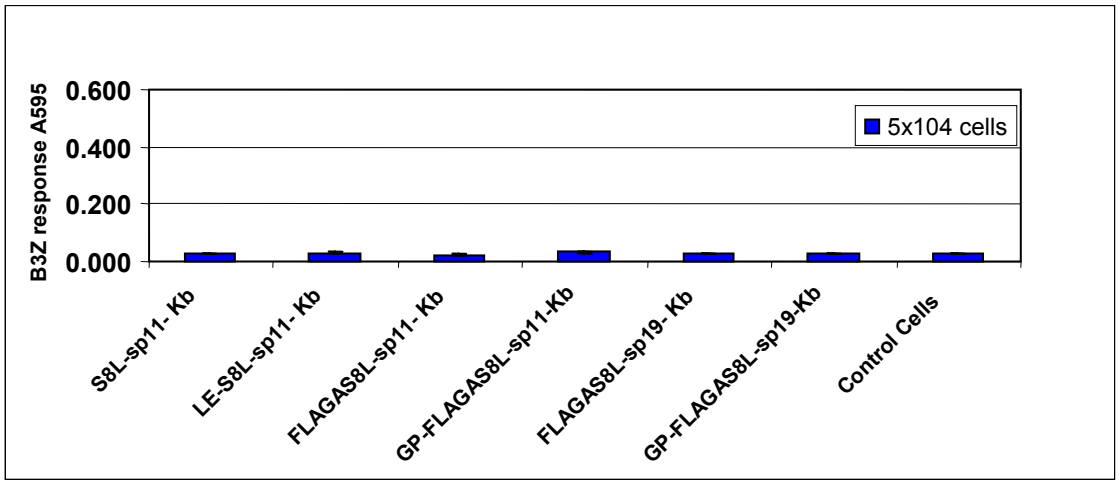

Figure 3.1.4d Stably expressed Ec7.1 cells were unable to elicit B3Z T cell responses.

Stably transfected Ec7.1 cells expressing the indicated constructs used in a standard B3Z LacZ assay.

3.1.4.2 Role of tapasin on peptide-K^b conjugates presentation

In the absence of ER-resident glycoprotein tapasin, TAP subunits are unstable (Garbi *et al*., 2003). MC4 cells are transformed fibroblasts derived from the tapasin knockout mouse (Garbi *et al*., 2001). In the absence of tapasin and TAP-mediated peptide transport, surface class I expression is drastically reduced. To check, whether tapasin influences the presentation of peptide-K^b conjugates, I transiently transfected the cells in a 96-well plate. Fourty eight hrs after transfection, the B3Z T cell assay was performed **(fig. 3.1.4e).**

It was interesting to observe that restoration of tapasin led to significantly improved presentation of extended conjugates both for spacer-11 as well as spacer-19 conjugates. The conjugates which did not have N-terminal extension (S8L-sp11-K^b/S8L-sp19-K^b) were unaffected by tapasin reconstitution. It was also interesting to note that in the construct extended with the sequence RKKR (Arg-Lys-Lys-Arg), the B3Z response remained high even in the absence of tapasin. These data suggest a contribution of tapasin and TAP to the formation of finally trimmed S8L:K^b complexes.

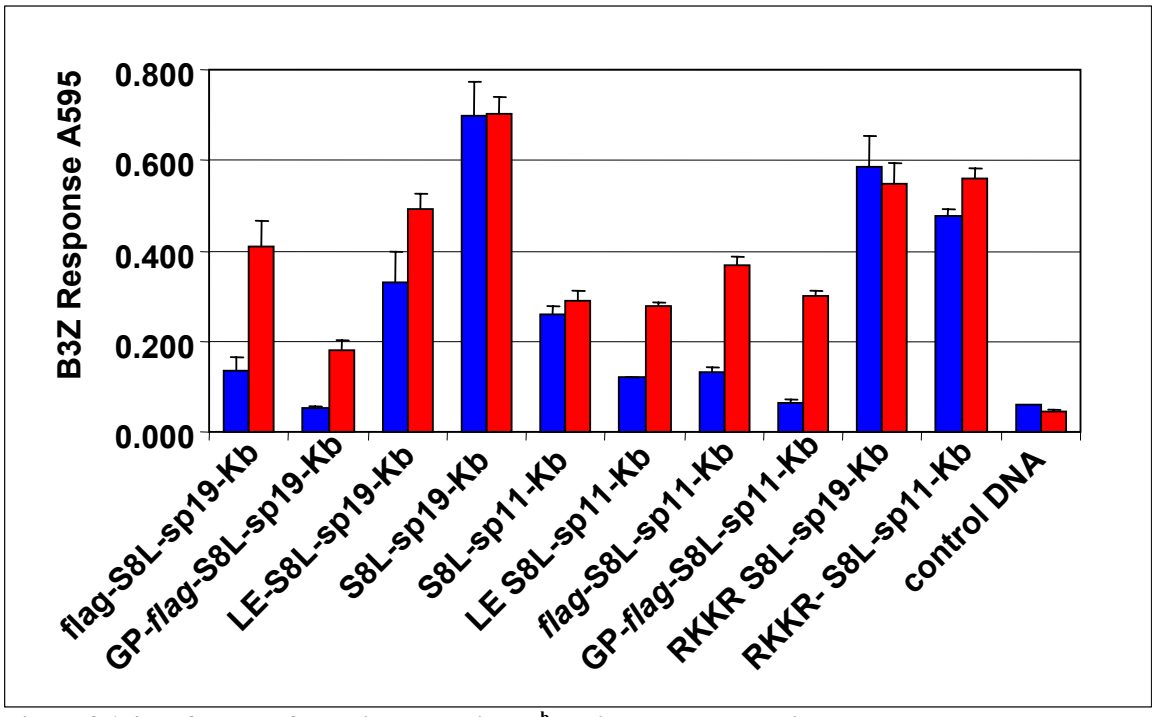

Figure 3.1.4e Influence of tapasin on peptide-K^b conjugates presentation.

1x 10^4 cells were seeded in a 96-well plate one day prior to transfection. 48 hrs after post transfection with the indicated S8L-Kb conjugates, cells were fixed followed by B3Z T cell activation assay. Blue bars represent tapasin knockout mouse cells (MC4) and red bars represent MC4 cell reconstituted with wild type mTpn cDNA.

3.1.4.3 Expression levels of TAP2 in Tpn$^{-/-}$ and TAP1$^{-/-}$ cells and in reconstituted cells

The expression levels of tapasin and TAP in reconstituted Tpn-deficient and TAP-deficient cells were assessed by Western blot. After 48 hrs of transient transfection, cells were lysed and proteins were separated by 10% SDS-PAGE. Western blot was performed using an anti-mouse TAP2 antibody. As a control, MC6 fibroblast cells derived from Tpn$^+$/TAP$^+$ B6 mice were taken which express all the components of the peptide loading complex. Calnexin was used as loading control for the Western blot.

In TAP1-deficient MCA cells, no TAP2 could be detected because TAP2 is unstable in the absence of TAP1. In tapasin-deficient MC4 cells, TAP2 expression was also undetectable. Transfection of mouse TAP1 cDNA into MCA cells and of mouse tapasin cDNA into MC4 cells partially restored TAP2 expression as shown in **figure 3.1.4f**. Apparently, this restoration was sufficient to cause improved B3Z responses.

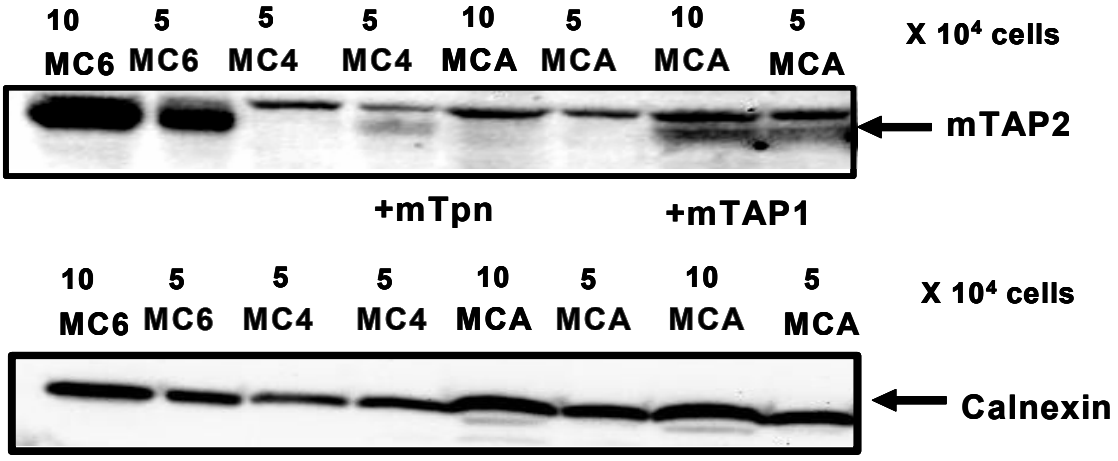

Figure 3.1.4f Analysis of expression level of Tpn and TAP in reconstituted cells

1 x 10^6 cells were lysed in 100 µl of 1% NP40 lysis buffer and protein was resolved by 10% SDS-PAGE followed by Western blot. The blot was developed using rabbit anti-mouse TAP2 and rabbit anti-calnexin polyclonal antibodies, respectively, and goat anti rabbit IgG peroxidase.

3.1.4.4 Role of ERp57/ER60 on peptide-K^b conjugates presentation.

ERp57 is a thiol-dependent oxidoreductase that has been shown to mediate disulfide bond formation in monoglycosylated glycoproteins. ERp57 may also function as general chaperone as it has been found to associate with non-cysteine containing glycoproteins. It was also suggested that ERp57 may act as protease. Within the peptide-loading complex, the function of ERp57 is not known. I have investigated whether ERp57 may have some role in peptide-K^b conjugates presentation. When I performed the experiments, ERp57 knockout mice were not available to assess its contribution to peptide loading. Therefore, I have used the siRNA gene silencing approach to downregulate this protein.

Downregulation of ERp57 by siRNA gene silencing

I explored the siRNA silencing approach to downmodulate the ERp57 as a possible trimming enzyme for N-terminally extended S8L conjugates. I made stably transfected ERp57 silenced cell line using pSUPER-derived plasmids (2269, 2272, and 2275), coding for 3 different small interfering hairpin, ERp57-specific RNA sequences driven by the H1-RNA promoter that were kindly provided by Dr. J. Neefjes, Amsterdam. A hygromycin resistance gene was inserted into this plasmid for selection of stable transfectants (F. Momburg, unpublished)

Using MC6 (wild type B6 TAP^{+}/Tpn^{+}), MC4 ($Tpn^{-/-}$) and MCA ($TAP1^{-/-}$) cell lines, I was able to downmodulate ERp57 protein levels to 4-6 % of the respective wild-type levels (**Fig.3.1.4g**).

In these ERp57-silenced cells, the cell surface expression of MHC class I was slightly reduced. However, I could not find significant changes in the processing of N-terminally extended peptide-K^{b} presentation in wild-type versus ERp57-silenced cells, suggesting that ERp57 played no essential role (**Fig. 3.1.4h and 3.1.4i**).

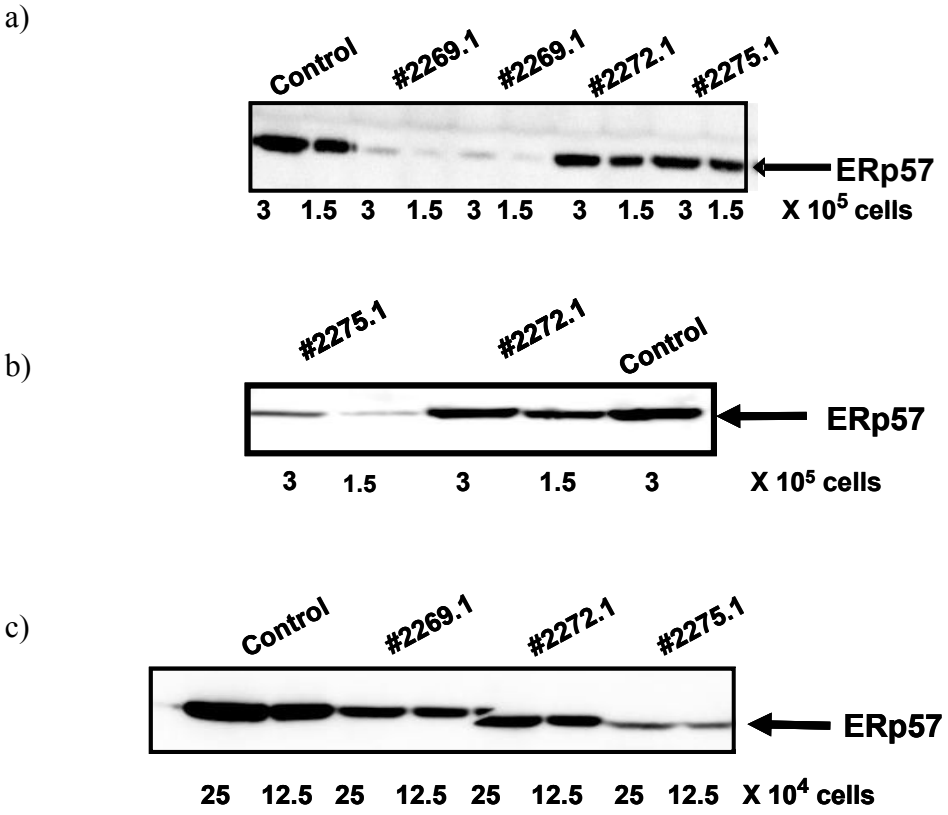

Figure 3.1.4g Analysis of expression levels of ERp57 in siRNA-silenced cells.

ERp57 downregulation was achieved using three different plasmids in which ERp57-specific siRNA was driven by the H1-RNA promoter. MC6, MC4 and MCA cells were transfected with the indicated constructs and selected with the antibiotic hygromycin. 1 x 10^{6} cells were lysed in 100 µl of 1% NP40 lysis buffer and protein was resolved in 10% SDS-PAGE followed by Western blot. The blot was developed using rabbit anti-mouse ER60 followed by anti-rabbit IgG peroxidase.

a) MC6 TAP^{+}/Tpn^{+} ERp57-silenced cells b) MC4 $Tpn^{-/-}$ ERp57-silenced cells c) MCA $TAP1^{-/-}$ ERp57-silenced cells

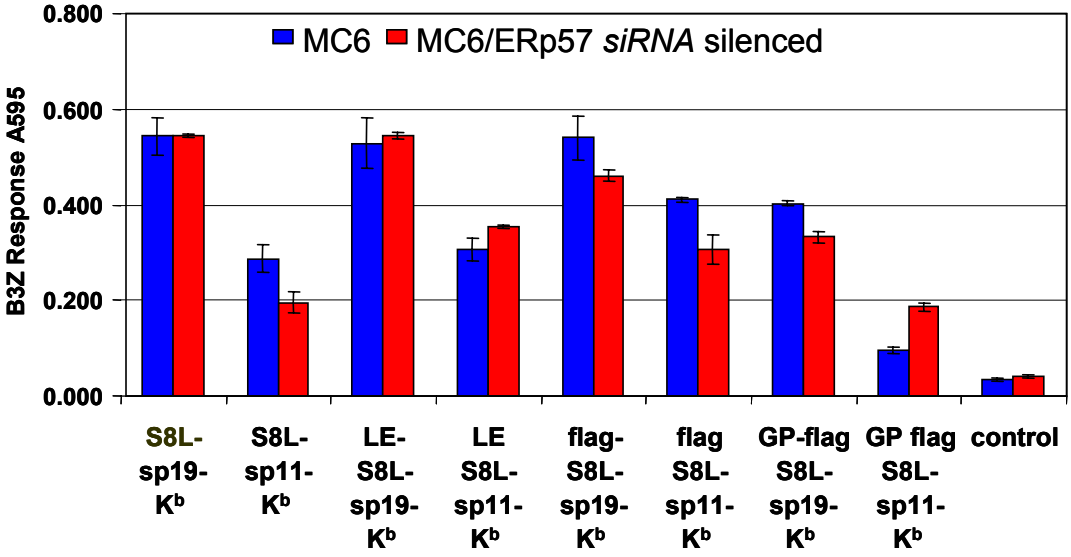

Figure 3.1.4h Influence of ERp57 on peptide-K^b conjugates presentation by PLC-proficient MC6 cells.

MC6 cells stably transfected with an ERp57 siRNA encoding plasmid (pFM2269) were transiently transfected with 0.4 μg/well of the indicated construct for 48 hrs, followed by the B3Z T cells assay.

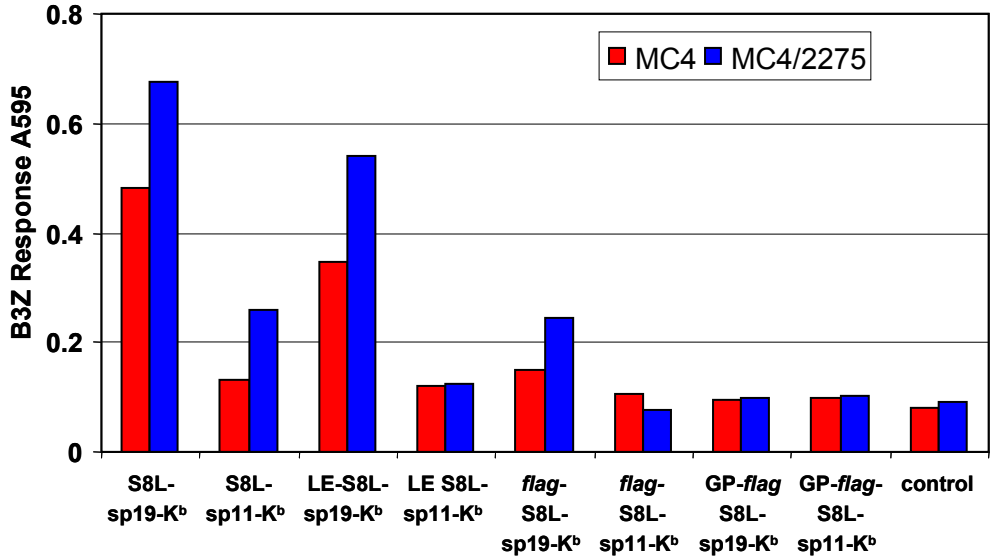

Figure 3.1.4i Influence of ERp57 on peptide-K^b conjugates presentation by tapasin-deficient cells.

MC6 cells stably transfected with an ERp57 siRNA encoded plasmid (pFM2275) were transiently transfected with 0.4 μg/well of the indicated construct for 48 hrs, followed by the B3Z T cells assay.

Summary of section 3.1.4

So far, we have seen that among the peptide loading complex components, the presence of TAP and tapasin enhanced presentation of N-terminally extended peptide-K^b conjugates presentation but not of optimally trimmed peptide conjugates. Whether these results could be attributed to a positive effect of TAP and tapasin on conjugate folding and ER egress, or whether it was due to retrotranslocation of misfolded conjugates followed by TAP-mediated peptide import, was addressed in the next section using inhibitors of cytosolic proteases (e.g. proteasomes, TPPII).

3.1.5 Kinetics of reappearance of peptide-K^b conjugates in P815 cells

In order to study the effect of proteasomal inhibitors, we first had to establish the kinetics of reappearance of S8L-loaded K^b molecules after removal of pre-existing complexes from the cell surface. The cell surface expression levels of different peptide-K^b conjugates at steady state were approximately similar as judged by FACS analysis (see **fig. 3.1.2a**). I wanted to analyze how much time was required for the reappearance of S8L:K^b complexes after an acid wash (pH 3.0) (Storkus *et al.*, 1993). The isotonic acid-wash technique has previously been employed to remove pre-existing peptides from the cell surface of MHC class I molecules (Serwold *et al.*, 2001; Serwold *et al.*, 2002). Unexpectedly, the rate of reappearance of S8L:K^b complexes from the *flag*-S8L-sp11-K^b construct was faster than from S8L-sp11-K^b which does not require N-terminal trimming **(Fig. 3.1.5).** Even 10 hours after the acid-wash, S8L:K^b complexes had not recovered in the P815 cells expressing the GP-*flag*-S8L-sp11-K^b construct. This suggested again that N-terminal trimming of this construct was very inefficient. The slower reappearance of S8L:K^b complexes in P815/S8L-sp11-K^b cells as compared with P815/*flag*-S8L-sp11-K^b cells might be explained by slightly lower expression levels of the former construct in these stably transfectant cell lines (**Fig 3.1.2a**). Under steady state conditions, i.e. without acid-wash, the production of S8L:K^b complexes from S8L-sp11-K^b, LE-S8L-sp11-K^b and *flag*-S8L-sp11-K^b conjugates were approximately equal.

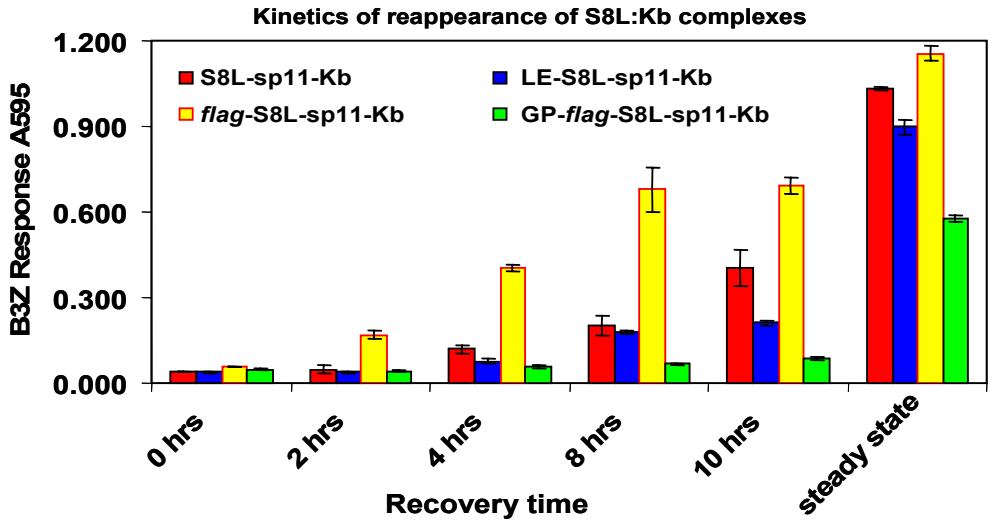

Figure 3.1.5 Reappearance of S8L:K^b complexes in acid-stripped P815 transfectants.

Stably transfected P815 cells expressing the indicated constructs were acid washed. 5 x 10^4 cells were transferred into 96-well plates and fixed after the indicated time periods. 5 x 10^4 B3Z cells were added for another 18 hrs and the LacZ assay was performed.

3.1.6 Effect of proteasomal inhibitors on peptide-K^b conjugates presentation

To determine whether the presentation of S8L:K^b complexes was due to cytosolic retrotransloaction of misfolded conjugates, subsequent degradation by proteasomes and import of free peptides via TAP, I tested the irreversibly binding proteasomal inhibitor lactacystin for its ability to block presentation. Stably transfected P815 cells, which express all components of the loading complex, were used for the acid-wash recovery assay. Various time points were chosen in order to allow for the reappearance of S8L:K^b complex formation in *flag*-S8L-sp11-K^b P815 cells. As a positive control I have taken RMA cells expressing ovalbumin in the cytosol, because the generation of the SIINFEKL epitope from cytosolic full-length OVA protein requires proteasomal activity. My result show that the S8L:K^b complex formation from *flag*-S8L-sp11-K^b was unaltered in lactacystin-treated, TAP-competent P815 cells (**Fig. 3.1.6a**).

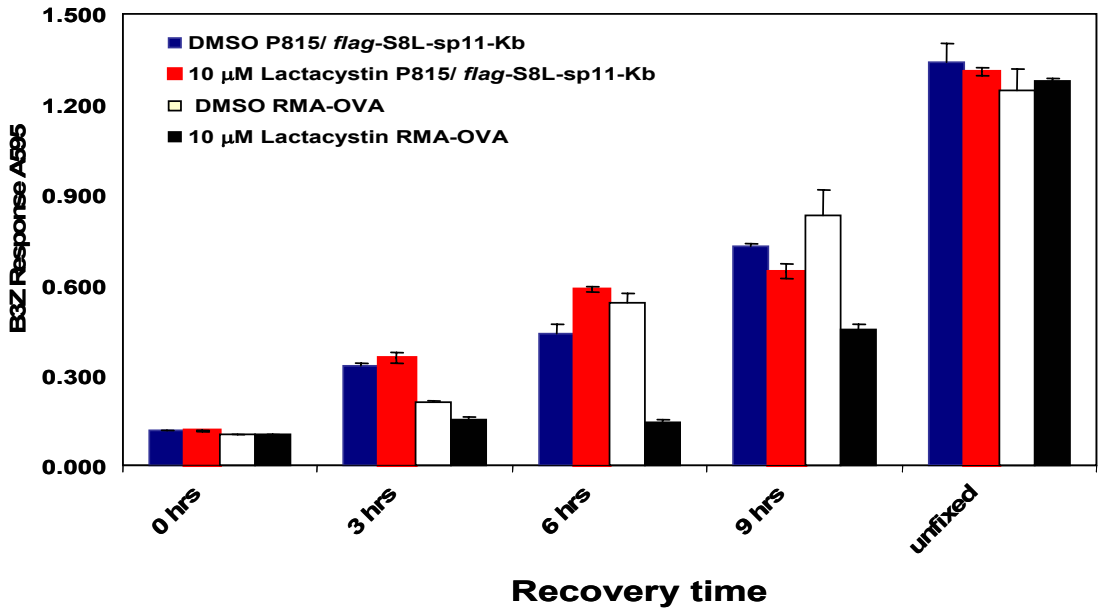

Figure 3.1.6a The proteasomal inhibitor lactacystin does not alter the cell surface reappearance of S8L:K^b complexes processed from an extended S8L-K^b conjugate.

P815 cells stably transfected with the construct flag-S8L-sp11-Kb and RMA cells stably expressing cytosolic OVA protein were treated with 10 µM lactacystin 30 min prior to acid wash treatment and cells were allowed to recover for indicated time points in the presence or absence of the proteasomal inhibitor. After each time point, cells were fixed. 5x 10^4 B3Z cells were added for another 18 hour and the LacZ assay was performed.

The presentation of S8L:K^b complex formation from cytosolic OVA protein was completely blocked at 6 hours of lactacystin treatment, but than slowly recovered. This is likely due to the consumption of this unstable compound. The experiment suggests

that proteasomes likely do not generate free SIINFEKL peptide from the conjugate and the observed presentation of S8L:K^b complexes to B3Z cells.

In another experiment (**Fig. 3.1.6b**), I have tested the peptide aldehyde proteasomal inhibitors, MG132 and LLnL, which, however, also inhibit the ER signal peptidase (Hughes *et al*., 1996).

As expected, our results indicate that the B3Z response was fully inhibited by treatment with LLnL and partially with MG132, but again the proteasome-specific inhibitors lactacystin did not impair the presentation. This finding suggests that the *flag*-S8L-sp11-K^b conjugate needs to be inserted into the ER membrane with the help of signal peptidase in order to detect presentation.

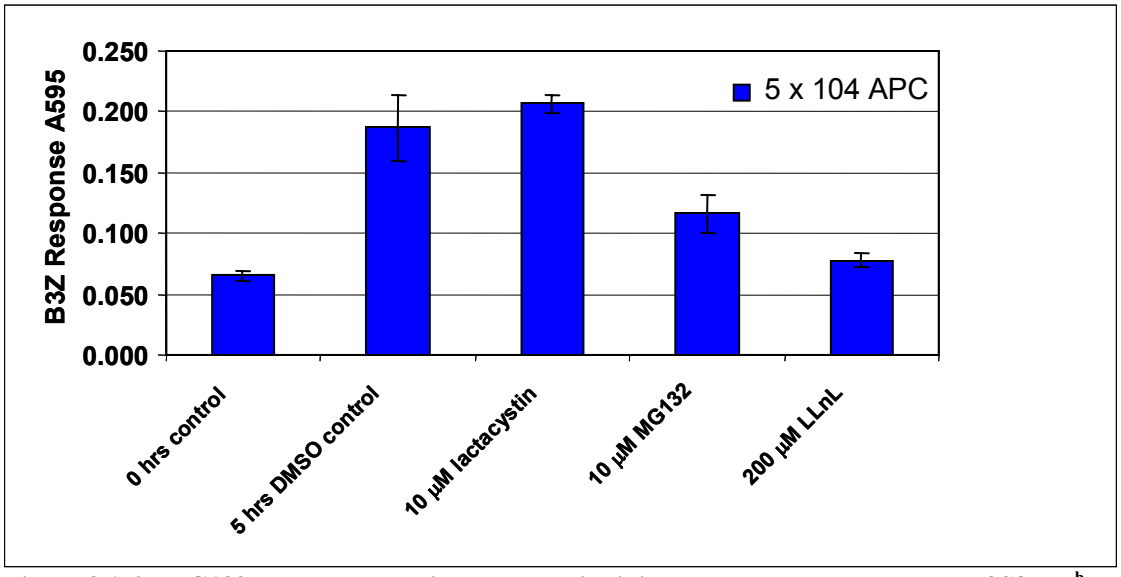

Figure 3.1.6b MG132 and LLnL peptide aldehyde inhibitors block the reappearance of S8L:K^b complexes.

P815 cells stably transfected with the construct *flag*-S8L-sp11-K^b were treated with 10 µM lactacystin, 10 µM MG132 or 200 µM LLnL 30 min prior to acid wash treatment. Cells were allowed to recover for 5 hrs in the presence or absence (DMSO) of inhibitors. Thereafter cells were fixed and 5 x 10^4 B3Z cells were added for another 18 hrs followed by the LacZ assay.

To investigate whether the cytosolic aminopeptidase, tripeptidyl peptidase II (TPP II), plays a role in peptide-K^b conjugates processing, I have treated the same cells (i.e., P815/*flag*-S8L-sp11-K^b) overnight with butabindide, which is a potent inhibitor of TPPII, followed by the acid-wash recovery assay. TPPII, a cytosolic subtilisin-like peptidase, was shown to digest proteasomal products and to exhibits endo- as well as exopeptidase activity (Reits et al., 2004). TPPII thus can act in concert with the

proteasome in the degradation of cytosolic proteins and peptides.

As shown in **figure 3.1.6c**, even after using high concentrations of butabindide and long incubation times, presentation remained unaffected. This indicates that TPP II does not play a significant role for the processing of *flag*-S8L-sp11-K^b conjugates.

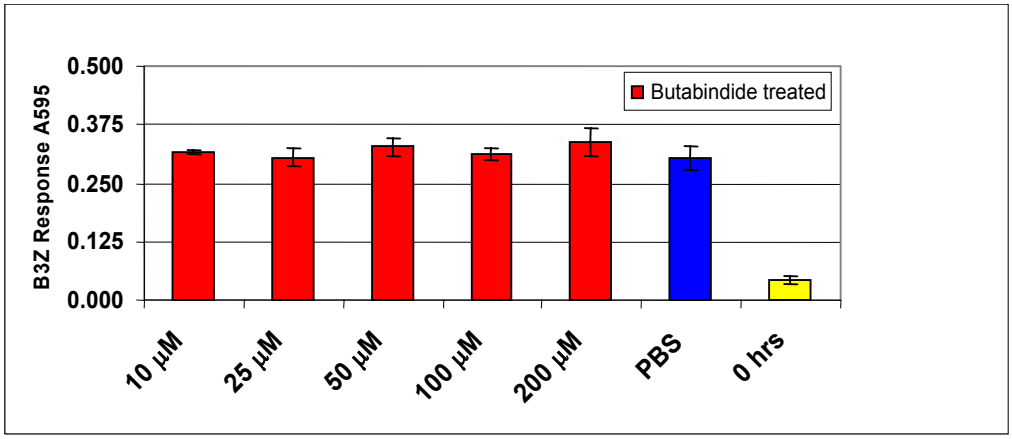

Figure 3.1.6c TPP II inhibition assay.

P815 cells stably transfected with the construct *flag*-S8L-sp11-K^b were treated with different concentrations of butabindide overnight prior to acid wash treatment and 5 hrs recovery in the presence or absence of inhibitor. After 5 hrs cells were fixed, 5x 10^4 B3Z cells were added for another 18hrs and the LacZ assay was performed. Red bars represent butabindide treated cells, the blue bar represents PBS-treated cells and the yellow bar shows cells that were immediately fixed after the acid wash.

3.1.7 Effect of aminopeptidase inhibitors on peptide-K^b conjugates presentation to B3Z T-cell hybridoma.

Ours experiments using exogenously added extended peptides **(see Fig. 3.1.3a and 3.1.3b)** and the available literature suggest that N-terminal extensions of S8L are poorly recognized by B3Z (Paz *et al*., 1999). Therefore, I was interested whether inhibitors of aminopeptidases were able to block the presentation of N-terminally extended conjugates.

To this end, I have tested several known aminopeptidase inhibitors at sub-toxic concentrations. The cell viability was always checked by the MTT assay and the Trypan Blue exclusion method, respectively.

P815 cells stably expressing N-terminally extended S8L-K^b conjugates and S8L-K^b were used in reappearance assays in the presence of aminopeptidase inhibitors. Cells were pre-incubated overnight in the presence or absence of inhibitors, acid-washed, and

allowed to recover for 12 hrs in the presence of the same inhibitors. Cell surface expression of S8L/K^b complexes were monitored using the B3Z T cell hybridoma.

TABLE 2

AMINOPEPTIDASE INHIBITOR	USED CONC.	EFFECT
Amastatin	10 μM	No
Bestatin	10 μM	No
LCMK	75 μM	No
Leucinethiol	125 μM	No
1,10-phenanthroline	2.5 μM	No
$ZnCl_2$	100 μM	No

I was unable to inhibit the presentation by treatment with any of these aminopeptidase inhibitors **(Table 2)**.

3.1.7.1 Effect of ERAP1/ERAAP on presentation of peptide-K^b conjugates.

While we were looking for the effect of aminopeptidase inhibitors, two groups (N. Shastri at the University of California, Berkeley, USA, and K. L. Rock, MIT, Boston, USA) had simultaneously discovered an ER-resident aminopeptidase in mouse cells and human cells, respectively (Serwold *et al*., 2002; York *et al*., 2002). They have named this enzyme ERAAP in the mouse and ERAP1 for human, respectively.

ERAP1 or ERAAP:

ERAAP is a member of the M1 family of zinc metalloproteases that are defined by a highly conserved His-Glu-X-X-His-X_{18}-Glu motif in the core peptidase unit. It has a leader sequence and is localized in endoplasmic reticulum. In human cells, a second ER aminopeptidase L-RAP/ERAP2/MAMS has also been described (Tanioka *et al*., 2003; Tanioka *et al*., 2005).

3.1.7.2 Influence of ERAAP silencing on peptide-K^b conjugates presentation

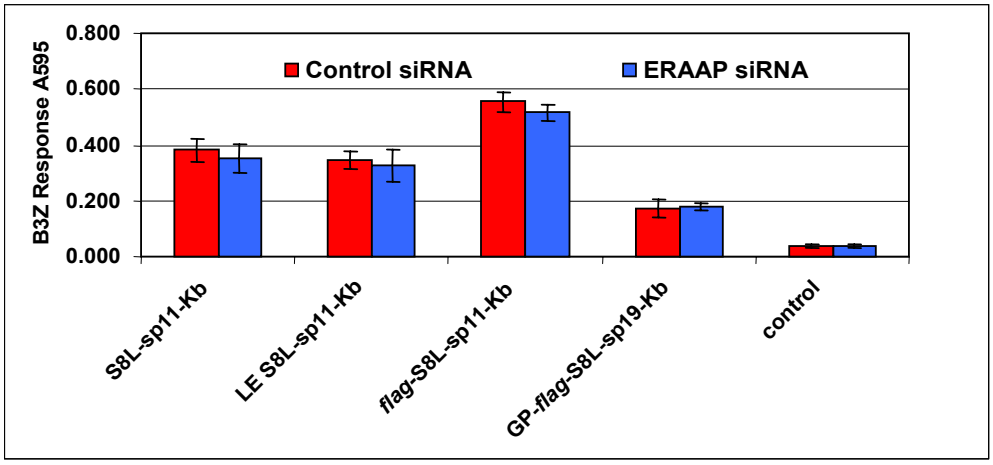

Figure 3.1.7a Effect of mouse ERAAP siRNA in peptide-K^b conjugates.

Stably expressed P815 cells with above mentioned construct were transiently transfected with control and ERAAP siRNA for 72 hrs. 1x10^4 cells fixed APC were co-cultured with 5 x 10^4 B3Z cells overnight in a 96-well plate for 18 hrs followed by the LacZ assay. All the conjugates were in triplicate and experiments were repeated three times.

I explored the siRNA silencing approach to downmodulate the ER aminopeptidase ERAAP as possible trimming enzyme for N-terminal extended S8L conjugates. However, I could not find any significant changes as compared with control siRNA-transfected cells, suggesting that ERAAP does not play a role in the processing of N-terminally extended conjugates **(Fig. 3.1.7a)**.

3.1.7.3 Overexpression of known ER aminopeptidases

Next, I overexpressed ER aminopeptidases to study their influence on peptide-K^b conjugate presentation. For this analysis I have taken the TAP-deficient fibroblast cell line MCA, derived from the TAP1$^{-/-}$ mouse. MCA cells were transiently co-transfected for 48 hrs with various N-terminally extended conjugates and cDNAs for human ERAP1 (York *et al*., 2002), its mouse homologous ERAAP (Serwold *et al*., 2002) as well as human ERAP2/L-RAP/MAMS. As shown in **figure 3.1.7b**, I could not detect an effect of aminopeptidase co-expression on the efficiency of S8L:K^b complex presentation to B3Z. The overexpression of ERAP1, ERAAP and MAMS was verified by rabbit antisera against ERAAP and MAMS and anti-His-tag antibody detecting (His)6-conjugated MAMS (data not shown). Apparently, the known ER aminopeptidase/s that are involved in the trimming of peptides imported by TAP, did

not significantly contribute the processing of our peptide-K^b conjugates.

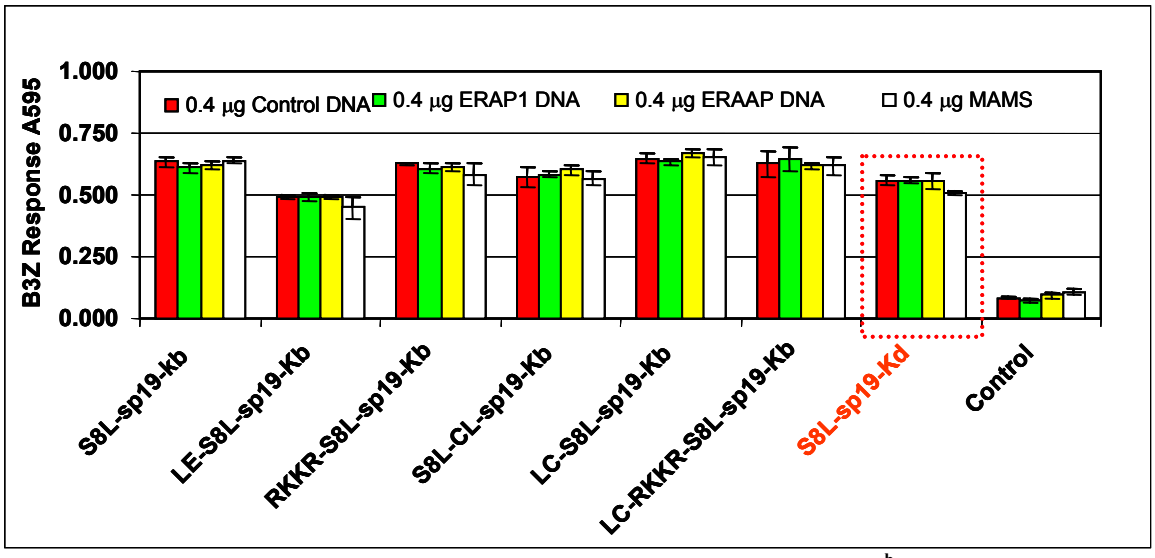

Figure 3.1.7b Effect of overexpression of ER aminopeptidases on peptide-K^b conjugates presentation

1x 10^4 MCA cells were transiently co-transfected with cDNAs for the indicated aminopeptidases and 0.4 µg/wells peptide-K^b conjugates for 48 hrs in a 96-well plate. After the transfection, cells were co-culture with 5 x 10^4 B3Z T cell hybridoma for another 18 hrs followed by LacZ assay.

Another very important observation was made while studying the presentation of the SIINFEKL peptide tethered to the unrelated MHC class I molecule H-$2K^d$ by a 19 residue linker. This conjugate itself can not induce the B3Z T cell response which specifically recognizes S8L/K^b but not S8L/K^d. As shown in **figure 3.1.7b** next to the control, there was an efficient response to S8L-sp19-K^d. It can be concluded that S8L peptide was librated from S8L-sp19-K^d by an endopeptidase.

Except for signal peptidase which is not predicted to cleave after the SIINFEKL sequence in our conjugates, there is no evidence for an endopeptidase activity in the ER lumen (Shastri *et al*., 2002). As these cells were TAP deficient, peptide retranslocation and proteasomal cleavage could be ruled out. The findings therefore indicated processing in a post-ER compartment (See part II).

3.1.8 Influence of MHC I glycosylation on peptide-K^b conjugates presentation.

MHC class I is a type I glycoprotein and it acquires a proper conformation with the help of the lectin-like chaperones calnexin and calreticulin. Mouse H-$2K^b$ molecules have two N-glycosylation sites (**Asn**-X-Ser/Thr Berg and Grinnell, 1993; Rademacher *et al.*, 1988) at position 86, which is known to interact with calreticulin, and an other one at

176, which is a target for calnexin.

In the *flag*-S8L-sp19-K^b construct, the mutations **N86S** and **N176Q** were introduced individually or together. All mutants showed a two-fold reduction (**fig.3.1.8a**), suggesting that the function of calreticulin and calnexin, which participate in the murine TAP-associated loading complex, were indirectly required for the processing of the conjugates.

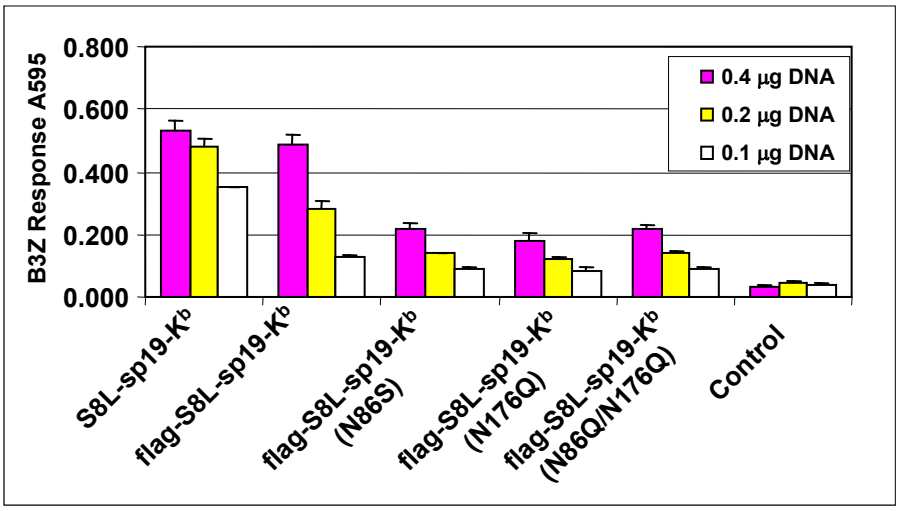

Figure 3.1.8a Influence of glycosylation on presentation of transiently transfected peptide-K^b conjugates.

1 x 10^4 P815 cells were seeded in a 96-well plate in triplicates one day prior to transfection. 48 hrs post transfection, cells were fixed followed by the B3Z T cell activation assay.

This observed reduction could be also due to misfolding and enhanced ER-associated degradation in the absence of a proper interaction with calnexin and calreticulin. I also made stable cell lines of these glycosylation mutants which were expressed in P815 cells. As shown in **(Fig. 3.1.8b)**, the wild-type and non-glycosylated *flag*-S8L-sp19-K^b variants were presented with equal efficiency in stably transfected P815 cells. Apparently, the processing defects of incompletely glycosylated K^b mutants were subtle and thus not detectable under steady-state conditions.

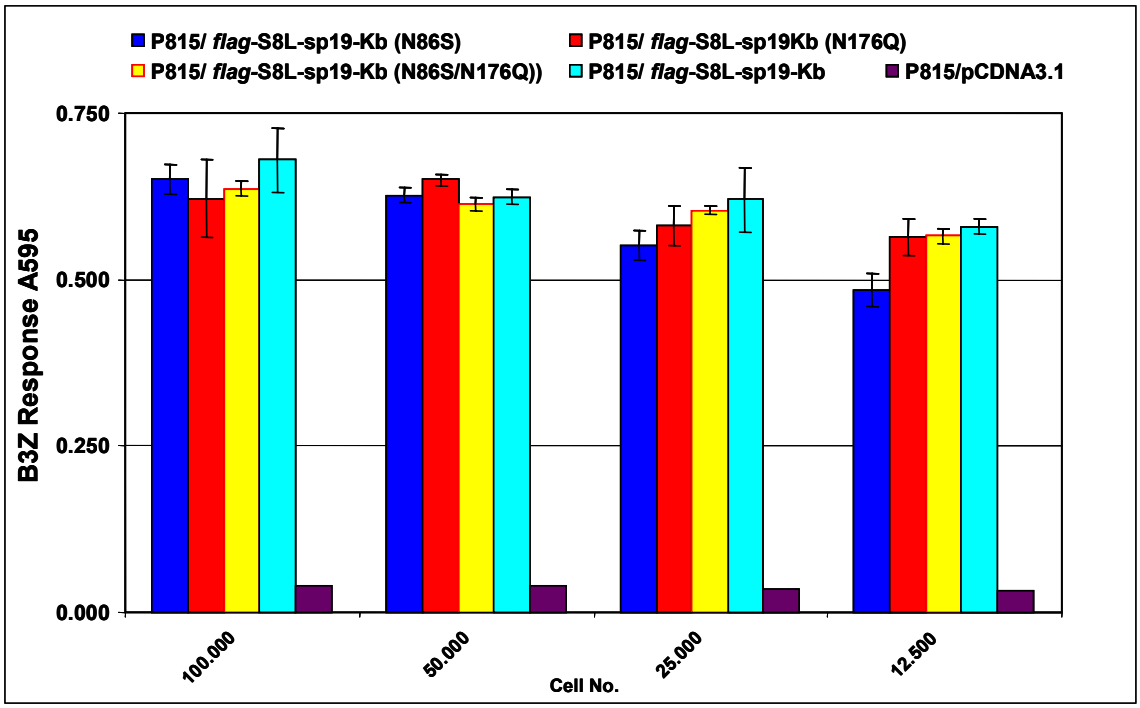

Figure 3.1.8b Stable expression of glycosylation mutants and influence of antigen processing/presentation

Stably transfected P815 cells with the indicated glycosylation mutant conjugates were analyzed. Peptide-K^b conjugates expressing P815 cells were titrated as mentioned. 5 x 10^4 B3Z T cells were added for 18 hrs followed by the LacZ assay.

3.1.9 Are B3Z cells themselves involved in the processing of conjugates?

In one report it was claimed that B3Z cells themselves can cause the proteolysis of some exogenous soluble proteins (Diegel *et al*., 2003). To rule out such kind of phenomenon I performed the B3Z assay in the presence of chymostatin, a serum protease inhibitor that was reported to block the proteolysis by a B3Z-associated protease. P815 cells expressing the *flag*-S8L-sp11-K^b conjugate were co-cultured with B3Z cells pretreated with 200 μM chymostatin, which was present during the entire assay. I could not find any influence of chymostatin treatment indicating that B3Z-associated serum proteases were not responsible for conjugate processing (**Fig. 3.1.9**).

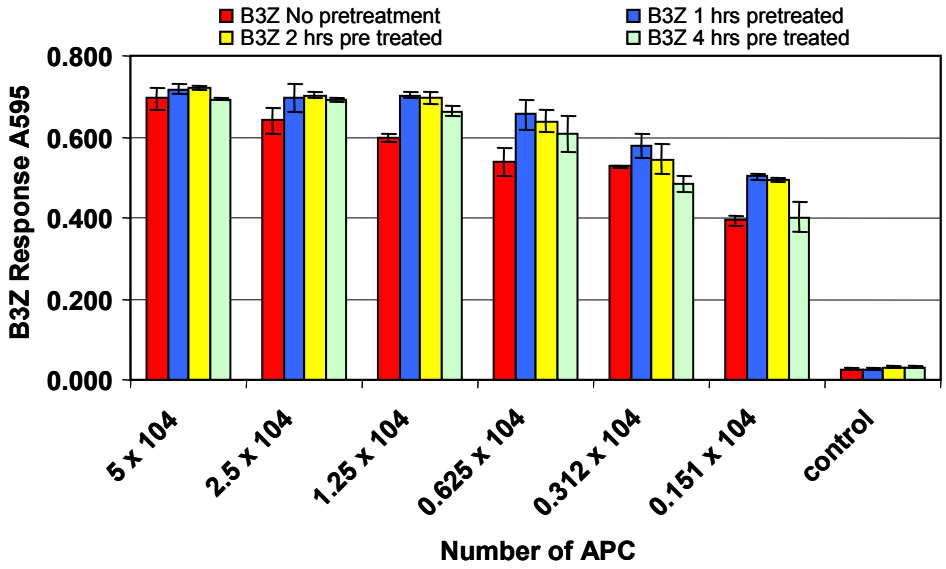

Figure 3.1.9 Effect of chymostatin on conjugates presentation

Stably expressing *flag*-S8L-sp-11-K^b P815 cells were used in a T cell stimulation assay with B3Z cells, pretreated with 200 μM chymostatin followed by co-incubation with the transfectants in the presence of 200 μM chymostatin. For control, B3Z cells received no pretreatment and chymostatin was absent during the assay.

3.1.10 Are trimmed or untrimmed peptides presented?

The experiments described so far suggested the processing of peptides from our conjugates but I sought additional biochemical evidence to prove this point. Maleimide polyethylene glycol (PEG-mal is a 5 kDa polymer which covalently couples to free cysteines (Yang *et al*., 2003). I transfected peptide-K^b conjugates containing single cysteine residues either N- or C-terminally adjacent to the S8L epitopes. Live cells expressing cysteine-carrying conjugates were incubated with PEG-mal. If free cysteine residue were available in S8L-loaded K^b complexes, the chemical conjugation of the bulky PEG moieties should interfere with TCR binding and suppress the response of B3Z cells.

TAP-deficient MCA cells were transiently transfected with the constructs shown in **Fig 3.1.10**.

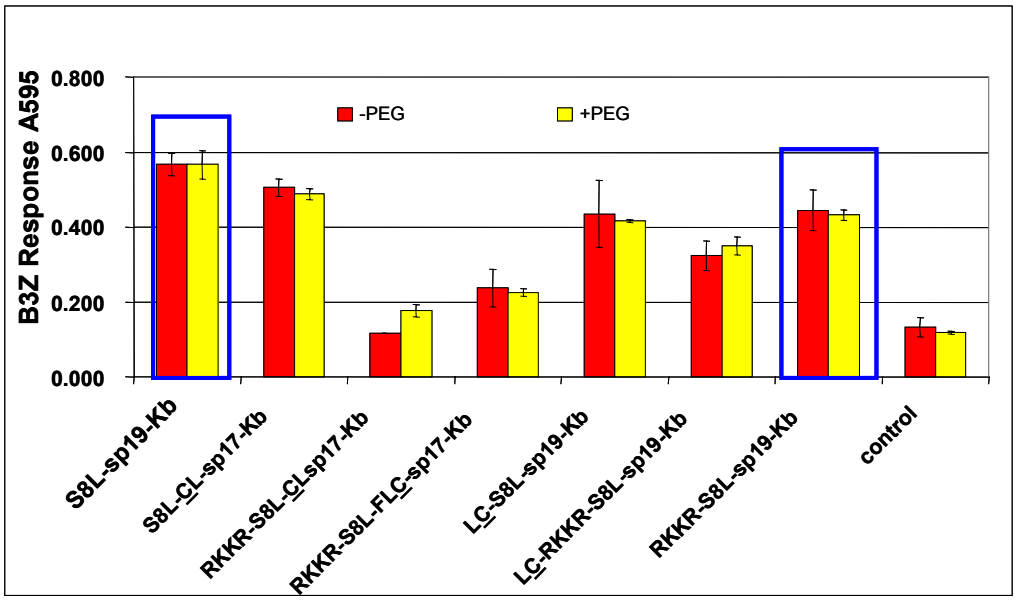

Figure 3.1.10 Effect of PEGylation on the presentation of conjugates containing N- or C-terminally adjacent, unpaired cysteine residues.

1x 10^4 MCA cells were transiently transfected with 0.4 µg/well DNA of the indicated constructs in 96-well plates. 48 hrs after transfection, cells were washed twice with D-PBS and then treated with 2 µM PEG-mal for another 20 minutes followed by extensive washing and fixation. The PEG-mal treated cells were co-culture with 5 x 10^4 B3Z cells/well for 18 hrs and the lacZ assay was performed.

I included two controls (S8L-sp19-K^b and RKKR-S8L-sp19-K^b) which contained no unpaired cysteine residues. However, I could not find any deference between PEG-mal treated and untreated cells. This negative result again suggests that the S8L epitopes had been processed out of the sequence context prior to K^b binding. Incubation of transfectants with PEG-mal was able to increase the apparent molecular weight of subpopulation of K^b-peptide conjugates as visualized in Western blot using C-terminally His-tagged conjugates (data not shown), indicating successful PEGylation.

3.1.11 Effect of N- and C-terminal flanking residues on conjugates presentation

To explore the influence of different amino acids at the N-terminal flank on S8L trimming, I generated a series of N–terminally substituted constructs. MCA cells were transfected for 48 hrs followed by the B3Z T cell activation assay.

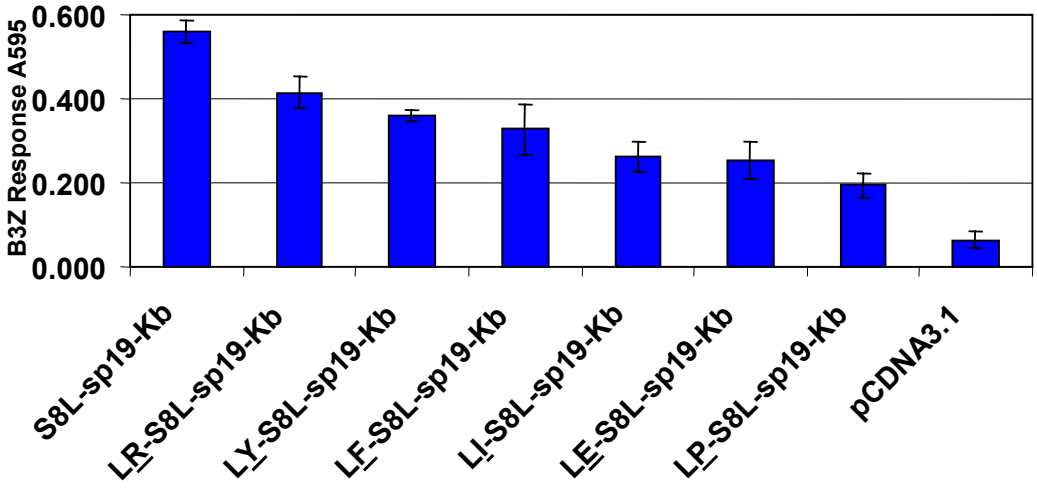

Figure 3.1.11a Role of flanking amino acids on N-terminal trimming

1x 10^4 MCA cells were transiently transfected with 0.4 µg/well DNA of the indicated constructs for 48 hrs followed by the B3Z T cell activation assay. All transfections were done in 96-well plate and samples were in triplicate.

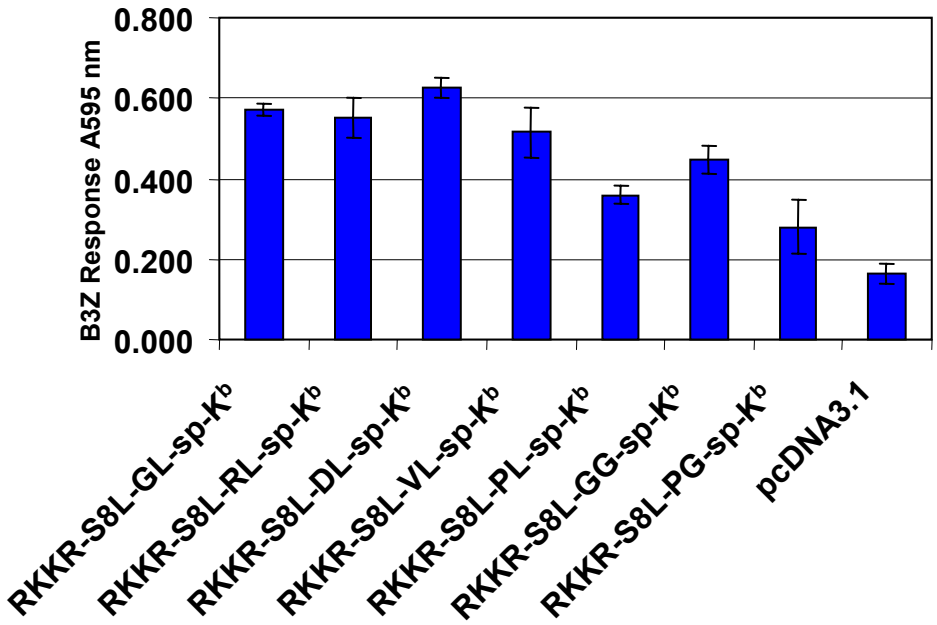

Figure 3.1.11b Role of flanking amino acids on C-terminal trimming

1x 10^4 MCA cells were transiently transfected with 0.4 µg/well DNA of the indicated constructs for 48 hrs followed by the B3Z T cell activation assay. All transfections were done in 96-well plate and samples were in triplicate.

As shown in figure **3.1.11a** clear differences were observed in the efficiencies of presentation using LX-S8L-sp19-K^b constructs with X= proline (P) and glutamine (E) having the lowest efficiencies. Apparently, the unknown trimming amino-peptidase activity in charge exhibits a preference for particular amino acids. Furthermore, I have analyzed the effect of C-terminal flanks of SL8 by replacing the flanking residues Phe-Leu in the sp19 linker of RKKR-S8L-sp19-K^b constructs by various XL sequences, PG and GG, respectively. Again, flanking proline residues reduced the efficiency of processing and presentation (figure **3.1.11b**).

3.1.12 Is the B3Z response due to ER processing or are alternative pathways involved?

Since the processing of peptide-K^b conjugates was not detectably affected by inhibitors of ER/cytosolic proteases, I reasoned that it may be a function of alternative class I processing pathways. Therefore, I treated the cells with bafilomycinA_1 (Baf A_1), which is a potent proton pump inhibitor that prevents the acidification of endosomes and lysosomes. As shown in figure 3.1.12, to our surprise I found that in bafilomycin A_1-treated cells the presentation of *flag*-S8L-K^b was completely abolished. Bafilomycin A_1 was not cytotoxic at the concentrations used in our experiments. These data strongly suggested that N-terminal trimming took place in acidic compartments, where pH regulation is most important for vesicular trafficking and the function of endoproteases (cathepsins).

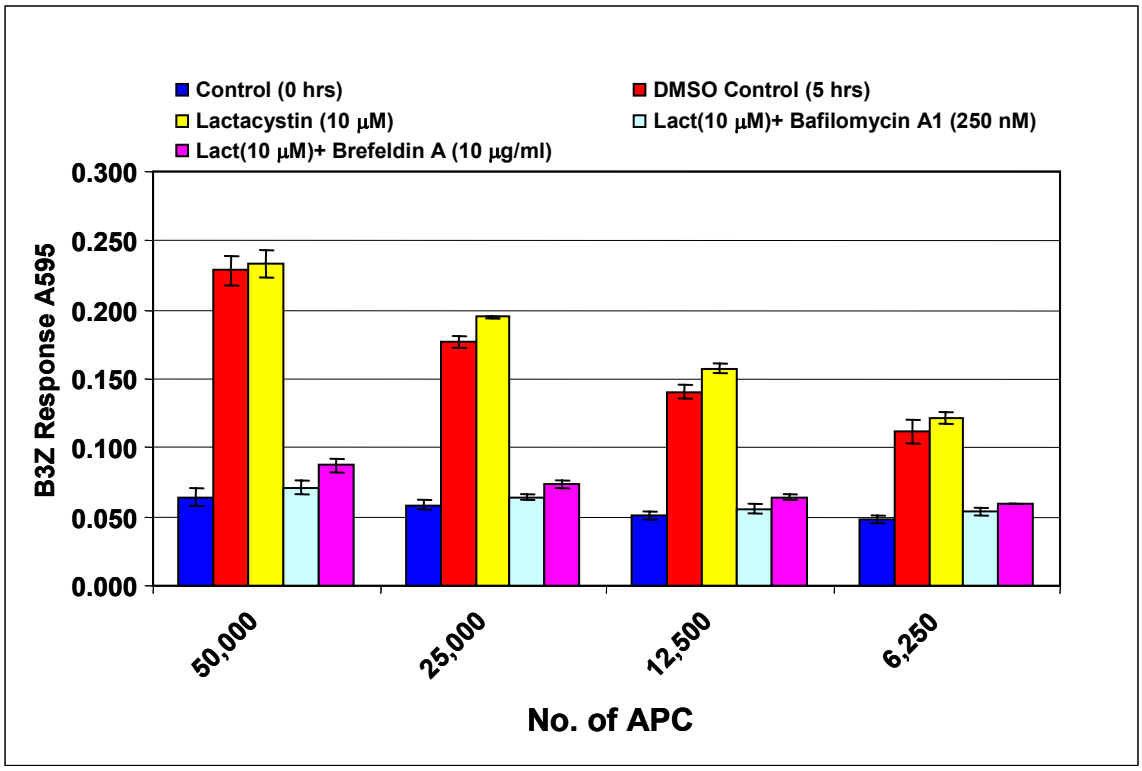

Figure 3.1.12 Role of alternative class I pathways in TAP-proficient P815 cells

P815 cells stably transfected with the construct *flag*-S8L-sp11-K^b were treated with 10 μM lactacystin, 10 μM lactacystin + 2.5 μM $BafA_1$, 10 μM lactacystin + Brefeldin A (10 μg/ml) for 30 min prior to acid wash treatment. Cells were allowed to recover for 5 hrs in the presence of the inhibitors. After 5 hrs cells were fixed. 5 x 10^4 B3Z cells were added for another 18 hrs followed by the LacZ assay.

In order to further study the route of processing of peptide-K^b conjugates presentation by P815 cells, I did the acid wash recovery assay in presence of brefeldin A, which blocks the newly synthesized class I molecules from the ER to the cell surface. I found that the presentation to B3Z was suppressed (**fig 3.1.12**, pink bar), suggesting that newly synthesized conjugates, rather then recycling conjugates were processed and presented. At this point, it is important to note, however, that brefeldin A also inhibits transport of recycling MHC class II molecules from endosomes to the cell surface (Pond and Watts, 1997).

PART II.

3.2 Alternative presentation/cleavage in endocytic compartments.

As I have seen in Figure 3.1.12 (bafilomycin treatment), the presentation of *flag*-S8L-sp11-K^b conjugates was pH dependent. Therefore we focused our attention towards processing in endocytic compartments. I have mostly used TAP-deficient MCA and RMA-S cells for further studies to avoid any influence of cytosolic proteases/proteasomes. In addition I have also used the TAP-proficient Ltk^- cells (H-$2K^k$) which do not express endogenous H-$2K^b$.

3.2.1 Role of endosomal compartments for the presentation of peptide-K^b conjugates.

We made the unexpected observation that even if the SIINFEKL analogues were linked to a class I molecules of another haplotype, i.e. H-$2K^d$, an efficient T cell response was seen (**Fig. 3.1.7b**; S8L-sp19-K^d). To prove that the B3Z T cell hybridoma did not recognize the SIINFEKL in the context of H2-K^d, I analyzed Ltk^- cells that lack endogenous K^b. In Ltk^- cells, S8L-sp19-K^d and RKKR-S8L-sp19-K^d conjugates required co-transfection of K^b to be presented (**Fig 3.2.4f**). Apparently peptide-K^d conjugates were cleaved by endopeptidase(s) and exopeptidase(s), and then the finally trimmed peptides were loaded onto H-$2K^b$ expressed in the same cell. To elucidate the mechanism of this intriguing result, I conducted transient transfections of various extended peptide-K^b conjugates along with S8L-sp19-K^d in MCA cells. Pre-existing S8L:K^b complexes were removed from the cell surface by acid wash treatment which was followed by recovery in presence/absence of chloroquine, a drug known to alter the pH of endolysosomal compartments. Chloroquine is a weak base which neutralizes the organelle pH. It has been used to decrease the degradation of endocytosed material by inhibiting endolysosomal hydrolytic enzymes.

As shown in figure 3.2.1a, in the presence of chloroquine not only S8L-sp19-K^d presentation was inhibited, but the presentation of S8L-sp19-K^b and of all N-terminally extended variants were also suppressed. This finding suggests that all the observed B3Z presentations were due to free peptide bound to K^b and not due to spacer-linked peptide-K^b conjugates. This observation was fully confirmed using the vacuolar proton pump inhibitor, folimycin **(Fig. 3.2.1d)**

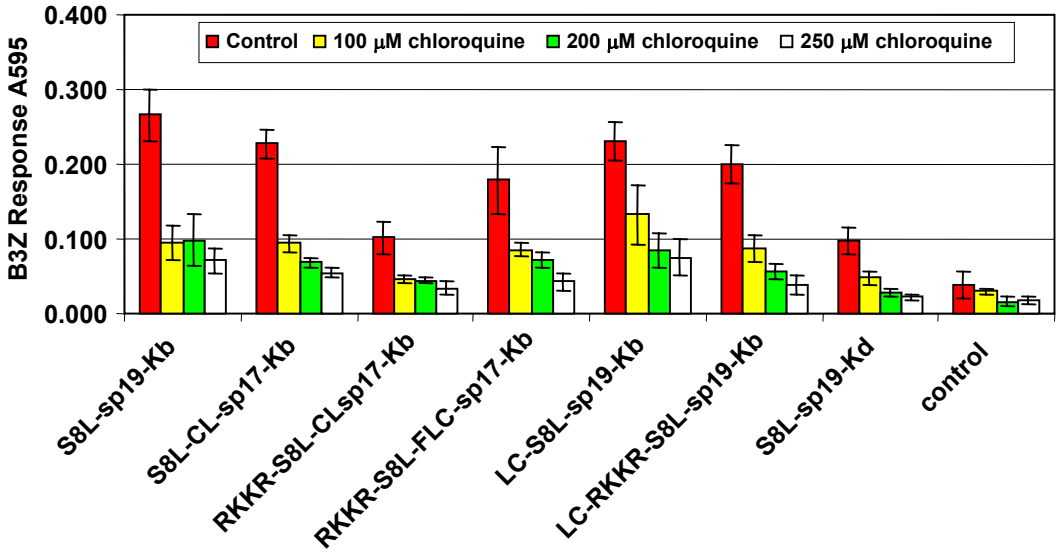

Figure: 3.2.1a Effect of pH increase on the presentation of peptide-K^b conjugates

MCA cells were transiently transfected in a 96-well plate for 48 hrs followed by an acid wash for 3 min. Cells were then allowed to recover in absence/presence of chloroquine in graded doses for another 12 hrs. At the end of the recovery time, cells were fixed followed by the B3Z T cell assay.

To further elucidate the role of endosome-dependent presentation, I have also used another weak base, primaquine, which accumulates in protonated forms and consequently neutralizes the endosomal and lysosomal pH (Reid and Watts, 1990). Once again, I have used MCA cells and transiently transfected the cells with peptide-K^b and -K^d conjugates. In addition, I transfected a construct in which the C-terminal portion of OVA protein was covalently linked to the N-terminal end of the transmembrane portion of the transferrin receptor (TfR). TfR is known recycles through early endosomes. If protein processing occurred in early endosomes, we would expect presentation of TfR-OVA. The cells were pre-incubated with various doses of primaquine and then the acid wash recovery assay was performed in the presence and absence of primaquine. As shown in figure 3.2.1b, the response of the B3Z hybridoma was inhibited by higher doses of primaquine. TfR-OVA was, however, unable to produce a detectable response. The viability of chloroquine- or primaquine-treated cells was 95% after 12 hrs of treatment. The treatment of TAP-deficient MCA cells with primaquine, bafilomycin A_1 or chloroquine did not affect their capacity to present exogenously added S8L peptide **(Fig. 3.2.1c)**, indicating that the extent of newly synthesized K^b molecules was not impaired.

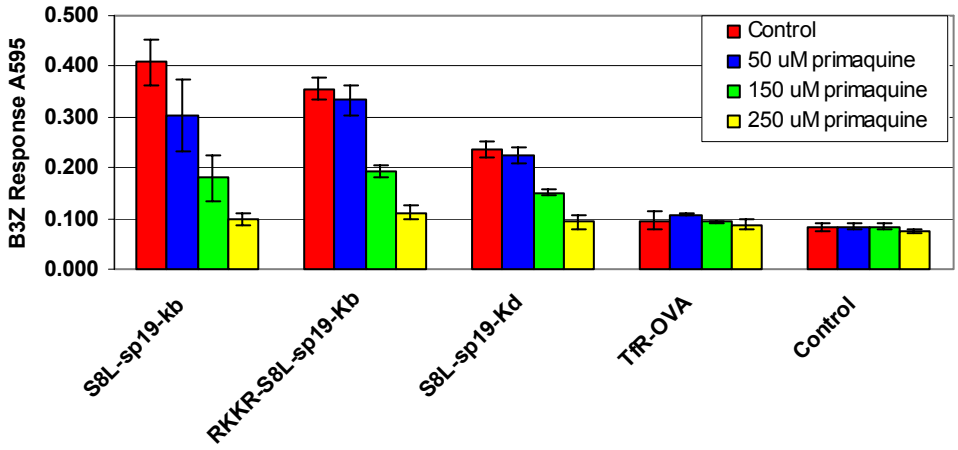

Figure 3.2.1b Effect of pH increase on the presentation of peptide-K^b conjugates

MCA cells were transiently transfected for 48hrs. Cells were pretreated for 60 min with the indicated amounts of primaquine followed by the acid wash recovery assay for 12 hrs in the presence of primaquine. After that, the cells were washed 2 times to remove primaquine followed by fixation and the B3Z T cell assay.

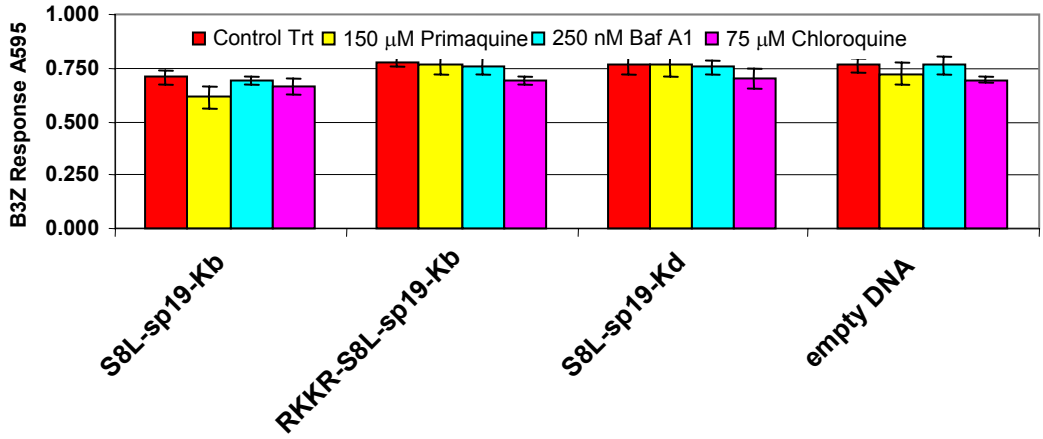

Figure 3.2.1c Effect of pH increase on the presentation of exogenous S8L peptides

MCA cells pre-treated with primaquine, bafilomycin A_1 or chloroquine were incubated with exogenous S8L peptide 1 μM for 1 hour at 37^{o}C followed three washes with D-PBS, fixation and the B3Z T cell assay.

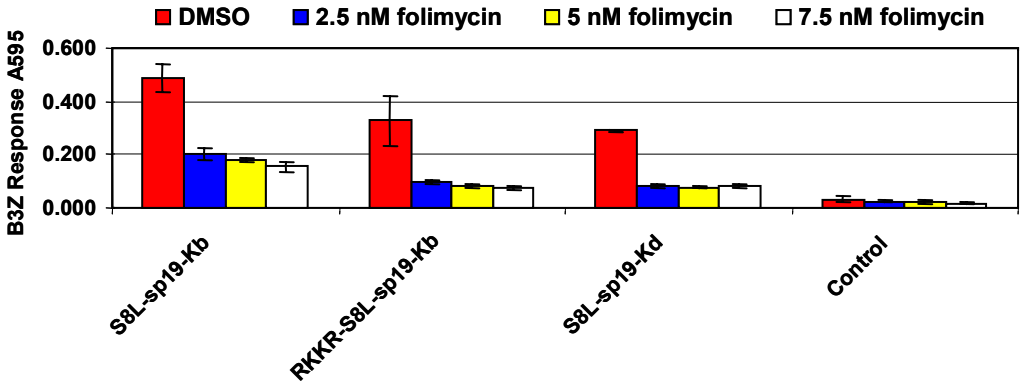

Figure 3.2.1d Influence of endosomal pH alteration by the proton pump inhibitor folimycin.
MCA cells were transiently transfected for 48hrs. Cells were pretreated for 60 minute with the indicated amounts of folimycin followed by the acid wash recovery assay for 12 hrs in the presence of folimycin. After that, the cells were washed 2 times to remove folimycin followed by fixation and the B3Z T cell assay.

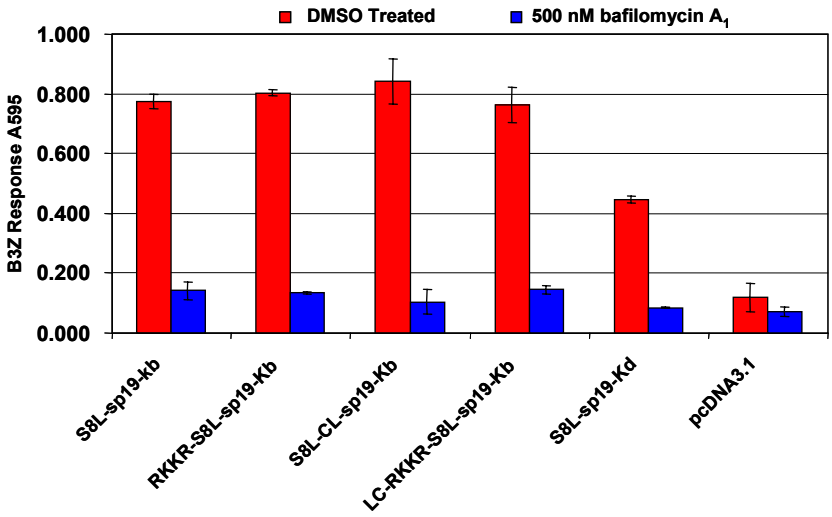

Figure 3.2.1e Influence of endosomal pH alteration by the proton pump inhibitor bafilomycin A_1.
MCA cells were transiently transfected for 48hrs. Cells were pretreated for 60 minute with the 500 nM bafilomycin A_1 followed by the acid wash recovery assay for 12 hrs in the presence of bafilomycin A_1. After that, the cells were washed 2 times to remove the bafilomycin followed by fixation and the B3Z T cell assay.

I also generated stable transfectants of TAP-deficient RMA-S cells (H-2K^b) expressing the S8L-sp19-K^d(Y341P) or S8L-sp19-K^d (T328A, S329A, S332A; exon 7 Ser/Thr) mutants) conjugates (see sec. 3.2.3), since RMA-S expresses endogenous K^b molecules that might be loaded with S8L epitopes processed from K^d conjugates.

First I analyzed the time needed for the recovery of S8L:K^b complexes after the acid wash. RMA-S transfectants were treated with isotonic low pH buffer (pH 3.0) followed by recovery for different time periods. As shown in **figure 3.2.1f**, SIINFEKL-loaded K^b molecules reappeared after 3-6 hours. On the basis of these results, I have chosen a 6 hrs standard recovery time for stably transfected RMA-S cells.

Cells treated with primaquine, bafilomycin and folimycin showed a significant inhibition of S8L:K^b complex formation as judged by B3Z responses. This inhibition was 71% by primaquine, 56 % by bafilomycin A$_1$ and 53 % by folimycin during the 6 hrs recovery (**Fig. 3.2.1g**). I could not use higher doses of above inhibitors as they were toxic.

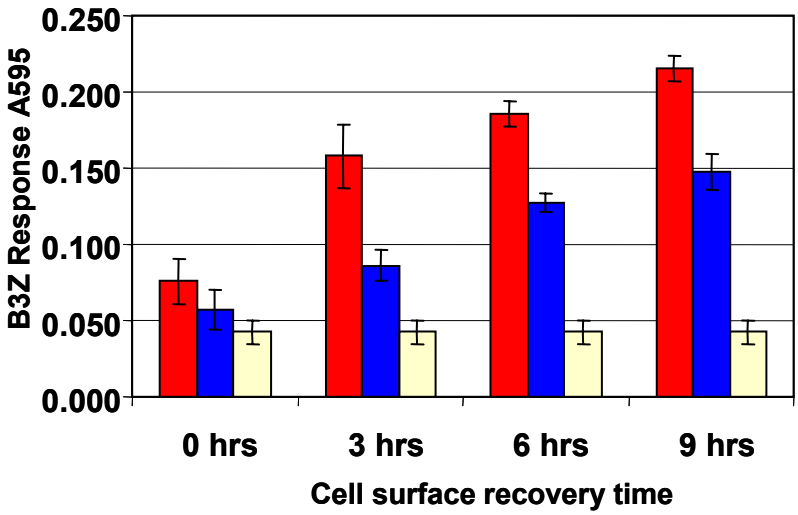

Figure 3.2.1f Recovery of S8L:K^b complexes in acid-washed RMS-S transfectants

1x 10^6 RMA-S stably transfected with S8L-sp19-K^d (Y341P; red bars) or S8L-sp19-K^d (Ser/Thr mutants, blue bars) were acid washed for 3 min followed by recovery for the times. Cells were fixed at the given time and after the end of the assay 5 x 10^4 RMA-S cells were co-cultured in a 96-well plate with 5 x 10^4 B3Z cells, followed by the LacZ assay. Untransfected RMA-S cells were used as control (yellow bars). All samples were in triplicates.

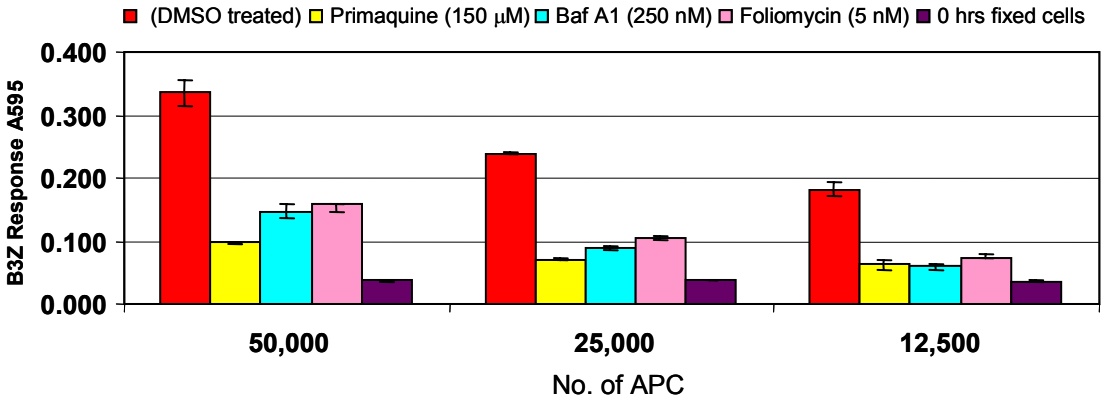

Figure 3.2.1g Effect of pH alteration on conjugates presentation by RMA-S transfectants.
$1x10^6$ RMA-S cells expressing S8L-sp19-K^d (Y341P) were pre-incubated for 60 min with the above mentioned inhibitors followed by acid wash for 3 min and recovery for another 6 hrs in the presence of inhibitors or DMSO for control. After the assay, cells were twice washed with D-PBS followed by fixation. $1x10^5$ fixed APC were co-cultured in a 96-well plate with $5 x10^4$ B3Z cells for 18 hrs, followed by the LacZ assay. All the samples were in triplicates.

These results using RMA-S transfectants demonstrate that the inhibitory effect of lysosomotropic amines and V-type proton pump blockers also applied to the processing of peptide-MHC class I conjugates by T-lymphoma cells. It was still unclear at this stage whether the observed downmodulations of B3Z responses were due to a decrease in the activity of endopeptidases, as the activation of various endopeptidases requires low pH, or whether the endosomal trafficking and recycling to the cell surface was blocked (Dunn and Maxfield, 1992).

3.2.2 Cathepsin inhibitors partially block the presentation.

Our data suggested that the C-terminus of SIINFEKL was liberated by endopeptidases sensitive to endosomal pH alteration. The two classes of intracellular proteases implicated in antigen presentation are aspartate and cysteine proteases. I assessed the role of cathepsins using known inhibitors for aspartic and cysteine-type cathepsins.

First, I used cysteine protease inhibitors blocking the cathepsin B, L, S, H etc. It was shown before by Rock and colleagues that MHC class I ligands can be generated in endocytic compartments and that the generation of SIINFEKL peptide from OVA protein is inhibited in Cat $S^{-/-}$ $TAP^{-/-}$ knockout cells and in the presence of the cysteine protease inhibitor leupeptin in wild-type cells (Shen *et al*., 2004).

I treated RMA-S cells stably expressing the SIINFKL-sp19-K^d (Y342P) conjugate overnight with the cysteine protease inhibitors leupeptin and cystatin followed by an acid-wash recovery in the presence of these inhibitors for 6 hrs. Subsequently, cells were washed thrice with D-PBS to remove residual amounts of inhibitor, fixed and incubated with the B3Z cells.

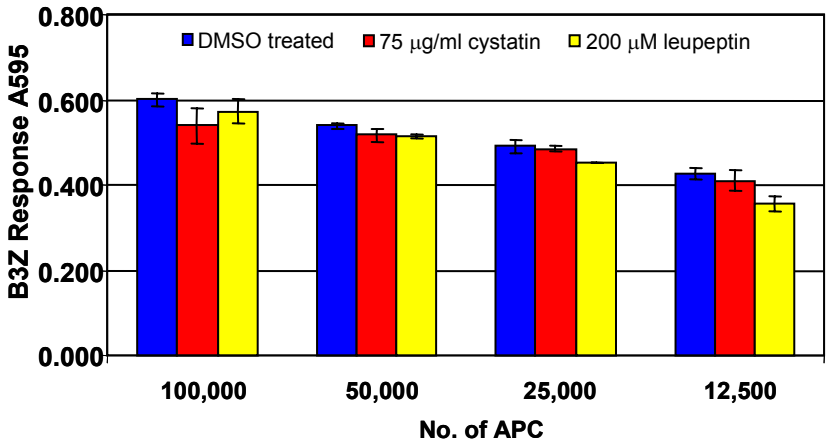

Figure 3.2.2a Effect of cysteine proteases inhibitors on the presentation of the S8L-sp19-K^d conjugate by RMA-S cells.

Stably expressing RMA-S cells were treated overnight with the depicted inhibitors followed by an acid-wash recovery in absence or presence of inhibitors. Cells were fixed and the B3Z assay was performed.

However, I could not find any inhibition using these cysteine protease inhibitors suggesting that cysteine proteases such as cathepsin S were not involved in conjugate processing. In another series of experiments I used pepstatin A, an inhibitor of aspartic-type cathepsin D and E, and observed a partial inhibition of S8L:K^b complex generation. Apparently, cathepsin D or E were involved in the processing of S8L-sp19-K^d conjugates (**Fig. 3.2.2b**).

When I treated the cells with cysteine protease inhibitor (leupeptin) and aspartic protease inhibitor (pepstatin A) together, unexpected results were observed. As shown in **(Fig. 3.2.2c)**, leupeptin had antagonistic effects on pepstatin A and similar effects were seen with cystatin, another cysteine protease inhibitor. It seemed that the activity of aspartic-type protease inhibitors was controlled by a cysteine protease. Similar results were obtained using TAP-deficient MCA fibroblasts as APC (data not shown)

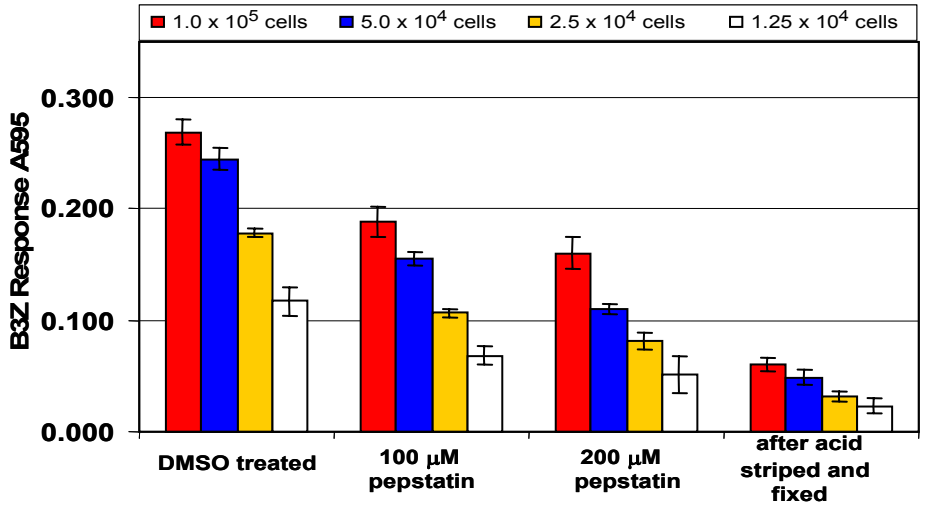

Figure 3.2.2b Effect of pepstatin A on RMA-S expressing S8L-sp19-K^d conjugates

1 x 10^6 stably expressing RMA-S cells were treated o/n with indicated amount of pepstatin A (inhibitor of aspartic-type cathepsin) followed by acid-wash recovery in the presence or absence of inhibitor. Cells were fixed and seeded into a 96-well plate followed by addition of 5x10^4 B3Z T cell. After 18hrs LacZ assay was performed.

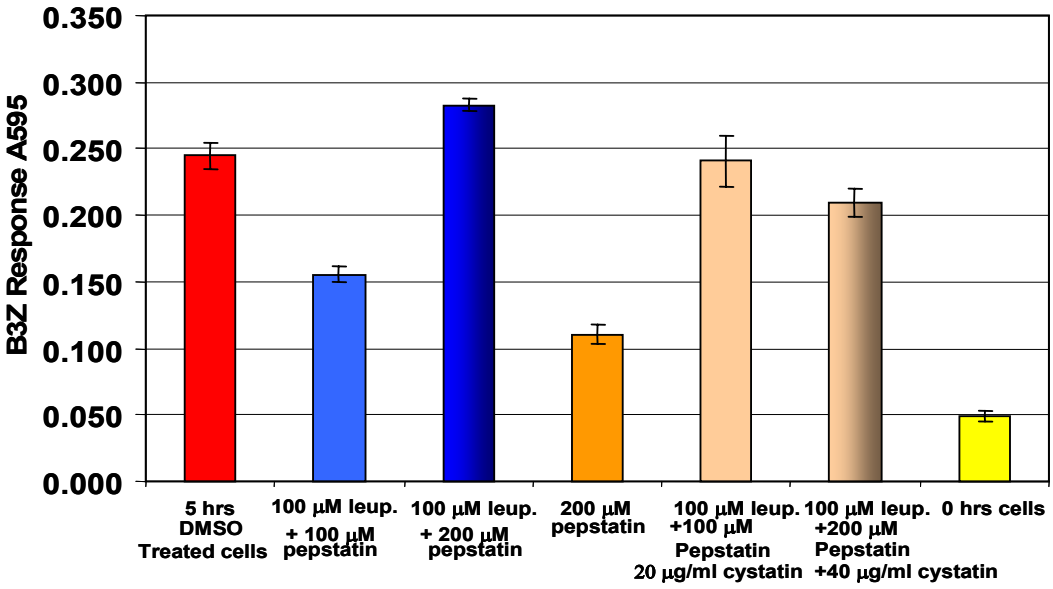

Figure 3.2.2c Effect of cathepsin inhibitors on RMA-S expressing S8L-sp19-K^d conjugates

1 x 10^6 stably expressing RMA-S cells were treated overnight with indicated amount of inhibitors followed by acid-wash recovery in the presence or absence of inhibitor. Cells were fixed and seeded into a 96-well plate followed by addition of 5 x10^4 B3Z T cell. After 18hrs LacZ assay was performed.

Related observations were made by Honey *et al*., who reported that mature cathepsin L protein levels in B cells, but not DCs or macrophages, were increased in the absence of cathepsin S (Honey *et al*., 2001).

However, in their case both proteases belong to the cysteine-type family and the authors proposed that cathepsin S may play a role in the degradation of mature cathepsin L protein. In our case, I speculate that in T cells (note that RMA-S is a T-lymphoma) as well in fibroblasts, the activity of aspartic proteases, which is responsible for observed S8L:K^b complex generation, might be positively regulated by cysteine proteases.

3.2.3 Effect of tyrosine/serine residues in the cytoplasmic tail of mouse MHC class I for endocytosis

The MHC class I cytoplasmic domain has one conserved tyrosine residue (encoded by exon 6) and two serine residues (encoded by exon 7), the second of which is the major site of cytoplasmic tail phosphorylation (Guild and Strominger, 1984) (**Figure 3.2.3 a**).

Species	MHC class I cytoplasmic tail sequence
Mouse	-RRRNTGGKGGD**Y**ALAPG___SQT**S**DL**S**LPDCKV---
Rat	-RKRNTGGKGGD**Y**APAPGRDSSQS**S**DV**S**LPDCKA
Rabbit	-KKHSSDGKGGR**Y**TPAAGGHRDQG**S**DD**S**LMP
Dog	-RKQRSGGKGPG**Y**SHAARDDSAQG**S**DV**S**LTAPRV
Cat	-RKKFSGGKGPR**Y**SHAARDDSTQG**S**DS**S**VMAPKV
Horse	-RKKRSGEKRGI**Y**VQAANSDSAQG**S**DA**S**LPQ_KV
Sheep	-RKKCSGEKRGT**Y**TQASSNDSAQG**S**DV**S**LTVHKV
Bull	--KKRSGEKGGN**Y**IQASSSDSAQG**S**DV**S**LTVPKV
Human	-RRKSSDRKGGS**Y**TQAASSDSAQG**S**DV**S**LTACKV
Seal	-RKKRSGGKGPG**Y**SHAARDDSAQG**S**DV**S**LTAP
Chicken	--RRHAGKKGKG**Y**NIAPDREGGSSSL**S**TG**S**NPAI
Xenopus	--KKRAGKPDAG**Y**TAAANRDSPPS**S**IV**S**A
Reptile	---VYFKKRQDG**Y**NKTPTN__DGG**S**NS**S**GEGGNVNI
Shark	-RKKAGQKT__G**Y**NPAKTSDKAES**S**SN**S**SATA
Zebrafish	---YRRHK___GFKPVPQNTSDGG**S**DN**S**SRT

(Adopted from Lizee *et. al.,* 2003)

Figure 3.2.3a Conserved amino acid residues in the cytoplasmic tail of MHC class I heavy chains from different species.

Splicing of exon 7 occurs naturally in some cell types resulting in MHC class I molecules that cannot be internalized efficiently in lymphoblastoid cell lines (Vega and Strominger, 1989). It was also reported that tyrosine/serine residues in the cytoplasmic domain of cell surface receptor are necessary, but not sufficient, for internalization through coated pits. MHC I molecules were reported to undergo endocytosis via clathrin-independent pathways in Hela cells (Naslavsky *et al*., 2003; Naslavsky *et*

al., 2004), but in T cells they are internalized in clathrin-coated pits via AP-2 mediated endocytosis (Machy *et al*., 1987). Some MHC I molecules recycle along with Arf6-associated early endosomes back to cell surface (Caplan *et al*., 2002; Powelka *et al*., 2004) while some proceed on to late endosomes/lysosomes for degradation (Naslavsky *et al*., 2003). The conserved MHC class I cytoplasmic tyrosine residue was reported to be pivotal for proper endolysosomal targeting in DCs and subsequent cross-presentation of exogenously derived antigens (Lizee *et al*., 2003). In human T cells, it was reported, however, that the internalization and signaling for T cell activation by cytoplasmic tail-deleted class I remain similar to wild type class I (Gur *et al*., 1990; Gur *et al*., 1997) .

To identify the cytoplasmic tail-derived signals for endocytosis/recycling, I generated tyrosine and serine mutants of our S8L-sp19-$K^{b/d}$ and RKKR-S8L-sp19-$K^{b/d}$ conjugates, which were efficiently presented by TAP-deficient cells.

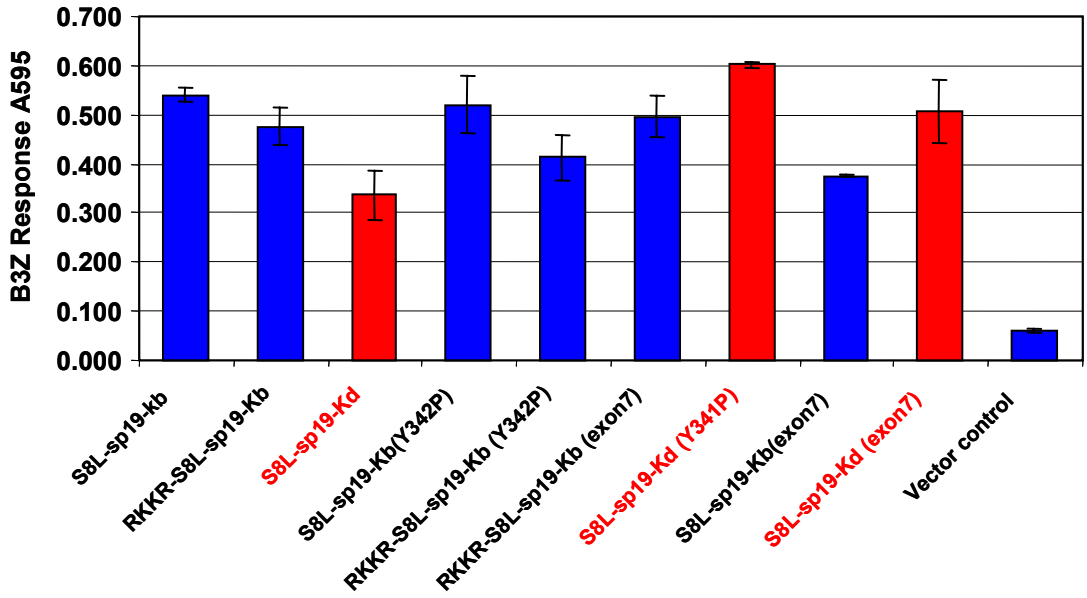

Figure 3.2.3b Effect of point mutations in the cytoplasmic tail of peptide-MHC conjugates.
1 x 10^4 MCA cells were transiently transfected with 0.4 µg/wells DNA in 96-well plates for 48 hrs followed by the B3Z T cell activation assay.

The conserved tyrosine residue in the cytoplasmic tail was replaced by proline, 2 serine and 1 threonine residues in exon 7 were replaced by alanine, later denoted as exon7 mutants. I transiently transfected MCA cells with these cytoplasmic tail mutants along with their wild-type constructs for 48 hrs before fixation and co-culture with B3Z cells **(Fig. 3.2.3b)**.

We reasoned that if the mentioned serine/tyrosine residue in the cytoplasmic tail were important for endocytosis, then we would not observe processing and presentation of peptide-K^b and K^d conjugates. The unreduced presentation of cytoplasmic tail mutants shows that neither a tyrosine-based internalization signal nor serine phosphorylation is critical for the internalization and processing of our conjugates.

3.2.4 Class I molecules are internalized by clathrin-dependent and independent mechanisms

Endocytosis pathways are used by cells for the internalization of nutrients, signal transduction regulation, and modulation of plasma membrane composition. There are several endocytic pathways that can mediate the internalization of many different proteins. One of the pathways is clathrin-dependent endocytosis, defined by a requirement for clathrin, which is major component of the endocytic vesicle coat. A clathrin-independent pathway depends on cholesterol-rich membrane domains (i.e. raft, which can also be encased by the protein caveolin to form membrane invaginations called caveolae). To investigate the mode of class I internalization from the cell surface of transfected MCA $TAP^{-/-}$ cells, I used the sterol-binding agent filipin as well as the cationic amphiphilic compound chlorpromazine to block the clathrin-independent and dependent internalization pathways, respectively (Naslavsky *et al*., 2004; Orlandi and Fishman, 1998). Filipin binds to cholesterol, a major component of glycolipid microdomains and caveolae, and disrupt caveolar structure and function. In contrast, chlorpromazine acts on the clathrin-dependent pathway and inhibits receptor-mediated endocytosis by reducing the number of coated pit-associated receptors at the cell surface and causing the accumulation of clathrin and AP-2 in an endosomal compartment (Orlandi and Fishman, 1998). Filipin complex and chlorpromazine were individually able to induce a partial inhibition of the presentation of K^b linked peptide conjugates in reappearance assays while K^d linked peptide conjugates substantially lost the presentation **(Fig. 3.2.4a)**. Thus, both internalization pathways were apparently involved in the endocytosis of peptide-MHC class I conjugates.

PI3 kinase inhibitors were reported to block an Arf6-dependent, early endosomal recycling pathway utilized by class I molecules in HeLa cells (Naslavsky *et al*., 2003). The PI3K inhibitor inhibitors wortmannin and 3-methyladenine had either no effect on

the presentation of peptide-MHC class I conjugates in TAP$^{-/-}$ MCA cells or even slightly enhanced it (**Fig. 3.2.4b and 3.2.4c**). These results suggest that such as Arf6-dependent pathway was irrelevant for the targeting of our peptide fusions to acidic processing compartments.

To investigate whether newly synthesized or pre-existing class I-peptide fusion molecules were used for the production of S8L:K^{b} complexes, I performed the reappearance assay in the presence of the protein synthesis inhibitor cycloheximide (data not shown). Since this treatment did not impair the presentation of (RKKR-)S8L-K$^{b/d}$ conjugates, we conclude that the presentation was solely based on the processing of pre-existing, recycling class I molecules.

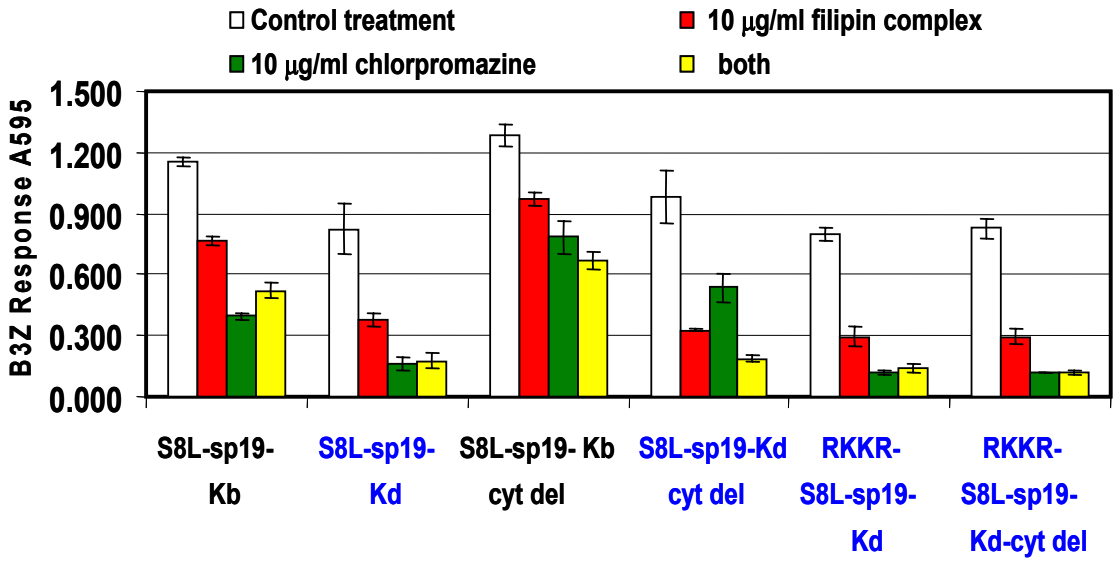

Figure 3.2.4a Mode of conjugates internalization using chloropromazine and filipin complexes.
The MCA cells were transiently transfected with 0.8 µg DNA/wells in a 96-well plate for 48 hrs. After transfection, cells were 60 min pretreated with 10 µg/ml of the mentioned inhibitors followed by an acid wash and recovery for 11 hrs in the presence of the same concentration of inhibitors. After that, cells were washed 2 times followed by fixation and the B3Z T cells assay.

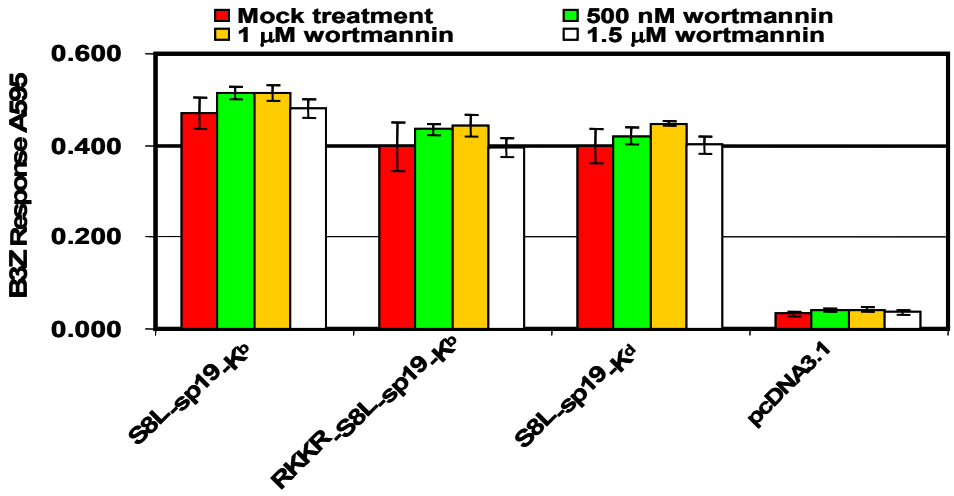

Figure 3.2.4b Effect of the PI3K inhibitor wortmannin on the presentation of peptide-K$^{b/d}$ conjugates

5 x 10^4 MCA cells transiently expressing above depicted peptide conjugates were pre-incubated with graded amounts of wortmannin for 60 min followed by acid wash for 3 min. Wortmannin was present during the 11 hours recovery time. After the recovery time, cells were washed twice with D-PBS followed by fixation and the B3Z LacZ assay.

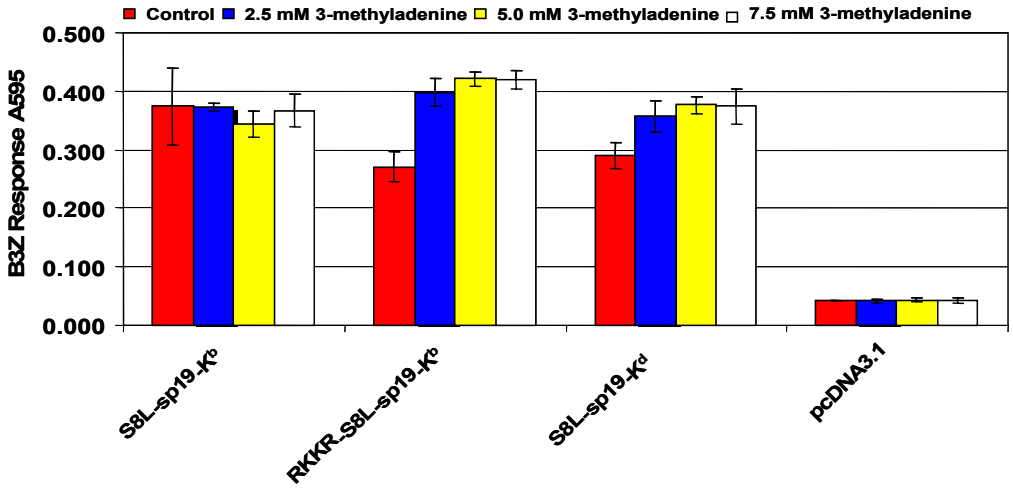

Figure 3.2.4c Effect of the PI3K inhibitor 3-methyladenine on the presentation of peptide-K$^{b/d}$ conjugates

5 x 10^4 MCA cells transiently expressing the above depicted peptide conjugates were pre-incubated overnight with graded amounts of 3-methyladenine followed by an acid wash for 3 min. During the 11 hours recovery time 3-methyladenine was also present in the same concentrations. After the assay, cells were washed twice with D-PBS followed by fixation and the B3Z LacZ assay.

As my results suggest that the endocytosis of the peptide-MHC I conjugates does not require the cytoplasmic tail. Because recycling of peptide-loaded K^b back to the cell surface might, however, require the cytoplasmic tail, I have transfected Ltk^- cells (H-$2K^k$) with both cytoplasmic tail-deleted and corresponding control conjugates.

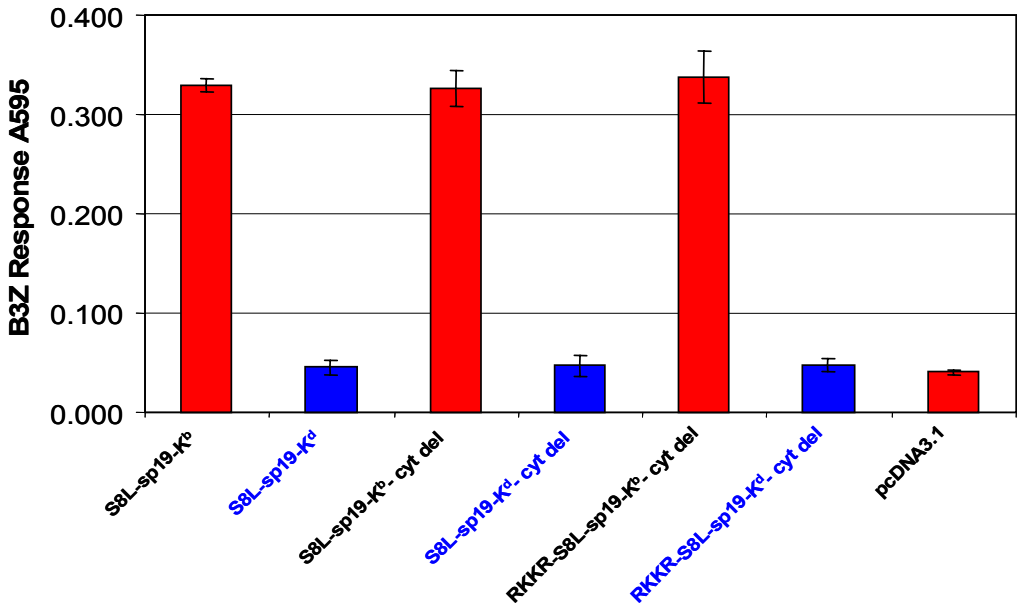

Figure: 3.2.4d Presentation of K^d conjugates requires endogenous H-$2K^b$

1 x 10^5 Ltk^- cells were transiently transfected using 0.4 µg DNA/well with above depicted conjugates in a 96-well plate for 48 hrs followed by the B3Z T cell activation assay. All transfections were done in a 96-well plate in triplicates.

As shown in Figure 3.2.4d, none of the S8L-sp19-K^d conjugates and their variants were able to produce a B3Z response after transfection into K^b-deficient Ltk^- cells. S8L-sp19-K^b and extended variants presentation were, however, well presented. If I co-transfected the peptide-K^d conjugates along with K^b cDNA, presentation was restored (**Fig 3.2.4e**). It was interesting to observe that the cytoplasmic tail of presenting K^b molecules could be deleted without losing the B3Z response, suggesting that cytoplasmic tail does not have any significant role in recycling of peptide-loaded K^b.

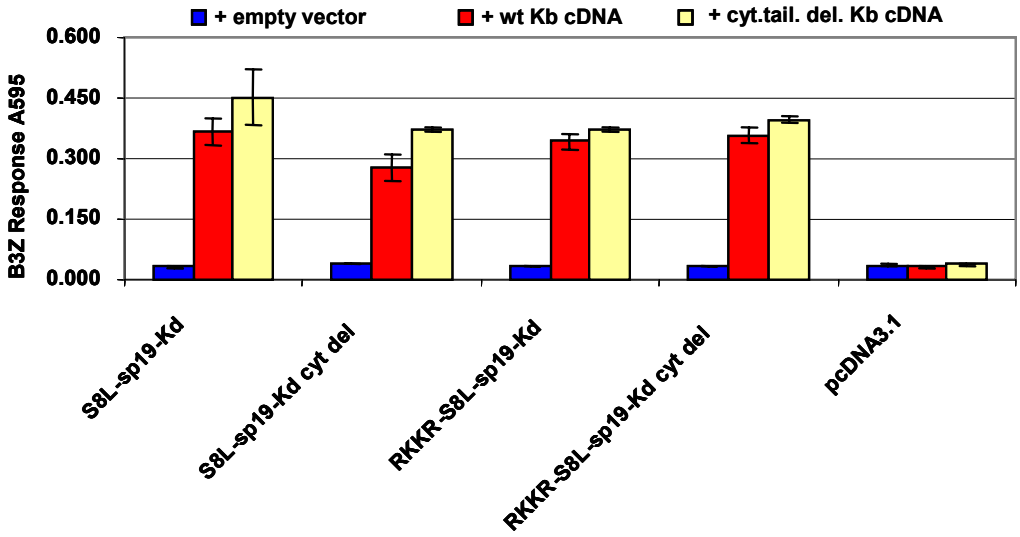

Figure 3.2.4e Presentation was independent of cytoplasmic tail signals of recycling, peptide loaded MHC class I molecules.

1 x 10^5 Ltk^- cells were transiently transfected using 0.4 µg DNA/well with above depicted conjugates in 96-well plates for 48 hrs followed by the B3Z T cell activation assay. All transfections were done in a 96-well plate in triplicates.

3.2.5 Intracellular localization of S8L:K^b complex formation.

Sorting to endocytic organelles has long been recognized as a means of degradation for long-lived proteins as well as various extracellular endocytosed proteins. Apart from the degradative fate of most proteins sent to late endosomes/lysosomes, a selected set of proteins appear quite stable in these internal vesicles. These proteins include tetraspanins (CD63, CD81 and CD82) and MHC II molecules which are found in specialized late-endosome-like compartments (MIIC).

Late endosomes are prelysosomal endocytic organelles. When viewed with the electron microscope, late endosomes are more spherical than early endosomes and more juxtanuclear, being concentrated near the microtubule organizing center. They are differentiated from early endosomes by their lower lumenal pH, different protein composition and association with different GTPases of the rab family. Multilamellar membranes with the late endosomes are frequently associated with mannose-6-phosphate receptors (M6PR) which is used as marker protein for late endosomes. Lamp1 protein is also found in late endosomes but it is also quite abundant in lysosomes. Lysosomes are differentiated by lacking M6PR. EEA1 is used a marker for early endosomes. EEA1 and M6PR marker proteins were used to study the localization of

S8L:K^b complexes in MCA cells. I transiently transfected MCA cells with EGFP-tagged S8L-K^b and S8L-K^d conjugates for 48 hrs and then the cells were plated on coverslips. The cells were fixed in 4 % paraformaldehyde followed by antibody staining with EEA1 and M6PR for early and late endosomes, respectively. For detection of the S8L:K^b complex, I used the monoclonal antibody 25.D1-16.

As shown in **figure 3.2.5a and b**, S8L:K^b complex formation in S8L-sp19-K^d-EGFP transfected MCA cells was detected in both in early and late endosomes. Many 25.D1-16^+ vesicles co-stained with EEA1 and only a minor fraction co-stained with M6PR. Thus, S8L:K^b complexes appeared predominantly in early endosomes.

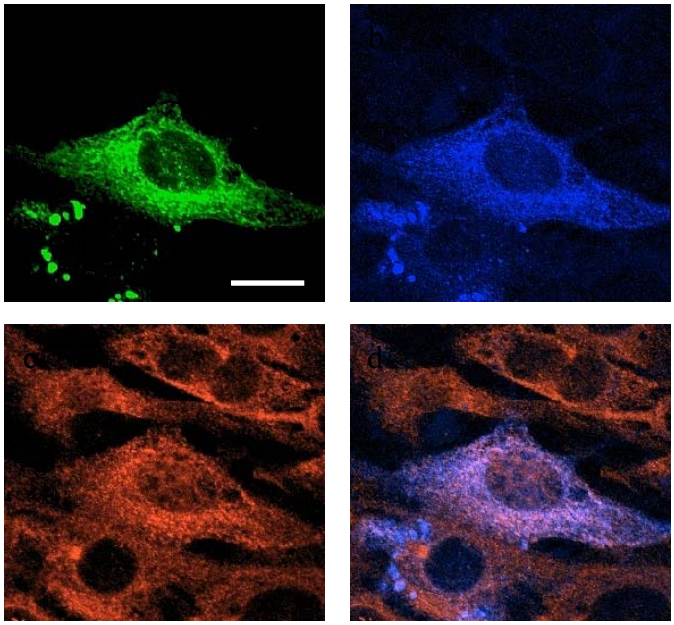

Figure 3.2.5a S8L:K^b co-localizes with EEA1-positive endosomes in S8L-sp19-K^d-EGFP expressing MCA cells. MCA cells were transiently transfected with the S8L-sp19-Kd-EGFP conjugate for 48 hrs in a 6-well plate and then transferred onto a poly-L-lysine coated coverslip followed by fixation with 4% paraformaldehyde for 10 min. These fixed cells were stained with 25. D1-16 mAb and EEA1 polyclonal antibody followed by secondary antibodies anti-mouse IgG-Cy5 and anti-rabbit IgG TRITC, respectively. Mowiol mounted cells were processed for confocal microscopy. The bar represents 20µm.

a) EGFP b) EEA1 c) 25.D1-16 d) Merge of b and c , depicted in the false color vesicles co-staining for EEA1 and 25.D1-16 appears in the false color white.

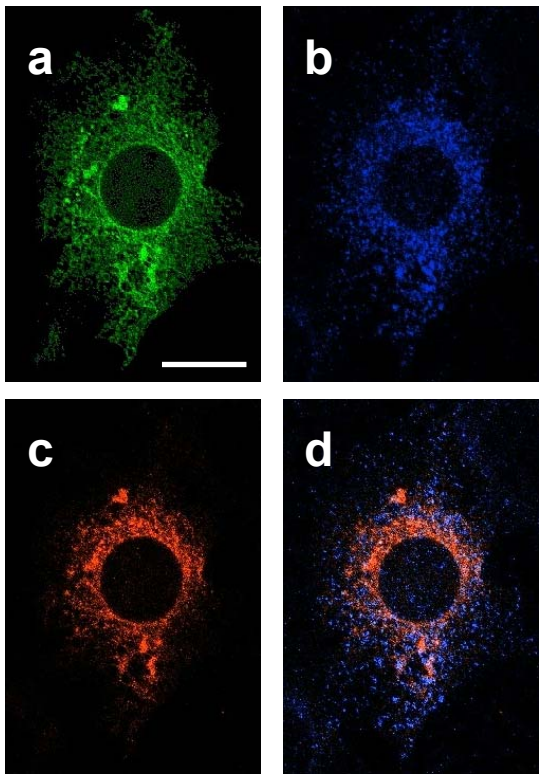

Figure 3.2.5b S8L:K^b complexes colocalizes with M6PR positive late-endosomes in S8L-sp19-K^d-EGFP tagged expressing MCA cells.
MCA cells were transiently transfected with the S8L-sp19-K^d-EGFP conjugate for 48 hrs in a 6-well plate and then transferred into poly L-lysine coated coverslip, followed by fixation with 4% paraformaldehyde for 10 min. These fixed cells were stained with 25.D1-16 mAb and M6PR polyclonal antibody followed by secondary antibodies Cy5-conjugated anti-mouse and TRITC-conjugated anti rabbit, respectively. Mowiol mounted cells were processed for confocal microscopy. a) EGFP b) M6PR c) 25.D1-16 d) Merge of b and c, depicted in the false color vesicles co-staining for M6PR and 25.D1-16 appears in the false color white.

The bar represents 20µm.

4. Discussion

The endogenous antigen processing pathway is considered to be the main source for processed peptides that are presented by MHC class I on the cell surface. Peptides liberated from proteins in the cytosol by proteasomes and other proteolytic systems are transported by the heterodimeric TAP into the ER lumen, where they bind to nascent MHC class I molecules. Most data on antigen processing fit well with the concept of distinct endogenous and exogenous pathways for generating peptides for MHC class I and MHC class II, respectively. Exogenous antigens are processed in early and late endosomes and presented by MHC class II molecule. However, there is an increasing evidence for the processing and presentation of exogenous antigens by MHC class I molecules. Likewise, cytoplasmic proteins can be presented by MHC class II molecules (Paludan *et al*., 2005; Tewari *et al*., 2005).

Constitutive endocytosis of MHC class I molecules from the cell surface via coated pits, transit through a primaquine-sensitive vesicular compartment and their *de novo* expression on the cell surface have been demonstrated in various cell types. The actual delivery of MHC class I molecules to endosomal compartments, in which they could capture processed peptides, has not been well defined.

To elucidate the mechanisms underlying this novel phenomenon, I generated fusion proteins of the OVA epitope SIINFEKL with K^b and K^d MHC class I molecules in different sequence contexts. How will these N-terminally extended peptide-MHC-I conjugates present the peptides? Is there any role of components peptide loading complexe (PLC), such as TAP, tapasin, calnexin, calreticulin and ERp57 in the presentation of such? Previously, a number of approaches have been described to make recombinant single chain MHC class I molecules by linking either peptide-β2-microglobulin or peptide MHC or peptide-β2m-MHCI. Among them, peptide-MHC class I D^d (White *et al*., 1999), K^d (Mottez *et al*., 1995) and human HLA-A2 molecules (Kang et al., 1997; Toshitani et al., 1996) successfully presented peptides after transfection into mammalian cells. Interestingly, attempts to make a functional single-chain peptide-MHC conjugate in bacteria was not successful (Sylvester-Hvid *et al*., 1999). Thus T cells can recognize MHC molecules with a peptide linked to the amino terminus of the MHC heavy chain.

4.1 Analysis of peptide-MHC class I conjugates by T cells

Previous studies suggest that the S8L-spacer-K^b fusion protein may bind the covalently linked S8L peptide and present it to T cells as an intact "single-chain" class I molecule (Mottez *et al*., 1995; Yu *et al*., 2002). N-terminally extended epitopes have not been studied in this respect. Furthermore, peptides >15 residues binding to K^b molecules have been reported (Joyce *et al*., 1994). Therefore, it was necessary to establish the specificity and sensitivity of B3Z hybridoma cells towards N- and C-terminally extended variants of the S8L peptide.

The mAb 25.D1-16, which recognizes the SIINFEKL epitope in conjunction with H-$2K^b$, was initially used to detect S8L/K^b complex generation. I believed that this antibody would not tolerate the N- or C-terminal SIINFEKL extension, but using free synthetic peptides in cytofluorometry I found that this antibody is reactive with N-terminally extended SIINFEKL analogues (data not shown). The selectivity against N- or C-terminal extension of SIINFEKL was very pronounced in B3Z T cells. So most experiments of this work relied on the B3Z hybridoma (Karttunen *et al*., 1992).

Previous work has shown that B3Z responses to S8L analogues extended at the N terminus by a single amino acid was comparable to S8L (Buchholz *et al*., 1995). S8L variants C-terminally extended by single residue required, however, >1000 times higher concentrations (Shastri *et al*., 1995). Our experiments with synthetic peptides indicated that N-terminal extension of S8L by 2-5 residues reduced the B3Z responses approximately 1000-fold. C-terminal extension by 4 residues either decreased the B3Z by 3-5 orders of magnitude (see **fig. 3.1.3a/b)**. The superior presentation of S8L-FLGG as compared with S8L-GGGA is in line with a report showing that hydrophobic residues at P9 and P10 improve the binding of C-terminally extended analogues of an 8-mer Kb ligand (Hörig *et al*., 1999). Biterminally extended analogues were unable to stimulate significant B3Z responses at concentrations up to 100 μM (**see fig. 3.1.3a/b)**. This is consistent with earlier findings showing extremely poor binding of double-extended epitopes to various purified mouse class I molecules including K^b (Stryhn *et al*., 2000).

Except S8L-sp19-$K^{b/d,}$ all peptide-class I conjugates used for this study were biterminally extended and thus, in all likelihood, their recognition by B3Z required exo-

and endoproteolytic processing.

4.2 Role of loading complex components on peptide-MHC I conjugate.

Using the T cell hybridoma B3Z and the monoclonal antibody 25.D1-16, which both recognize S8L-loaded K^b molecules, I found that significant levels of the S8L-K^b epitope were generated from most of the investigated unextended and N-terminally extended S8L-class I fusion proteins after transient transfection of $TAP1^{-/-}$ mouse fibroblasts. Similar results were obtained using tapasin-deficient murine fibroblasts, that express no TAP proteins due a lack of the TAP-stabilizing activity of tapasin (Garbi *et al*., 2003), as well as the TAP2-deficient T lymphoma line RMA-S. In TAP and Tpn-deficient cells, long extended peptide conjugates were less efficiently presented as compared to optimal peptide conjugates (S8L-K^b) and after restoring the TAP and tapasin expression in these cells I found enhanced presentation. Although I have shown that proteasomes do not contribute significantly to the presentation of S8L peptide from our conjugates, it is possible that TAP may contribute as stabilizing factor. Using a chemical cross linker approach Lacaille and Androlewicz (Lacaille and Androlewicz, 1998) found that subtle conformational changes occur in the TAP heterodimer upon the binding of peptides. The viral inhibitor ICP47 also has a deleterious effect on the heterodimer structure of the TAP, in addition to its role in blocking the peptide transport from the cytoplasmic side. Moreover, TAP association influenced the conformation of MHC class I molecules in the ER (Owen and Pease, 1999). It is also possible that some extended conjugates may not efficiently leave the ER until they are loaded with free peptides supplied by TAP to the ER. Similarly, in tapasin deficient cells, TAP expression is drastically reduced and tapasin restoration enhances TAP stabilization resulting in higher peptide supply to the ER.

I was unable to see any influence of ERp57 silencing on the presentation of our extended peptide-K^b conjugates and thus it seems that ERp57 was largely dispensable for proper conjugate folding and ER egress. B cells from conditionally ERp57 knockout mice show reduced MHC class I expression, however (N. Garbi, pers. communication), indicating that ERp57 does play a role in the maturation of class I molecules.

4.3 Role of endo- and exopeptidase on N-or C-terminal trimming

Of the 8 studied LX-S8L extensions, Leu-Pro had the lowest presentation efficiency (see **Fig. 3.1.11a**). Moreover, addition of Gly-Pro to the N-terminal *flag* peptide

extension strongly reduced presentation. This finding suggested processing of our conjugates by the ER aminopeptidase ERAP1/ERAAP which inefficiently trims X-Pro-Xn peptides (Serwold *et al*., 2001; Serwold *et al*., 2002). Using cells with overexpressed or silenced ERAP1 I could not obtain evidence for an involvement of ERAP1 in the trimming of our peptide-class I conjugates (see **fig. 3.1.7a & 7b**). There is evidence that the degradation of a few proteins is initiated by limited proteolysis in the ER. Signal peptidase, signal peptide peptidase and furin that recycles between ER have been implicated in such cleavages (reviewed in (Schmitz and Herzog, 2004). While our peptide-class I conjugates generally required signal peptidase to remove the ER signal sequence, it was of interest to assess the role of furin which has been previously shown to contribute to the generation of class I-binding peptides (Gil-Torregrosa *et al*., 2000; Gil-Torregrosa *et al*., 1998). Constructs containing a potential furin cleavage motif (RKKR or LCRKKR) as N-terminal extension of S8L were presented with remarkable efficiency but they were not sensitive to a peptide ketone inhibitor of furin, suggesting that furin was not involved in processing.

The database www.syfpeithi.de lists 21 class I ligands derived from the ectodomain of various other class I molecules that bind to 16 different class I allomorphs. Therefore, I reasoned that MHC class I molecules themselves might be well-suited carriers of peptide antigen as, by definition, they would reach all intracellular compartments harboring class I molecules that can be loaded with peptides. I showed that S8L epitope can be liberated from the amino terminal end of K^d for subsequent loading onto K^b molecules co-expressed by the antigen presenting cells. Similar to the respective K^b constructs, also the N-terminally extended RKKR-S8L-K^d fusion protein was efficiently processed for presentation to B3Z. Without exception, the processing of the S8L epitope from the investigated peptide conjugates was significantly blocked when reappearance assays were performed in the presence of lysosomotropic amines or inhibitors of the vacuolar proton pump. These drugs interfere with the function of endolysosomal proteases that require acidic pH for optimal function as well as with vesicular trafficking in the endosomal pathway (reviewed in Gruenberg, 2001; Watts, 2001). Following recovery from acid stripping in the presence of acidification inhibitors, the presentation of exogenous S8L peptide by the transfectants was not affected suggesting that the surface expression of newly synthesized class I molecules was not impaired. In the same line, surface stainings for K^b and K^d after recovery from acid stripping and

fixation proved that transport through the classical secretory pathway was not affected by bafilomycin A_1 (data not shown). Taken together, endolysosomal compartments appear to be solely responsible for the TAP-independent processing of the membrane-associated model antigens used for our study.

In TAP-competent cells, peptides can be processed out membrane-associated proteins by using the ER retrotranslocation and proteasomal processing pathway (Bacik *et al*., 1997; Mosse *et al*., 1998; Selby *et al*., 1999). S8L-MHC class I conjugates were efficiently presented by TAP-competent P815 mastocytoma cells and by Ltk^- cells. While the proteasome inhibitor lactacystin had no effect, proton pump inhibitors substantially suppressed the generation of the S8L epitopes provided by K^b or K^d fusion proteins. Thus, also in TAP-proficient cells these antigens are degraded by the alternative pathway.

Unexpectedly, also the presentation of S8L-sp19-K^b molecules was substantially blocked by inhibitors of endosomal acidification. In this fusion protein, K^b may be able to bind the S8L peptide without endoproteolytic cleavage through the linker sequence as suggested by previous work using S8L-β2m-K^b single-chain trimers and peptide-β2m fusions (Uger and Barber, 1998; Yu *et al*., 2002). I cannot rule out that a minor fraction of S8L-K^b single-chain dimers in fact presented S8L in the unprocessed form, however, the similar sensitivity of S8L-K^b and S8L-K^d to bafilomycin suggests that both conjugates were subjected to processing in the same endosomal vesicles.

Cysteine proteases have been implicated in the processing of exogenous OVA administered to TAP-deficient dendritic cells or macrophages in the form of biodegradable microspheres (Shen *et al*., 2004) or *E. coli* producing MBP-OVA (Campbell *et al.*, 2000). The aspartic protease inhibitor pepstatin A blocked B3Z responses to RMA-S/S8L-K^d in reappearance assays, strongly suggesting an involvement of cathepsin D or E in processing. In these cells, inhibition by pepstatin A was antagonized by cysteine protease inhibitors, suggesting that aspartic-type cathepsins may regulate the function of cysteine-type cathepsins. In some experiments using MCA transfectants we also observed a modest inhibition of antigen presentation by the cysteine-type cathepsin inhibitor leupeptin. As pointed out for MHC class II antigen processing, there seems to be functional redundancy of endolysosomal cathepsins (Villadangos and Ploegh, 2000). The broadly expressed cysteine-type cathepsins B, H

and L, which often cleave after basic residues, and the aspartic-type cathepsins D and E, which preferentially cut bonds flanked by hydrophobic residues (www.merops.sanger.ac.uk), could together account for the liberation of S8L from different sequence contexts in the nonprofessional antigen presenting cells used here. The use of cell lines from cathepsin-deficient mice will be necessary to clarify the involvement of individual proteases.

4.5 Role of alternative pathway peptide-MHC conjugates antigen presentation.

In agreement with earlier studies using TAP-deficient professional antigen presenting cells (Kovacsovics-Bankowski and Rock, 1995[Reis e Sousa, 1995 #644; Reis e Sousa and Germain, 1995; Wick and Pfeifer, 1996), native soluble ovalbumin was poorly processed by the TAP-deficient T cells and fibroblasts. A transferrin receptor-OVA fusion protein, which localizes to early endosomes and was efficiently processed by TAP-competent B cell lines (Fernandes *et al.*, 2000), elicited no detectable B3Z response after transfection into TAP-deficient MCA cells. Also, the S8L-K^b fusion protein carrying an N-terminal extension of 137 OVA residues was inefficiently presented (see Fig.3.1.4b). It is conceivable that particular flanking sequences or restrictions imposed by secondary structures of folded polypeptides may interfere with processing in the alternative pathway. With the exception of proline, individual residues flanking the SIINFEKL sequence at the N- or C-terminal end had, however, no strong influence on the efficiency of generation of S8L:K^b complexes. This finding underscores that the TAP-independent pathway can, under certain circumstances, be remarkably efficient.

The cytoplasmic tail of MHC class I molecules contains a serine phosphorylation site, a conserved tyrosine residue as well as lysine residues that can be conjugated with ubiquitin. Individual sequence motifs or the entire cytoplasmic tail have been suggested to control internalization and/or late endosomal targeting of class I molecules, however, no coherent picture has emerged (Bartee *et al*., 2004; Davis *et al*., 1997; Gur *et al*., 1997; Lizee *et al.*, 2003; Vega and Strominger, 1989). Cell type-specific prerequisites for internalization and endosomal trafficking and differences between the class I allomorphs studied may account for the observed discrepancies. One of the main findings of my thesis is that the entire cytoplasmic tail of K^b or K^d peptide fusion molecules can be deleted without any loss of the presentation capacity of transiently

transfected TAP-deficient cells. Moreover, the cytoplasmic tails of both the presenting

K^b molecules as well as the peptide-carrying K^d molecules were dispensable (see **Fig. 3.2.4e)**. Our results are in apparent conflict with results by Lizée and colleagues who reported that K^b molecules with a mutated tyrosine residue in the cytoplasmic tail fail to mediate cross-presentation of OVA by dendritic cells (Lizee *et al*., 2003). It is possible that dendritic cells employ special targeting signals to mediate trafficking of K^b to late endosomes, whereas in nonprofessional APC default mechanisms involved in the constitutive internalization of cell surface proteins for turn-over may be sufficient to target class I molecules to processing compartments.

Autophagy is one of the main pathways of the degradation of endogenous proteins (Dissanayake *et al*., 2005; Paludan *et al*., 2005; Yorimitsu and Klionsky, 2005) and organelles (Cuervo, 2004). One might expect that our S8L conjugates may follow this route of processing. After treating the cells with 3-methyladenine, which is described as a potent inhibitor of autophagy, I could, however, not find a reduction of presentation suggesting that autophagy is not a source of conjugate delivery for S8L:K^b complex formation.

I used filipin and chlorpromazine to block internalization by the clathrin-independent pathway and dependent pathways, respectively (Naslavsky *et al*., 2004; Orlandi and Fishman, 1998). Both filipin and chlorpromazine partially blocked the reappearance of S8L:K^b complexes after acid stripping and also showed a synergistic effect. Thus, both endocytosis pathways appear to be operative in MCA cells regardless of the presence of a cytoplasmic tail. It remains to be investigated how cytoplasmic tail-deficient class I-molecules can be targeted into clathrin-coated pits. The alternative role of clathrin-dependent and –independent endocytosis may explain why the PI3-kinase inhibitors wortmannin and 3-methyladenine had no effect on antigen presentation in our antigenic system.

Intracellular Localization of S8L:K^b complexes was investigated a by confocal immunofluorescence microscopy. I have observed that in case of S8L-K^b conjugates, the 25.D1-16 epitope generation was predominantly seen in early endosomes and for S8L-K^d conjugates it was observed in late as well as in early endosomes. It might be possible that the slightly acidic pH in early endosomes is sufficient to process and load

an autologous linked peptide (i. e., S8L-sp19-K^b). In case of K^d conjugates, it was apparent that they must be completely processed in order to be loaded onto K^b molecules for recognition by B3Z T cells. I have observed S8L:K^b complexes in EEA+ early endosomes and M6PR+ late endosomes by confocal microscopy, but additional confirmation of these findings by electron microscopically studies would be desirable.

In the present thesis evidence is presented for targeting of MHC class I-associated peptides to endosomal vesicles for degradation. In the TAP-independent vacuolar pathway, a T cell epitope could be cleaved out various sequence contexts and loaded onto recycling K^b molecules. This alternative pathway was not only operative in TAP-deficient non-professional antigen presenting cells but also in wild-type cells. The vacuolar processing of membrane-associated antigens for class I presentation appears to be unexpectedly efficient. Therefore, the vacuolar pathway may be exploited in future vaccination strategies directed at tumor cells, representing non-professional antigen presenting cells which often downmodulate the proteasome/TAP-dependent pathway.

5. References

Adams, J. (2003). The proteasome: structure, function, and role in the cell. Cancer Treatment Reviews *29*, 3-9.

Almond, J. B., and Cohen, G. M. (2002). The proteasome: a novel target for cancer chemotherapy. Leukemia *16*, 433-443.

Anderson, K., Cresswell, P., Gammon, M., Hermes, J., Williamson, A., and Zweerink, H. (1991). Endogenously synthesized peptide with an endoplasmic reticulum signal sequence sensitizes antigen processing mutant cells to class I- restricted cell-mediated lysis. J Exp Med *174*, 489-492.

Aniento, F., Emans, N., Griffiths, G., and Gruenberg, J. (1993). Cytoplasmic dynein-dependent vesicular transport from early to late endosomes. J Cell Biol *123*, 1373-1387.

Anton, L. C., Snyder, H. L., Bennink, J. R., Vinitsky, A., Orlowski, M., Porgador, A., and Yewdell, J. W. (1998). Dissociation of proteasomal degradation of biosynthesized viral proteins from generation of MHC Class I-associated antigenic peptides. J Immunol *160*, 4859-4868.

Aridor, M., Bannykh, S., Rowe, T., and Balch, W. (1995). Sequential coupling between COPII and COPI vesicle coats in endoplasmic reticulum to Golgi transport. J Cell Biol *131*, 875-893.

Bacik, I., Snyder, H. L., Anton, L. C., Russ, G., Chen, W., Bennink, J. R., Urge, L., Otvos, L., Dudkowska, B., Eisenlohr, L., and Yewdell, J. W. (1997). Introduction of a glycosylation site into a secreted protein provides evidence for an alternative antigen processing pathway: Transport of precursors of major histocompatability complex class I-restricted peptides from the endoplasmic reticulum to the cytosol. J Exp Med *186*, 479-487.

Baker, B. M., Turner, R. V., Gagnon, S. J., Wiley, D. C., and Biddison, W. E. (2001). Identification of a crucial energetic footprint on the alpha1 Helix of human histocompatibility leukocyte antigen (HLA)-A2 that provides functional interactions for recognition by Tax Peptide/HLA-A2-specific T cell receptors. J Exp Med *193*, 551-562.

Bartee, E., Mansouri, M., Hovey Nerenberg, B. T., Gouveia, K., and Fruh, K. (2004).

Downregulation of Major Histocompatibility Complex Class I by human ubiquitin ligases related to viral immune evasion proteins. J Virol *78*, 1109-1120.

Beismann-Driemeyer, S., and Tampe, R. (2004). Function of the antigen transport complex TAP in cellular immunity. Angew Chem Int Ed Engl *43*, 4014-4031.

Beninga, J., Rock, K. L., and Goldberg, A. L. (1998). Interferon-gamma can stimulate post-proteasomal trimming of the N terminus of an antigenic peptide by inducing leucine aminopeptidase. J Biol Chem *73*,18734-18742.

Berg, D. T., and Grinnell, B. W. (1993). Pro to Gly (P219G) in a silent glycosylation site results in complete glycosylation in tissue plasminogen activator. Protein Sci *2*, 126-127.

Bevan, M. J. (1976). Cross priming for a secondary cytotoxic respsonse to minor H antigens with H 2 congenic cells which do not cross react in the cytotoxic assay. J Exp Med *143*, 1283-1288.

Billingham, R., Bren, L., and Medawar, P. (1953) Activity acquired tolerance of foreign cells . Nature *172*, 603-606.

Bogyo, M., Verhelst, S., Bellingard-Dubouchaud, V., Toba, S., and Greenbaum, D. (2000). Selective targeting of lysosomal cysteine proteases with radiolabeled electrophilic substrate analogs. Chem Biol *7*, 27-38.

Bonifacino, J. S., and Traub, L. M. (2003). Signals for sorting of transmembrane proteins to endosomes and lysosomes. Annual Review of Biochemistry *72*, 395-447.

Brooks, P., Murray, R. Z., Mason, G. G., Hendil, K. B., and Rivett, A. J. (2000). Association of immunoproteasomes with the endoplasmic reticulum. Biochem J *352*, 611–615.

Brossart, P., and Bevan, M. J. (1997). Presentation of exogenous protein antigens on major histocompatability complex class I molecules by dendritic cells: Pathway of presentation and regulation by cytokines. Blood *90*, 1594-1599.

Brouwenstijn, N., Serwold, T., and Shastri, N. (2001). MHC class I molecules can direct proteolytic cleavage of antigenic precursors in the endoplasmic reticulum.

Immunity *15*, 95-104.

Brown, F. D., Rozelle, A. L., Yin, H. L., Balla, T., and Donaldson, J. G. (2001). Phosphatidylinositol 4,5-bisphosphate and Arf6-regulated membrane traffic. J Cell Biol *154*, 1007-1018.

Brown, M. G., Driscoll, J., and Monaco, J. J. (1991). Structural and serological similarity of MHC-linked LMP and proteasome (multicatalytic proteinase) complexes. Nature *353*, 355 - 357.

Bucci, C., Parton, R., Mather, I., Stunnenberg, H., Simons, K., Hoflack, B., and Zerial, M. (1992). The small GTPase rab5 functions as a regulatory factor in the early endocytic pathway. Cell *70*, 715-728.

Bucci, C., Thomsen, P., Nicoziani, P., McCarthy, J., and van Deurs, B. (2000). Rab7: A key to lysosome biogenesis. Mol Biol Cell *11*, 467-480.

Buchholz, D., Scott, P., and Shastri, N. (1995). Presentation without Proteolytic Cleavage of Endogenous Precursors in the MHC Class I Antigen Processing Pathway. J Biol Chem *270*, 6515-6522.

Campbell, D. J., Serwold, T., and Shastri, N. (2000). Bacterial proteins can be processed by macrophages in a transporter associated with antigen processing-independent, cysteine protease-dependent manner for presentation by MHC class I molecules. J Immunol *164*, 168-175.

Caplan, S., Naslavsky, N., Hartnell, L. M., Lodge, R., Polishchuk, R. S., Donaldson, J. G., and Bonifacino, J. S. (2002). A tubular EHD1-containing compartment involved in the recycling of major histocompatibility complex class I molecules to the plasma membrane. EMBO J *21*, 2557-2567.

Carbonetti, N. H., Irish, T. J., Chen, C. H., O'Connell, C. B., Hadley, G. A., McNamara, U., Tuskan, R. G., and Lewis, G. K. (1999). Intracellular Delivery of a Cytolytic T-Lymphocyte Epitope Peptide by Pertussis Toxin to Major Histocompatibility Complex Class I without Involvement of the Cytosolic Class I Antigen Processing Pathway. Infect Immun *67*, 602-607.

Cerundolo, V., Benham, A., Braud, V., Mukherjee, S., Gould, K., Macino, B., Neefjes,

J., and Townsend, A. (1997). The proteasome-specific inhibitor lactacystin blocks presentation of cytotoxic T lymphocyte epitopes in human and murine cells. Eur J Immunol *1*, 336-341.

Chapman, H. A., Riese, R. J., and Shi, G. P. (1997). Emerging roles for cysteine proteases in human biology. Annu Rev Physiol *59*, 63-88.

Chefalo, P. J., and Harding, C. V. (2001). Processing of exogenous antigens for presentation by class I MHC molecules involves post-golgi peptide exchange influenced by peptide-MHC complex stability and acidic pH. J Immunol *167*, 1274-1282.

Coulombe, R., Grochulski, P., Sivaraman, J., Menard, R., Mort, J., and Cygler, M. (1996). Structure of human procathepsin L reveals the molecular basis of inhibition by the prosegment. EMBO J *15*, 5492-5503.

Cuervo, A. (2004). Autophagy: many paths to the same end. Mol Cell Biochem *263*, 55-72.

Cyglera, M., and Mort, J. S. (1997). Proregion structure of members of the papain superfamily. Mode of inhibition of enzymatic activity. Biochimie *79*, 645-652.

David, V., Hochstenbach, F., Rajagopalan, S., and Brenner, M. (1993). Interaction with newly synthesized and retained proteins in the endoplasmic reticulum suggests a chaperone function for human integral membrane protein IP90 (calnexin). J Biol Chem *268*, 9585-9592.

Davis, D., Reyburn, H., Pazmany, L., Chiu, I., Mandelboim, O., and Strominger, J. (1997). Impaired spontaneous endocytosis of HLA-G. Eur J Immunol *27*, 2714-2719.

Degen, E., and Williams, D. (1991). Participation of a novel 88-kD protein in the biogenesis of murine class I histocompatibility molecules. J Cell Biol *112*, 1099-1115.

Dela Cruz, C. S., Tan, R., Rowland-Jones, S. L., and Barber, B. H. (2000). Creating HIV-1 reverse transcriptase cytotoxic T lymphocyte target structures by HLA-A2 heavy chain modifications. Int Immunol *12*, 1293-1302.

Deres, K., Beck, W., Faath, S., Jung, G., and Rammensee, H.-G. (1993). MHC/Peptide Binding Studies indicate Hierarchy of Anchor Residues. Cellular Immunology *151*,

158-167.

Dick, T. P., Bangia, N., Peaper, D. R., and Cresswell, P. (2002). Disulfide bond isomerization and the assembly of MHC class I-peptide complexes. Immunity *16*, 87-98.

Diedrich, G., Bangia, N., Pan, M., and Cresswell, P. (2001). A role for calnexin in the assembly of the MHC class I loading complex in the endoplasmic reticulum. J Immunol *166*, 1703-1709.

Diegel, M. L., Chen, F., Laus, R., Graddis, T. J., and Vidovic, D. (2003). Major Histocompatibility Complex Class I-Restricted Presentation of Protein Antigens without Prior Intracellular Processing. Scand J Immunol *58*, 1-8.

Dissanayake, S. K., Tuera, N., and Ostrand-Rosenberg, S. (2005). Presentation of endogenously synthesized MHC class II-restricted epitopes by MHC class II cancer vaccines is independent of Transporter Associated with Ag Processing and the proteasome. J Immunol *174*, 1811-1819.

Dittie, A., Klumperman, J., and Tooze, S. (1999). Differential distribution of mannose-6-phosphate receptors and furin in immature secretory granules. J Cell Sci *112*, 3955-3966.

Doms, R., Keller, D., Helenius, A., and Balch, W. (1987). Role for adenosine triphosphate in regulating the assembly and transport of vesicular stomatitis virus G protein trimers. J Cell Biol *105*, 1957-1969.

Dunn, K., and Maxfield, F. (1992). Delivery of ligands from sorting endosomes to late endosomes occurs by maturation of sorting endosomes. J Cell Biol *117*, 301-310.

Eisenlohr, L., Bacik, I., Bennink, J., Bernstein, K., and Yewdell, J. (1992). Expression of a membrane protease enhances presentation of endogenous antigens to MHC class I-restricted T lymphocytes. Cell *71*, 963-972.

Elliott, T., Willis, A., Cerundolo, V., and Townsend, A. (1995). Processing of major histocompatibility class I-restricted antigens in the endoplasmic reticulum. J Exp Med *181*, 1481-1491.

Enenkel, C., Lehmann, A., and Kloetzel, P. M. (1998). Subcellular distribution of

proteasomes implicates a major location of protein degradation in the nuclear envelope–ER network in yeast. Embo J *17*, 6144–6154.

Evans, G., Margulies, D., Camerini-Otero, R., Ozato, K., and Seidman, J. (1982). Structure and expression of a mouse major histocompatibility antigen gene, H-2Ld. PNAS *79*, 1994-1998.

Feng, Y., Press, B., and Wandinger-Ness, A. (1995). Rab 7: an important regulator of late endocytic membrane traffic. J Cell Biol *131*, 1435-1452.

Fernandes, D., Vidard, L., and Rock, K. (2000). Characterization of MHC class II-presented peptides generated from an antigen targeted to different endocytic compartments. Eur J Immunol *30*, 2333-2343.

Fremont, D., Stura, E., Matsumura, M., Peterson, P., and Wilson, I. (1995). Crystal Structure of an H-2Kb-Ovalbumin Peptide Complex Reveals the Interplay of Primary and Secondary Anchor Positions in the Major Histocompatibility Complex Binding Groove. PNAS *92*, 2479-2483.

Fruci, D., Niedermann, G., Butler, R. H., and van Endert, P. M. (2001). Efficient MHC Class I-Independent Amino-Terminal Trimming of Epitope Precursor Peptides in the Endoplasmic Reticulum. Immunity *15*, 467-476.

Galvin, K., Krishna, S., Ponchel, F., Frohlich, M., Cummings, D., Carlson, R., Wands, J., Isselbacher, K., Pillai, S., and Ozturk, M. (1992). The Major Histocompatibility Complex Class I Antigen-Binding Protein p88 is the Product of the Calnexin Gene. PNAS *89*, 8452-8456.

Garbi, N., Tan, P., Diehl, A. D., Chambers, B. J., Ljunggren, H.-G., Momburg, F., and Hammerling, G. J. (2000). Impaired immune responses and altered peptide repertoire in tapasin-deficient mice. *1*, 234-238.

Garbi, N., Tan, P., Momburg, F., and Hammerling, G. J. (2001). Role of tapasin in MHC class I antigen presentation in vivo. Adv Exp Med Biol *495*, 71-78.

Garbi, N., Tiwari, N., Momburg, F., and Hammerling, G. J. (2003). A major role for tapasin as a stabilizer of the TAP peptide transporter and consequences for MHC class I

expression. Eur J Immunol *33*, 264-273.

Garcia-Mata, R., Szul, T., Alvarez, C., and Sztul, E. (2003). ADP-Ribosylation Factor/COPI-dependent Events at the Endoplasmic Reticulum-Golgi Interface Are Regulated by the Guanine Nucleotide Exchange Factor GBF1. Mol Biol Cell *14*, 2250-2261.

Garred, Deurs, B. v., and Sandvig, K. (1995). Furin-induced Cleavage and Activation of Shiga Toxin. J Biol Chem *270*, 10817-10821.

Ghosh, P., Dahms, N. M., and Kornfeld, S. (2003). Mannose 6-phosphate receptors: new twists in the tale. Nat Rev Mol Cell Biol *4*, 202-213.

Gil-Torregrosa, B. C., Castano, A. R., Lopez, D., and Del Val, M. (2000). Generation of MHC Class I Peptide Antigens by Protein Processing in the Secretory Route by Furin. Traffic *1*, 641-651.

Gil-Torregrosa, B. C., Raul Castano, A., and Del Val, M. (1998). Major Histocompatibility Complex Class I Viral Antigen Processing in the Secretory Pathway Defined by the trans-Golgi Network Protease Furin. J Exp Med *188*, 1105-1116.

Gordon, R. D., Mathieson, B. J., Samelson, L. E., and et, a. (1976). The effect of allogeneic presensitization on H-Y graft survival and in vitro cell mediated responses to H-Y antigen. J Exp Med *144*, 810-820.

Gorer, P. A., Lymen, S., and Snell, S. D. (1948). Studies of genetic and antigenic basis of tumour transplantation. Linkage between a histocompatibility gene and fused in mice. Pro R Sco London B *135*, 499-505.

Gorvel, J., Chavrier, P., Zerial, M., and Gruenberg, J. (1991). rab5 controls early endosome fusion in vitro. Cell *64*, 915-925.

Grandea, A. G., 3rd, Comber, P. G., Wenderfer, S. E., Schoenhals, G., Fruh, K., Monaco, J. J., and Spies, T. (1998). Sequence, linkage to H2-K, and function of mouse tapasin in MHC class I assembly. Immunogenetics *48*, 260-265.

Grandea, A. r., Golovina, T., Hamilton, S., Sriram, V., Spies, T., Brutkiewicz, R., Harty, J., Eisenlohr, L., and Van Kaer, L. (2000). Impaired assembly yet normal trafficking of

MHC class I molecules in Tapasin mutant mice. Immunity *13*, 213-222.

Grant, E. P., Michalek, M. T., Goldberg, A. L., and Rock, K. L. (1995). Rate of antigen degradation by the ubiquitin-proteasome pathway influences MHC class I presentation. J Immunol *155*, 3750-3758.

Greener, T., Zhao, X., Nojima, H., Eisenberg, E., and Greene, L. E. (2000). Role of Cyclin G-associated Kinase in Uncoating Clathrin-coated Vesicles from Non-neuronal Cells. J Biol Chem *275*, 1365-1370.

Gromme, M., and Neefjes, J. (2002). Antigen degradation or presentation by MHC class I molecules via classical and non-classical pathways. Molecular Immunology *39*, 181-202.

Gromme, M., Uytdehaag, F. G. C. M., Janssen, H., Calafat, J., van Binnendijk, R. S., Kenter, M. J. H., Tulp, A., Verwoerd, D., and Neefjes, J. (1999). Recycling MHC class I molecules and endosomal peptide loading. PNAS *96*, 10326-10331.

Gruenberg, J. (2001). The endocytic pathway: a mosaic of domains. Nat Rev Mol Cell Biol *2*, 721-730.

Gruenberg, J., and Howell, K. E. (1989). Membrane Traffic in Endocytosis: Insights from Cell-Free Assays. Annual Review of Cell Biology *5*, 453-481.

Guermonprez, P., Saveanu, L., Kleijmeer, M., Davoust, J., Van Endert, P., and Amigorena, S. (2003). ER-phagosome fusion defines an MHC class I cross-presentation compartment in dendritic cells. Nature *425*, 397-402.

Guild, B., and Strominger, J. (1984). Human and murine class I MHC antigens share conserved serine 335, the site of HLA phosphorylation in vivo. J Biol Chem *259*, 9235-9240.

Guo, H. C., Jardetzky, T. S., Garrett, T. P., Lane, W. S., Strominger, J. L., and Wiley, D. C. (1992). Different length peptides bind to HLA-Aw68 similarly at their ends but bulge out in the middle. Nature *360*, 364-366.

Gur, H., El-Zaatari, F., Geppert, T., Wacholtz, M., Taurog, J., and Lipsky, P. (1990). Analysis of T cell signaling by class I MHC molecules: the cytoplasmic domain is not

required for signal transduction. J Exp Med *172*, 1267-1270.

Gur, H., Geppert, T. D., and Lipsky, P. E. (1997). Structural analysis of class I MHC molecules: The cytoplasmic domain is not required for cytoskeletal association, aggregation and internalization. Molecular Immunology *34*, 125-132.

Hammerling, G. J., Rusch, E., Tada, N., Kimura, S., and Hammerling, U. (1982). Localization of Allodeterminants on H-2Kb Antigens Determined with Monoclonal Antibodies and H-2 Mutant Mice. PNAS *79*, 4737-4741.

Harris, M. R., Yu, Y. Y. L., Kindle, C. S., Hansen, T. H., and Solheim, J. C. (1998). Calreticulin and Calnexin Interact with Different Protein and Glycan Determinants During the Assembly of MHC Class I. J Immunol *160*, 5404-5409.

Hochstenbach, F., David, V., Watkins, S., and Brenner, M. (1992). Endoplasmic Reticulum Resident Protein of 90 Kilodaltons Associates with the T- and B-Cell Antigen Receptors and Major Histocompatibility Complex Antigens During their Assembly. PNAS *89*, 4734-4738.

Honey, K., Duff, M., Beers, C., Brissette, W. H., Elliott, E. A., Peters, C., Maric, M., Cresswell, P., and Rudensky, A. (2001). Cathepsin S Regulates the Expression of Cathepsin L and the Turnover of gamma -Interferon-inducible Lysosomal Thiol Reductase in B Lymphocytes. J Biol Chem *276*, 22573-22578.

Hopkins, C., and Trowbridge, I. (1983). Internalization and processing of transferrin and the transferrin receptor in human carcinoma A431 cells. J Cell Biol *97*, 508-521.

Hopkins, C. R. (1983). The importance of the endosome in intracellular traffic. Nature *304*, 684-685.

Houde, M., Bertholet, S., Gagnon, E., Brunet, S., Goyette, G., Laplante, A., Princiotta, M., Thibault, P., Sacks, D., and Desjardins, M. (2003). Phagosomes are competent organelles for antigen cross-presentation. Nature *425*, 402-406.

Howarth, M., Williams, A., Tolstrup, A. B., and Elliott, T. (2004). Tapasin enhances MHC class I peptide presentation according to peptide half-life. PNAS *101*, 11737-11742.

Howell, D., Levitt, J. M., Foster, P. A., Guenther, M. M., Shawar, S. M., Rich, R. R., and Rodgers, J. R. (2000). Heterogeneity of RMA-S cell line: derivatives of RMA-S cells lacking H2-Kb and H2-Db expression. Immunogenetics *52*, 150-154.

Hoyt, M. A., and Coffino, P. (2004). Ubiquitin-free routes into the proteasome. Cell Mol Life Sci *61*, 1596-1600.

Hubbard, A. L., Stieger, B., and Bariles, J. R. (1989). Biogenesis of Endogenous Plasma Membrane Proteins in Epithelial Cells. Annual Review of Physiology *51*, 755-770.

Hughes, E., Ortmann, B., Surman, M., and Cresswell, P. (1996). The protease inhibitor, N-acetyl-L-leucyl-L-leucyl-leucyl-L- norleucinal, decreases the pool of major histocompatibility complex class I-binding peptides and inhibits peptide trimming in the endoplasmic reticulum. J Exp Med *183*, 1569-1578.

Hughes, E. A., and Cresswell, P. (1998). The thiol oxidoreductase ERp57 is a component of the MHC class I peptide-loading complex. Curr Biol *8*, 709-712.

Jackson, M., Cohen-Doyle, M., Peterson, P., and Williams, D. (1994). Regulation of MHC class I transport by the molecular chaperone, calnexin (p88, IP90). Science *263*, 384-387.

Jaulin, C., Romero, P., Luescher, I., Casanova, J., Prochnicka-Chalufour, A., Langlade-Demoyen, P., Maryanski, J., and Kourilsky, P. (1992). Most residues on the floor of the antigen binding site of the class I MHC molecule H-2Kd influence peptide presentation. Int Immunol *4*, 943-953.

Jones, B., and Janeway, C. A. J. (1981). Functional activities of antibodies against brain-associated T cell antigens. I. Induction of T cell proliferation. Eur J Immunol *11*, 584-592.

Kang, X., Robbins, P., Fitzgerald, E., Wang, R., Rosenberg, S., and Kawakami, Y. (1997). Induction of melanoma reactive T cells by stimulator cells expressing melanoma epitope-major histocompatibility complex class I fusion proteins. Cancer Res *57*, 202-205.

Karttunen, J., Sanderson, S., and Shastri, N. (1992). Detection of Rare Antigen-Presenting Cells by the lacZ T-Cell Activation Assay Suggests an Expression Cloning

Strategy for T-Cell Antigens. PNAS *89*, 6020-6024.

Katayama, T., Imaizumi, K., Yoneda, T., Taniguchi, M., Honda, A., Manabe, T., Hitomi, J., Oono, K., Baba, K., Miyata, S.*, et al.* (2004). Role of ARF4L in recycling between endosomes and the plasma membrane. Cell Mol Neurobiol *24*, 137-147.

Kawamoto, K., Yoshida, Y., Tamaki, H., Torii, S., Shinotsuka, C., Yamashina, S., and Nakayama, K. (2002). GBF1, a Guanine Nucleotide Exchange Factor for ADP-Ribosylation Factors, is Localized to the cis-Golgi and Involved in Membrane Association of the COPI Coat. Traffic *3*, 483-495.

Keller, P., and Simons, K. (1997). Post-Golgi biosynthetic trafficking. J Cell Sci *110*, 3001-3009.

Kleijmeer, M. J., Escola, J.-M., UytdeHaag, F. G. C. M., Jakobson, E., Griffith, J. M., Osterhaus, A. D. M. E., Stoorvogel, W., Melief, C. J. M., Rabouille, C., and Geuze, H. J. (2001). Antigen loading of MHC class I molecules in the endocytic tract. Traffic *2*, 124-137.

Klein, J., and Sato, A. (1998). Birth of the Major Histocompatibility Complex. Scand J Immunol *47*, 199-209.

Kloetzel, P. M. (2004). Generation of major histocompatibility complex class I antigens: functional interplay between proteasomes and TPPII. *5*, 661-669.

Koopmann, J. O., Post, M., Neefjes, J. J., Hammerling, G. J., and Momburg, F. (1996). Translocation of long peptides by transporters associated with antigen processing (TAP). Eur J Immunol *26*, 1720-1728.

Kornfeld, R., and Kornfeld, S. (1985). Assembly of Asparagine-Linked Oligosaccharides. Annual Review of Biochemistry *54*, 631-664.

Kovacsovics-Bankowski, M., and Rock, K. (1995). A phagosome-to-cytosol pathway for exogenous antigens presented on MHC class I molecules. Science *267*, 243-246.

Kulski, J. K., Shiina, T., Anzai, T., Kohara, S., and Inoko, H. (2002). Comparative genomic analysis of the MHC: the evolution of class I duplication blocks, diversity and complexity from shark to man. Immunol Rev *190*, 95-122.

Lacaille, V. G., and Androlewicz, M. J. (1998). Herpes Simplex Virus Inhibitor ICP47 Destabilizes the Transporter Associated with Antigen Processing (TAP) Heterodimer. J Biol Chem *273*, 17386-17390.

Lautscham, G., Rickinson, A., and Blake, N. (2003). TAP-independent antigen presentation on MHC class I molecules: lessons from Epstein-Barr virus. Microbes and Infection *5*, 291-299.

Lauvau, G., Gubler, B., Cohen, H., Daniel, S., Caillat-Zucman, S., and van Endert, P. M. (1999). Tapasin enhances assembly of transporters associated with antigen processing-dependent and -independent peptides with HLA-A2 and HLA-B27 expressed in insect cells. J Biol Chem *274*, 31349-31358.

Lemberg, M. K., Bland, F. A., Weihofen, A., Braud, V. M., and Martoglio, B. (2001). Intramembrane Proteolysis of Signal Peptides: An Essential Step in the Generation of HLA-E Epitopes. J Immunol *167*, 6441-6446.

Lewis, J. W., and Elliott, T. (1998). Evidence for successive peptide binding and quality control stages during MHC class I assembly. Current Biology *8*, 717-720.

Lindquist, J. A., Hammerling, G. J., and Trowsdale, J. (2001). ER60/ERp57 forms disulfide-bonded intermediates with MHC class I heavy chain. FASEB J *15*, 1448-1450.

Lindquist, J. A., Jensen, O. N., Mann, M., and Hammerling, G. J. (1998). ER-60, a chaperone with thiol-dependent reductase activity involved in MHC class I assembly. Embo J *17*, 2186-2195.

Lingeman, R. G., Joy, D. S., Sherman, M. A., and Kane, S. E. (1998). Effect of Carbohydrate Position on Lysosomal Transport of Procathepsin L. Mol Biol Cell *9*, 1135-1147.

Lippincott-Schwartz, J. (1993). Membrane cycling between the ER and Golgi apparatus and its role in biosynthetic transport. Subcell Biochem *21*, 95-119.

Liu, T., Zhou, X., Orvell, C., Lederer, E., Ljunggren, H., and Jondal, M. (1995). Heat-inactivated Sendai virus can enter multiple MHC class I processing pathways and generate cytotoxic T lymphocyte responses in vivo. J Immunol *154*, 3147-3155.

Lizee, G., Basha, G., Tiong, J., Julien, J., Tian, M., Biron, K., and Jefferies, W. (2003). Control of dendritic cell cross-presentation by the major histocompatibility complex class I cytoplasmic domain. Nature Immunology *4*, 1065-1073.

Ljunggren, H., and Karre, K. (1985). Host resistance directed selectively against H-2-deficient lymphoma variants. Analysis of the mechanism. J Exp Med *162*, 1745-1759.

Lybarger, L., Yu, Y. Y. L., Chun, T., Wang, C. R., Grandea III, A. G., Van Kaer, L., and Hansen, T. H. (2001). Tapasin enhances peptide-induced expression of H2-M3 molecules, but is not required for the retention of open conformers. Journal of Immunology *167*, 2097-2105.

Machy, P., Truneh, A., Gennaro, D., and Hoffstein, S. (1987). Major histocompatibility complex class I molecules internalized via coated pits in T lymphocytes. Nature *328*, 724-726.

Madden, D. R. (1995). The Three-Dimensional Structure of Peptide-MHC Complexes. Annual Review of Immunology *13*, 587-622.

Maloy, W., and Coligan, J. (1982). Primary structure of the H-2Db alloantigen II. Additional amino acid sequence information, localization of a third site of glycosylation and evidence for K and D region specific sequences. Immunogenetics *16*.

Martoglio, B., and Dobberstein, B. (1998). Signal sequences: more than just greasy peptides. Trends in Cell Biology *8*, 410-415.

Matlin, K., and Simons, K. (1983). Reduced temperature prevents transfer of a membrane glycoprotein to the cell surface but does not prevent terminal glycosylation. Cell *34*, 233-243.

McGrath, M. E. (1999). The lysosomal cysteine proteases. Annu Rev Biophys Biomol Struct *28*, 181-204.

Mellman, I. (1996). Membranes and sorting. Curr Opin Cell Biol *8*, 497-498.

Mesaeli, N., Nakamura, K., Zvaritch, E., Dickie, P., Dziak, E., Krause, K.-H., Opas, M., MacLennan, D. H., and Michalak, M. (1999). Calreticulin Is Essential for Cardiac Development. J Cell Biol *144*, 857-868.

Molinari, M., Eriksson, K. K., Calanca, V., Galli, C., Cresswell, P., Michalak, M., and Helenius, A. (2004). Contrasting Functions of Calreticulin and Calnexin in Glycoprotein Folding and ER Quality Control. Molecular Cell *13*, 125-135.

Momburg, F., Roelse, J., Hammerling, G. J., and Neefjes, J. J. (1994a). Peptide size selection by the major histocompatibility complex-encoded peptide transporter. J Exp Med *179*, 1613-1623.

Momburg, F., Roelse, J., Howard, J. C., Butcher, G. W., Hammerling, G. J., and Neefjes, J. J. (1994b). Selectivity of MHC-encoded peptide transporters from human, mouse and rat. Nature *367*, 648-651.

Momburg, F., Roelse, J., Neefjes, J., and Hammerling, G. J. (1994c). Peptide transporters and antigen processing. Behring Inst Mitt, 26-36.

Morrice, N. A., and Powis, S. J. (1998). A role for the thiol-dependent reductase ERp57 in the assembly of MHC class I molecules. Curr Biol *8*, 713-716.

Mosse, C. A., Meadows, L., Luckey, C. J., Kittlesen, D. J., Huczko, E. L., Slingluff, C. L., Jr., Shabanowitz, J., Hunt, D. F., and Engelhard, V. H. (1998). The Class I Antigen-processing Pathway for the Membrane Protein Tyrosinase Involves Translation in the Endoplasmic Reticulum and Processing in the Cytosol. J Exp Med *187*, 37-48.

Mottez, E., Langlade-Demoyen, P., Gournier, H., Martinon, F., Maryanski, J., Kourilsky, P., and Abastado, J. (1995). Cells expressing a major histocompatibility complex class I molecule with a single covalently bound peptide are highly immunogenic. J Exp Med *181*, 493-502.

Mukherjee, S., Ghosh, R. N., and Maxfield, F. R. (1997). Endocytosis. Physiol Rev *77*, 759-803.

Nagler, D., Storer, A., Portaro, F., Carmona, E., Juliano, L., and Menard, R. (1997). Major Increase in Endopeptidase Activity of Human Cathepsin B upon Removal of Occluding Loop Contacts. Biochemistry *36*, 12608 -12615.

Naslavsky, N., Weigert, R., and Donaldson, J. G. (2003). Convergence of non-clathrin- and clathrin-derived endosomes involves Arf6 inactivation and changes in

phosphoinositides. Mol Biol Cell *14*, 417-431.

Naslavsky, N., Weigert, R., and Donaldson, J. G. (2004). Characterization of a nonclathrin endocytic pathway: membrane cargo and lipid requirements. Mol Biol Cell *15*, 3542-3552.

Nebenfuhr, A., Ritzenthaler, C., and Robinson, D. G. (2002). Brefeldin A: Deciphering an Enigmatic Inhibitor of Secretion. Plant Physiol *130*, 1102-1108.

Neefjes, J. J., Momburg, F., and Hammerling, G. J. (1993). Selective and ATP-dependent translocation of peptides by the MHC-encoded transporter. Science *261*, 769-771.

Neefjes, J. J., Smit, L., Gehrmann, M., and Ploegh, H. L. (1992). The fate of the three subunits of major histocompatibility complex class I molecules. Eur J Immunol *22*, 1609-1614.

Neisig, A., Roelse, J., Sijts, A., Ossendorp, F., Feltkamp, M., Kast, W., Melief, C., and Neefjes, J. (1995). Major differences in transporter associated with antigen presentation (TAP)-dependent translocation of MHC class I-presentable peptides and the effect of flanking sequences. J Immunol *154*, 1273-1279.

Newman, R. H., Whitehead, P., Lally, J., Coffer, A., and Freemont, P. (1996). 20S human proteasomes bind with a specific orientation to lipid monolayers in vitro. Biochim Biophys Acta *1281*, 111-116.

Nichols, B. J., and Lippincott-Schwartz, J. (2001). Endocytosis without clathrin coats. Trends in Cell Biology *11*, 406-412.

Nie, Z., Hirsch, D. S., and Randazzo, P. A. (2003). Arf and its many interactors. Current Opinion in Cell Biology *15*, 396-404.

Niedermann, G., Butz, S., Ihlenfeldt, H., Grimm, R., Lucchiari, M. H., H, Jung, G., Maier, B., and Eichmann, K. (1995). Contribution of proteasome-mediated proteolysis to the hierarchy of epitopes presented by major histocompatibility complex class I molecules. Immunity *2*, 289-299.

Niedermann, G., King, G., Butz, S., Birsner, U., Grimm, R., Shabanowitz, J., Hunt, D.

F., and Eichmann, K. (1996). The proteolytic fragments generated by vertebrate proteasomes: Structural relationships to major histocompatibility complex class. PNAS *93*, 8572-8577.

Niu, T.-K., Pfeifer, A. C., Lippincott-Schwartz, J., and Jackson, C. L. (2004). Dynamics of GBF1, a Brefeldin A-sensitive Arf1 Exchange Factor at the Golgi. Mol Biol Cell, E04-07-0599.

Okudo, H., Urade, R., Moriyama, T., and Kito, M. (2000). Catalytic cysteine residues of ER-60 protease. FEBS Letters *465*, 145-147.

Orlandi, P. A., and Fishman, P. H. (1998). Filipin-dependent inhibition of cholera toxin: Evidence for toxin internalization and activation through caveolae-like domains. J Cell Biol *141*, 905-915.

Orr, H., Lopez de Castro, J., Lancet, D., and Strominger, J. (1979). Complete amino acid sequence of a papain-solubilized human histocompatibility antigen, HLA-B7. 2. Sequence determination and search for homologies. Biochemistry *18*, 5711-5720.

Ortmann, B., Androlewicz, M. J., and Cresswell, P. (1994). MHC class I/[beta]2-microglobulin complexes associate with TAP transporters before peptide binding. Nature *368*, 864-867.

Ortmann, B., Copeman, J., Lehner, P. J., Sadasivan, B., Herberg, J. A., Grandea, A. G., Riddell, S. R., Tampe, R., Spies, T., Trowsdale, J., and Cresswell, P. (1997). A critical role for tapasin in the assembly and function of multimeric MHC class I-TAP complexes. Science *277*, 1306-1309.

Owen, B. A. L., and Pease, L. R. (1999). TAP Association Influences the Conformation of Nascent MHC Class I Molecules. J Immunol *162*, 4677-4684.

Paludan, C., Schmid, D., Landthaler, M., Vockerodt, M., Kube, D., Tuschl, T., and Munz, C. (2005). Endogenous MHC class II processing of a viral nuclear antigen after autophagy. Science *307*, 593-596.

Paulsson, K. M., Kleijmeer, M. J., Griffith, J., Jevon, M., Chen, S., Anderson, P. O., Sjogren, H.-O., Li, S., and Wang, P. (2002). Association of Tapasin and COPI Provides a Mechanism for the Retrograde Transport of Major Histocompatibility Complex (MHC)

Class I Molecules from the Golgi Complex to the Endoplasmic Reticulum. J Biol Chem *277*, 18266-18271.

Paz , P., Brouwenstijn, N., Perry, R., and Shastri, N. (1999). Discrete proteolytic intermediates in the MHC class I antigen processing pathway and MHC I-dependent peptide trimming in the ER. Immunity *11*, 241-251.

Pelkmans, L., Kartenbeck, J., and Helenius, A. (2001). Caveolar endocytosis of simian virus 40 reveals a new two-step vesicular-transport pathway to the ER. Nature Cell Biology *3*, 473-483.

Peters, J. M. (1994). Proteasomes: protein degradation machines of the cell. Trends Biochem Sci *19*, 377-382.

Petersson, M., Charo, J., Salazar-Onfray, F., Noffz, G., Mohaupt, M., Qin, Z., Klein, G., Blankenstein, T., and Kiessling, R. (1998). Constitutive IL-10 Production Accounts for the High NK Sensitivity, Low MHC Class I Expression, and Poor Transporter Associated with Antigen Processing (TAP)-1/2 Function in the Prototype NK Target YAC-1. J Immunol *161*, 2099-2105.

Pond, L., and Watts, C. (1997). Characterization of transport of newly assembled, T cell-stimulatory MHC class II-peptide complexes from MHC class II compartments to the cell surface. J Immunol *159*, 543-553.

Porgador, A., Yewdell, J. W., Deng, Y., Bennink, J., and Germain, R. N. (1997). Localization, quantitation, and in situ detection of specific peptide-MHC class I complexes using a monoclonal antibody. Immunity *6*, 715-726.

Powelka, A. M., Sun, J., Li, J., Gao, M., Shaw, L. M., Sonnenberg, A., and Hsu, V. W. (2004). Stimulation-dependent recycling of integrin beta1 regulated by ARF6 and Rab11. Traffic *5*, 20-36.

Purcell, A. W., Gorman, J. J., Garcia-Peydro, M., Paradela, A., Burrows, S. R., Talbo, G. H., Laham, N., Chen Au, P., Reynolds, E. C., Lopez de Castro, J. A., and McCluskey, J. (2001). Quantitative and qualitative influences of tapasin on the class I peptide repertoire. Journal of Immunology *166*, 1016-1027.

Rademacher, T. W., Parekh, R. B., and Dwek, R. A. (1988). Glycobiology. Annual

Review of Biochemistry *57*, 785-838.

Radhakrishna, H., and Donaldson, J. G. (1997). ADP-Ribosylation Factor 6 Regulates a Novel Plasma Membrane Recycling Pathway. J Cell Biol *139*, 49-61.

Rammensee, H.-G., Friede, T., and Stevanovic, S. (1995). MHC ligands and peptide motifs: first listing. Immunogenetics *41*, 178-228.

Reid, P., and Watts, C. (1990). Cycling of cell-surface MHC glycoproteins through primaquine-sensitive intracellular compartments. Nature *346*, 655-657.

Reis e Sousa, C., and Germain, R. (1995). Major histocompatibility complex class I presentation of peptides derived from soluble exogenous antigen by a subset of cells engaged in phagocytosis. J Exp Med *182*, 841-851.

Reits, E., Benham, A., Plougastel, B., Neefjes, J., and Trowsdale, J. (1997). Dynamics of proteasome distribution in living cells. Embo J *16*, 6087-6094.

Reits, E., Griekspoor, A., Neijssen, J., Groothuis, T., Jalink, K., van Veelen, P., Janssen, H., Calafat, J., Drijfhout, J. W., and Neefjes, J. (2003). Peptide Diffusion, Protection, and Degradation in Nuclear and Cytoplasmic Compartments before Antigen Presentation by MHC Class I. Immunity *18*, 97-108.

Reits, E., Neijssen, J., Herberts, C., Benckhuijsen, W., Janssen, L., Drijfhout, J. W., and Neefjes, J. (2004). A major role for TPPII in trimming proteasomal degradation products for MHC class I antigen presentation. Immunity *20*, 495-506.

Reits, E. A., Vos, J. C., Gromme, M., and Neefjes, J. (2000). The major substrates for TAP in vivo are derived from newly synthesized proteins. Nature *404*, 774-778.

Riese, R. J., and Chapman, H. A. (2000). Cathepsins and compartmentalization in antigen presentation. Current Opinion in Immunology *12*, 107-113.

Ritz, U., Momburg, F., Pilch, H., Huber, C., Maeurer, M. J., and Seliger, B. (2001). Deficient expression of components of the MHC class I antigen processing machinery in human cervical carcinoma. International Journal Of Oncology *19*, 1211-1220.

Roberts, T. J., Sriram, V., Spence, P. M., Gui, M., Hayakawa, K., Bacik, I., Bennink, J.

R., Yewdell, J. W., and Brutkiewicz, R. R. (2002). Recycling CD1d1 Molecules Present Endogenous Antigens Processed in an Endocytic Compartment to NKT Cells. J Immunol *168*, 5409-5414.

Rock, K., York, I., and Goldberg, A. (2004). Post-proteasomal antigen processing for major histocompatibility complex class I presentation. Nat Immunol *5*, 670-677.

Rock, K. L., Gramm, C., Rothstein, L., Clark, K., Stein, R., Dick, L., Hwang, D., and Goldberg, A. L. (1994). Inhibitors of the proteasome block the degradation of most cell proteins and the generation of peptides presented on MHC class I molecules. Cell *78*, 761-771.

Sadasivan, B., Lehner, P. J., Ortmann, B., Spies, T., and Cresswell, P. (1996). Roles for calreticulin and a novel glycoprotein, tapasin, in the interaction of MHC class I molecules with TAP. Immunity *5*, 103-114.

Salazar-Onfray, F., Charo, J., Petersson, M., Freland, S., Noffz, G., Qin, Z., Blankenstein, T., Ljunggren, H., and Kiessling, R. (1997). Down-regulation of the expression and function of the transporter associated with antigen processing in murine tumor cell lines expressing IL-10. J Immunol *159*, 3195-3202.

Sambrook, J., and Russell, R. (2001). Molecular cloning: A laboratory manual, 3rd ed. Cold Spring, NY. Cold Spring Harbor Laboratory Press.

Sandvig, K., and van Deurs, B. (2002). Transport of protein toxins into cells: pathways used by ricin, cholera toxin and Shiga toxin. FEBS Letters *529*, 49-53.

Saper, M. A., Bjorkman, P. J., and Wiley, D. C. (1991). Refined structure of the human histocompatibility antigen HLA-A2 at 2.6 A resolution. J Mol Biol *219*, 277-319.

Saric, T., Beninga, J., Graef, C. I., Akopian, T. N., Rock, K. L., and Goldberg, A. L. (2001). Major Histocompatibility Complex Class I-presented Antigenic Peptides Are Degraded in Cytosolic Extracts Primarily by Thimet Oligopeptidase. J Biol Chem *276*, 36474-36481.

Saric, T., Chang, S. C., Hattori, A., York, I. A., Markant, S., Rock, K. L., Tsujimoto, M., and Goldberg, A. L. (2002). An IFN-gamma-induced aminopeptidase in the ER, ERAP1,

trims precursors to MHC class I-presented peptides. Nat Immunol *3*, 1169-1176.

Schmid, S. L. (1997). Clathrin-coated vesicle formation and protein sorting: an integrated process. Annu Rev Biochem *66*, 511-548.

Schmitz, A., and Herzog, V. (2004). Endoplasmic reticulum-associated degradation: exceptions to the rule. Eur J Cell Biol *83*, 501-510.

Schubert, U., Anton, L. C., Gibbs, J., Norbury, C. C., Yewdell, J. W., and Bennink, J. R. (2000). Rapid degradation of a large fraction of newly synthesized proteins by proteasomes. Nature *404*, 770-774.

Selby, M., Erickson, A., Dong, C., Cooper, S., Parham, P., Houghton, M., and Walker, C. M. (1999). Hepatitis C Virus Envelope Glycoprotein E1 Originates in the Endoplasmic Reticulum and Requires Cytoplasmic Processing for Presentation by Class I MHC Molecules. J Immunol *162*, 669-676.

Seliger, B., Schreiber, K., Delp, K., Meissner, M., Hammers, S., Reichert, T., Pawlischko, K., Tampe, R., and Huber, C. (2001). Downregulation of the constitutive tapasin expression in human tumor cells of distinct origin and its transcriptional upregulation by cytokines. Tissue Antigens *57*, 39-45.

Serwold, T., Gaw, S., and Shastri, N. (2001). ER aminopeptidases generate a unique pool of peptides for MHC class I molecules. Nature Immunology *2*, 644 - 651.

Serwold, T., Gonzalez, F., Kim, J., Jacob, R., and Shastri, N. (2002). ERAAP customizes peptides for MHC class I molecules in the endoplasmic reticulum. Nature *419*, 480-483.

Shastri, N., Schwab, S., and Serwold, T. (2002). Producing nature's gene-chips: The Generation of Peptides for Display by MHC Class I Molecules. Annual Review of Immunology *20*, 463-493.

Shastri, N., Serwold, T., and Gonzalez, F. (1995). Presentation of endogenous peptide/MHC class I complexes is profoundly influenced by specific C-terminal flanking residues. J Immunol *155*, 4339-4346.

Shen, L., Sigal, L. J., Boes, M., and Rock, K. L. (2004). Important role of cathepsin S in

generating peptides for TAP-independent MHC Class I crosspresentation *in vivo*. Immunity *21*, 155-165.

Snyder, H., Yewdell, J., and Bennink, J. (1994). Trimming of antigenic peptides in an early secretory compartment. J Exp Med *180*, 2389-2394.

Spies, T., Bresnahan, M., Bahram, S., Arnold, D., Blanck, G., Mellins, E., Pious, D., and DeMars, R. (1990). A gene in the human major histocompatibility complex class II region controlling the class I antigen presentation pathway. Nature *348*, 744-747.

Stanley, K. K., and Howell, K. E. (1993). TGN38/41: a molecule on the move. Trends in Cell Biology *3*, 252-255.

Stephens, D., Lin-Marq, N., Pagano, A., Pepperkok, R., and Paccaud, J. (2000). COPI-coated ER-to-Golgi transport complexes segregate from COPII in close proximity to ER exit sites. J Cell Sci *113*, 2177-2185.

Stoorvogel, W., Strous, G. J., Geuze, H. J., Oorschot, V., and Schwartz, A. L. (1991). Late endosomes derive from early endosomes by maturation. Cell *65*, 417-427.

Storkus, W., Zeh, H. r., Salter, R., and Lotze, M. (1993). Identification of T-cell epitopes: rapid isolation of class I-presented peptides from viable cells by mild acid elution. J Immunother *14*, 94-103.

Stryhn, A., Pedersen, L., Holm, A., and Buus, S. (2000). Longer peptide can be accommodated in the MHC class I binding site by a protrusion mechanism. Eur J Immunol *30*, 3089-3099.

Suh, W., Mitchell, E., Yang, Y., Peterson, P., Waneck, G., and Williams, D. (1996). MHC class I molecules form ternary complexes with calnexin and TAP and undergo peptide-regulated interaction with TAP via their extracellular domains. J Exp Med *184*, 337-348.

Sylvester-Hvid, C., Nielsen, L.-L. B., Hansen, N. J. V., Pedersen, L. O., and Buus, S. (1999). A Single-Chain Fusion Molecule Consisting of Peptide, Major Histocompatibility Gene Complex Class I Heavy Chain and beta2-Microglobulin Can Fold Partially Correctly, but Binds Peptide Inefficiently. Scand J Immunol *50*, 355-362.

Tanioka, T., Hattori, A., Masuda, S., Nomura, Y., Nakayama, H., Mizutani, S., and Tsujimoto, M. (2003). Human Leukocyte-derived Arginine Aminopeptidase: The third member of the oxytocinase subfamily of aminopeptidases. J Biol Chem *278*, 32275-32283.

Tanioka, T., Hattori, A., Mizutani, S., and Tsujimoto, M. (2005). Regulation of the human leukocyte-derived arginine aminopeptidase/endoplasmic reticulum-aminopeptidase 2 gene by interferon-gamma. FEBS J *272*, 916-928.

Tector, M., and Salter, R. D. (1995). Calnexin influences folding of human class I histocompatibility proteins but not their assembly with beta(2)-microglobulin. J Biol Chem *270*, 19638-19642.

Tewari, M., Sinnathamby, G., Rajagopal, D., and Eisenlohr, L. (2005). A cytosolic pathway for MHC class II-restricted antigen processing that is proteasome and TAP dependent. Nat Immunol *6*, 287-294.

Thomas, G. (2002). Furin at the cutting edge: from protein traffic to embryogenesis and disease. Nature Reviews Molecular Cell Biology

Nat Rev Mol Cell Biol *3*, 753-766.

Toshitani, K., Braud, V., Browning, M. J., Murray, N., McMichael, A. J., and Bodmer, W. F. (1996). Expression of a single-chain HLA class I molecule in a human cell line: Presentation of exogenous peptide and processed antigen to cytotoxic T lymphocytes. PNAS *93*, 236-240.

Townsend, A., Bastin, J., Gould, K., Brownlee, G., Andrew, M., Coupar, B., Boyle, D., Chan, S., and Smith, G. (1988). Defective presentation to class I-restricted cytotoxic T lymphocytes in vaccinia-infected cells is overcome by enhanced degradation of antigen. J Exp Med *168*, 1211-1224.

Townsend, A., Ohlen, C., Bastin, J., Ljunggren, H. G., Foster, L., and Karre, K. (1989). Association of class I major histocompatibility heavy and light chains induced by viral peptides. Nature *340*, 443-448.

Traub, L., and Kornfeld, S. (1997). The trans-Golgi network: a late secretory sorting

station. Curr Opin Cell Biol *9*, 527-533.

Trombetta, E. S., and Mellman, I. (2005). Cell biology of antigen processing in vitro and in vivo. Annu Rev Immunol *23*, 975-1028.

Trowsdale, J., Hanson, I., Mockridge, I., Beck, S., Townsend, A., and Kelly, A. (1990). Sequences encoded in the class II region of the MHC related to the 'ABC' superfamily of transporters. Nature *348*, 741-744.

Turk, B., Turk, D., and Turk, V. (2000). Lysosomal cysteine proteases: more than scavengers. Biochimica et Biophysica Acta (BBA) - Protein Structure and Molecular Enzymology *1477*, 98-111.

Turk, B., Turk, V., and Turk, D. (1997). Structural and functional aspects of papain-like cysteine proteinases and their protein inhibitors. Biol Chem *378*, 141-150.

Turk, V., and Bode, W. (1991). The cystatins: protein inhibitors of cysteine proteinases. FEBS Lett *285*, 213-219.

Uebel, S., Meyer, T. H., Kraas, W., Kienle, S., Jung, G., Wiesmller, K.-H., and Tamp, R. (1995). Requirements for Peptide Binding to the Human Transporter Associated with Antigen Processing Revealed by Peptide Scans and Complex Peptide Libraries. J Biol Chem *270*, 18512-18516.

Uger, R. A., and Barber, B. H. (1998). Creating CTL Targets with Epitope-Linked β2-Microglobulin Constructs. J Immunol *160*, 1598-1605.

Ullrich, O., Reinsch, S., Urbe, S., Zerial, M., and Parton, R. (1996). Rab11 regulates recycling through the pericentriolar recycling endosome. J Cell Biol *135*, 913-924.

Urade, R., Takenaka, Y., and Kito, M. (1993). Protein degradation by ERp72 from rat and mouse liver endoplasmic reticulum. J Biol Chem *268*, 22004-22009.

Van der Sluijs, P., Hull, M., Webster, P., Male, P., Goud, B., and Mellman, I. (1992). The small GTP-binding protein rab4 controls an early sorting event on the endocytic pathway. Cell *70*, 729-740.

Van Endert, P. M., Riganelli, D., Greco, G., Fleischhauer, K., Sidney, J., Sette, A., and

Bach, J. F. (1995). The peptide-binding motif for the human transporter associated with antigen processing. J Exp Med *182*, 1883-1895.

Van Kaer, L., Ashton-Rickardt, P., Ploegh, H., and Tonegawa, S. (1992). TAP1 mutant mice are deficient in antigen presentation, surface class I molecules, and CD4-8+ T cells. Cell *71*, 1205-1214.

Van, L., Jeroen, E. M., and Kearse, K. P. (1996). Deglucosylation of N-linked glycans is an important step in the dissociation of calreticulin-class I-TAP complexes. PNAS *93*, 13997-14001.

Vassilakos, A., Cohen-Doyle, M., Peterson, P., Jackson, M., and Williams, D. (1996). The molecular chaperone calnexin facilitates folding and assembly of class I histocompatibility molecules. Embo J *15*, 1495-1506.

Vega, M., and Strominger, J. L. (1989). Constitutive endocytosis of HLA class I antigens requires a specific portion of the intracytoplasmic tail that shares structural features with other endocytosed molecules. PNAS *86*, 2688-2692.

Verma, R., and Deshaies, R. (2000). A proteasome howdunit: the case of the missing signal. Cell *101*, 341-314.

Villadangos, J., and Ploegh, H. (2000). Proteolysis in MHC class II antigen presentation: who's in charge? Immunity *12*, 233-239.

von Figura, K., Gieselmann, V., and Hasilik, A. (1984). Antibody to mannose 6-phosphate specific receptor induces receptor deficiency in human fibroblasts. Embo J *3*, 1281-1286.

Watts, C. (2001). Antigen processing in the endocytic compartment. Curr Opin Immunol *13*, 26-31.

White, J., Crawford, F., Fremont, D., Marrack, P., and Kappler, J. (1999). Soluble Class I MHC with beta2-Microglobulin Covalently Linked Peptides: Specific Binding to a T Cell Hybridoma. J Immunol *162*, 2671-2676.

Wick, M., and Pfeifer, J. (1996). Major histocompatibility complex class I presentation of ovalbumin peptide 257-264 from exogenous sources: protein context influences the

degree of TAP-independent presentation. Eur J Immunol *26*, 2790-2799.

Williams, A. P., Peh, C. A., Purcell, A. W., McCluskey, J., and Elliott, T. (2002). Optimization of the MHC Class I Peptide Cargo Is Dependent on Tapasin. Immunity *16*, 509-520.

Yamashiro, D., Tycko, B., Fluss, S., and Maxfield, F. (1984). Segregation of transferrin to a mildly acidic (pH 6.5) para-Golgi compartment in the recycling pathway. Cell *37*, 789-800.

Yang, K., Basu, A., Wang, M., Chintala, R., Hsieh, M.-C., Liu, S., Hua, J., Zhang, Z., Zhou, J., Li, M.*, et al.* (2003). Tailoring structure-function and pharmacokinetic properties of single-chain Fv proteins by site-specific PEGylation. Protein Eng *16*, 761-770.

Yewdell, J., Norbury, C., and Bennink, J. (1999). Mechanisms of exogenous antigen presentation by MHC class I molecules in vitro and in vivo: implications for generating CD8+ T cell responses to infectious agents, tumors, transplants, and vaccines. Adv Immunology *73*, 1-77.

Yewdell, J., Schubert, U., and Bennink, J. (2001). At the crossroads of cell biology and immunology: DRiPs and other sources of peptide ligands for MHC class I molecules. J Cell Sci *114*, 845-851.

Yorimitsu, T., and Klionsky, D. J. (2005). Atg11 Links Cargo to the Vesicle-forming Machinery in the Cytoplasm to Vacuole Targeting Pathway. Mol Biol Cell, E04-11-1035.

York, I., Mo, A., Lemerise, K., Zeng, W., Shen, Y., Abraham, C., Saric, T., Goldberg, A., and Rock, K. (2003). The cytosolic endopeptidase, thimet oligopeptidase, destroys antigenic peptides and limits the extent of MHC class I antigen presentation. Immunity *18*, 429-440.

York, I. A., Chang, S., Saric, T., Keys, J., Favreau, J., Goldberg, A., and Rock, K. L. (2002). The ER aminopeptidase ERAP1 enhances or limits antigen presentation by trimming epitopes to 8–9 residues. Nature Immunology *3*, 1177 - 1184.

Yu, Y. Y. L., Netuschil, N., Lybarger, L., Connolly, J. M., and Hansen, T. H. (2002).

Cutting Edge: Single-Chain Trimers of MHC Class I Molecules Form Stable Structures That Potently Stimulate Antigen-Specific T Cells and B Cells. J Immunol *168*, 3145-3149.

Zapun, A., Darby, N. J., Tessier, D. C., Michalak, M., Bergeron, J. J. M., and Thomas, D. Y. (1998). Enhanced Catalysis of Ribonuclease B Folding by the Interaction of Calnexin or Calreticulin with ERp57. J Biol Chem *273*, 6009-6012.

Zapun, A., Petrescu, S. M., Rudd, P. M., Dwek, R. A., Thomas, D. Y., and Bergeron, J. J. (1997). Conformation-independent binding of monoglucosylated ribonuclease B to calnexin. Cell *88*, 29-38.

Zeidler, R., Eissner, G., Meissner, P., Uebel, S., Tampe, R., Lazis, S., and Hammerschmidt, W. (1997). Downregulation of TAP1 in B Lymphocytes by Cellular and Epstein-Barr Virus-Encoded Interleukin-10. Blood *90*, 2390-2397.

Zuniga, M. C., Wang, H., Barry, M., and McFadden, G. (1999). Endosomal/Lysosomal Retention and Degradation of Major Histocompatibility Complex Class I Molecules Is Induced by Myxoma Virus. Virology *261*, 180-192.

6. Acknowledgements

From experience I can tell you that these last pages of a PhD thesis are the most widely read pages of the entire publication. It is a pleasure to thank the many people who made this thesis possible.

It is difficult to overstate my gratitude to my Ph.D. supervisor, Priv.-Doz. Dr. Frank Momburg. With his enthusiasm, inspiration, and his great efforts to explain things clearly and simply I managed to finish my thesis on time.

I would like to acknowledge the support given by Prof. Gunter J. Hammerling and critical review of my thesis.

Throughout my thesis-writing period, I can't forget a few friends who provided encouragement, sound advice, good teaching, good company, and lots of good ideas. Among them, Vinaygam, who provided me with excellent south Indian food and home accommodation whenever I needed it in night time after experiments. Suresh and Kishore, who were always ready to help me to improve my English and for scientific discussion, Badri for teaching me PyMOL and reading the thesis time to time.

I am indebted to my many colleagues for providing a stimulating and fun environment in the lab where I have learned a lot and grown up. I am especially grateful to Natalio Garbi, Thomas, Mario, Tewfik, Martina, Mustafa at the DKFZ. Natalio was particularly helpful in teaching me the B3Z assay which was extensively used during my PhD time and at the same time patiently discussed lots of new things in the MHC class I antigen presentation pathway.

I wish to thank my friend in India, Jaya who helped me to start my PhD in Germany. My thanks go to Ravi, Anmol. I can't forget the moral support provided by my friend Jitnedra, Frankfurt, for helping me get through difficult times, and for all the emotional support, comraderie, entertainment, and caring he provided. Thanks to Vishal for reminding me to finish my thesis on time.

My thanks goes to Nitin, for providing me access to confocal microscopy and critical tips for cell staining, without that it would have been difficult to solve all problems in time.

My greatest thanks go to my fiancé Meetu, for calling me from India and taking care of myself from far away. Your support has been priceless and thesis would not have completed without your help.

Lastly, and most importantly, I wish to thank my parents, especially my mother, for her understanding. Her love encouraged me to work hard to pursue my PhD in Germany. Her firm and kind-hearted personality has affected me to be steadfast and never bend to difficulty. She always lets me know that she is proud of me, which motivated me to work harder and do my best. My thanks go to my youngest sister Vandana for giving me support and fun time when I had difficult times.

Neeraj Tiwari

April 20, 2005